

The impact of intertidal areas on the carbonate system of the southern North Sea

Fabian Schwichtenberg^{1,6}, Johannes Pätsch^{1,5}, Michael Ernst Böttcher^{2,3,4}, Helmuth Thomas⁵,
Vera Winde², Kay-Christian Emeis⁵

¹ Theoretical Oceanography, Universität Hamburg, Bundesstr. 53, D-20146 Hamburg, Germany

² Geochemistry & Isotope Biogeochemistry Group, Department of Marine Geology, Leibniz Institute of Baltic Sea Research (IOW), Seestr. 15, D-18119 Warnemünde, Germany

³ Marine Geochemistry, University of Greifswald, Friedrich-Ludwig-Jahn Str. 17a, D-17489 Greifswald, Germany

⁴ Department of Maritime Systems, Interdisciplinary Faculty, University of Rostock, Albert-Einstein-Str. 21, D-18059 Rostock, Germany

⁵ Institute of Coastal Research, Helmholtz Zentrum Geesthacht (HZG), Max-Planck-Str. 1, D-21502 Geesthacht, Germany

⁶ Present Address: German Federal Maritime and Hydrographic Agency, Bernhard-Nocht-Str. 78, D-20359 Hamburg, Germany

Correspondence to Johannes Pätsch (johannes.paetsch@uni-hamburg.de)

Abstract

The coastal ocean is strongly affected by ocean acidification because of its shallow water depths, low volume, and the closeness to terrestrial dynamics. Earlier observations of dissolved inorganic carbon (DIC) and total alkalinity (TA) in the southern part of the North Sea, a Northwest-European shelf sea, revealed lower acidification effects than expected. It has been assumed that anaerobic degradation and subsequent TA release in the adjacent back-barrier tidal areas ('Wadden Sea') in summer time is responsible for this phenomenon. In this study the exchange rates of TA and DIC between the Wadden Sea tidal basins and the North Sea and the consequences for the carbonate system in the German Bight are estimated using a 3-D ecosystem model. The aim of this study is to differentiate the various sources contributing to observed high summer TA concentrations in the southern North Sea.

30 Measured TA and DIC concentrations in the Wadden Sea are considered as model boundary
31 conditions. This procedure acknowledges the dynamic behaviour of the Wadden Sea as an
32 area of effective production and decomposition of organic material. According to the
33 modelling results, 39 Gmol TA yr⁻¹ were exported from the Wadden Sea into the North Sea,
34 which is less than a previous estimate, but within a comparable range. The interannual
35 variabilities of TA and DIC concentrations, mainly driven by hydrodynamic conditions, were
36 examined for the years 2001 – 2009. Dynamics in the carbonate system is found to be
37 related to specific weather conditions. The results suggest that the Wadden Sea is an
38 important driver for the carbonate system in the southern North Sea. On average 41 % of TA
39 inventory changes in the German Bight were caused by riverine input, 37 % by net transport
40 from adjacent North Sea sectors, 16 % by Wadden Sea export, and 6 % are caused by
41 internal net production of TA. The dominant role of river input for the TA inventory
42 disappears when focussing on TA concentration changes due to the corresponding
43 freshwater fluxes diluting the marine TA concentrations. The ratio of exported TA versus DIC
44 reflects the dominant underlying biogeochemical processes in the Wadden Sea. Whereas,
45 aerobic degradation of organic matter plays a key role in the North Frisian Wadden Sea
46 during all seasons of the year, anaerobic degradation of organic matter dominated in the
47 East Frisian Wadden Sea. Despite of the scarcity of high-resolution field data it is shown that
48 anaerobic degradation in the Wadden Sea is one of the main contributors of elevated
49 summer TA values in the southern North Sea.

50

51 **1. Introduction**

52 Shelf seas are highly productive areas constituting the interface between the inhabited
53 coastal areas and the global ocean. Although they represent only 7.6 % of the world ocean's
54 area, current estimates assume that they contribute approximately 21 % to total global
55 ocean CO₂ sequestration (Borges, 2011). At the global scale the uncertainties of these
56 estimates are significant due to the lack of spatially and temporally resolved field data. Some
57 studies investigated regional carbon cycles in detail (e.g., Kempe & Pegler, 1991; Brasse et
58 al., 1999; Reimer et al., 1999; Thomas et al., 2004; 2009; Artioli et al., 2012; Lorkowski et al.,
59 2012; Burt et al., 2016; Shadwick et al., 2011; Laruelle et al., 2014; Carvalho et al., 2017) and
60 pointed out sources of uncertainties specifically for coastal settings.

61 However, natural pH dynamics in coastal- and shelf- regions, for example, have been shown
62 to be up to an order of magnitude higher than in the open ocean (Provoost et al, 2010).

63 Also, the nearshore effects of CO₂ uptake and acidification are difficult to determine,
64 because of the shallow water depth and a possible superposition by benthic-pelagic
65 coupling, and strong variations in fluxes of TA are associated with inflow of nutrients from
66 rivers, pelagic nutrient driven production and respiration (Provoost et al., 2010), submarine
67 groundwater discharge (SGD; Winde et al., 2014), and from benthic-pelagic pore water
68 exchange (e.g., Billerbeck et al., 2006; Riedel et al., 2010; Moore et al., 2011; Winde et al.,
69 2014; Santos et al., 2012; 2015; Brenner et al., 2016; Burt et al., 2014; 2016; Seibert et al.,
70 2019). Finally, shifts within the carbonate system are driven by impacts from watershed
71 processes and modulated by changes in ecosystem structure and metabolism (Duarte et al.,
72 2013).

73 Berner et al. (1970) and Ben-Yakoov (1973) were among the first who investigated elevated
74 TA and pH variations caused by microbial dissimilatory sulphate reduction in the anoxic pore
75 water of sediments. At the Californian coast, the observed enhanced TA export from
76 sediments was related to the burial of reduced sulphur compounds (pyrite) (Dollar et al.,
77 1991; Smith & Hollibaugh, 1993; Chambers et al., 1994). Other studies conducted in the
78 Satilla and Altamaha estuaries and the adjacent continental shelf found non-conservative
79 mixing lines of TA versus salinity, which was attributed to anaerobic TA production in
80 nearshore sediments (Wang & Cai, 2004; Cai et al., 2010). Iron dynamics and pyrite
81 formation in the Baltic Sea were found to impact benthic TA generation from the sediments
82 (Gustafsson et al., 2019; Łukawska-Matuszewska and Graca, 2017).

83 The focus of the present study is the southern part of the North Sea, located on the
84 Northwest-European Shelf. This shallow part of the North Sea is connected with the tidal
85 basins of the Wadden Sea via channels between barrier islands enabling an exchange of
86 water, and dissolved and suspended material (Rullkötter, 2009; Lettmann et al., 2009;
87 Kohlmeier and Ebenhöf, 2009). The Wadden Sea extends from Den Helder (The
88 Netherlands) in the west to Esbjerg (Denmark) in the north and covers an area of about
89 9500 km² (Ehlers, 1994). The entire system is characterised by semidiurnal tides with a tidal
90 range between 1.5 m in the westernmost part and 4 m in the estuaries of the rivers Weser
91 and Elbe (Streif, 1990). During low tide about 50 % of the area are falling dry (van Beusekom

92 et al., 2019). Large rivers discharge nutrients into the Wadden Sea, which in turn shows a
93 high degree of eutrophication, aggravated by mineralisation of organic material imported
94 into the Wadden Sea from the open North Sea (van Beusekom et al., 2012).

95 In comparison to the central and northern part of the North Sea, TA concentrations in the
96 southern part are significantly elevated during summer (Salt et al., 2013; Thomas et al.,
97 2009; Brenner et al., 2016; Burt et al., 2016). The observed high TA concentrations have
98 been attributed to an impact from the adjacent tidal areas (Hoppema, 1990; Kempe &
99 Pegler, 1991; Brasse et al., 1999; Reimer et al., 1999; Thomas et al., 2009; Winde et al.,
100 2014), but this impact has not been rigorously quantified. Using several assumptions,
101 Thomas et al. (2009) calculated an annual TA export from the Wadden Sea / Southern Bight
102 of 73 Gmol TA yr⁻¹ to close the TA budget for the southern North Sea.

103 The aim of this study is to reproduce the elevated summer concentrations of TA in the
104 southern North Sea with a 3D biogeochemical model that has TA as prognostic variable.
105 With this tool at hand, we balance the budget TA in the relevant area on an annual basis.
106 Quantifying the different budget terms, like river input, Wadden Sea export, internal pelagic
107 and benthic production, degradation and respiration allows us to determine the most
108 important contributors to TA variations. In this way we refine the budget terms by Thomas
109 et al. (2009) and replace the original closing term by data. The new results are discussed on
110 the background of the budget approach proposed by Thomas et al. (2009).

111 **2. Methods**

112 **2.1. Model specifications**

113 ***2.1.1. Model domain and validation area***

114 The ECOHAM model domain for this study (Fig. 1) was first applied by Pätsch et al. (2010).
115 For model validations (magenta: validation area, Fig. 1), an area was chosen that includes
116 the German Bight as well as parts along the Danish and the Dutch coast. The western
117 boundary of the validation area is situated at 4.5° E. The southern and northern boundaries
118 are at 53.5° and 55.5° N, respectively. The validation area is divided by the magenta dashed
119 line at 7° E into the western and eastern part. For the calculation of box averages of DIC and
120 TA a bias towards the deeper areas with more volume and more data should be avoided.
121 Therefore, each water column covered with data within the validation area delivered one

122 mean value, which is calculated by vertical averaging. These mean water column averages
123 were horizontally interpolated onto the model grid. After this procedure average box values
124 were calculated. In case of box-averaging model output, the same procedure was applied,
125 but without horizontal interpolation.

126 **2.1.2. The hydrodynamic module**

127 The physical parameters temperature, salinity, horizontal and vertical advection as well as
128 turbulent mixing were calculated by the submodule HAMSOM (Backhaus, 1985), which was
129 integrated in the ECOHAM model. It is a baroclinic primitive equation model using the
130 hydrostatic and Boussinesq approximation. It is applied to several regional sea areas
131 worldwide (Mayer et al., 2018; Su & Pohlmann, 2009). Details are described by Backhaus &
132 Hainbucher (1987) and Pohlmann (1996). The hydrodynamic model ran prior to the
133 biogeochemical part. Daily result fields were stored for driving the biogeochemical model in
134 offline mode. Surface elevation, temperature and salinity resulting from the Northwest-
135 European Shelf model application (Lorkowski et al., 2012) were used as boundary conditions
136 at the southern and northern boundaries. The temperature of the shelf run by Lorkowski et
137 al. (2012) showed a constant offset compared with observations (their Fig. 3), because
138 incoming solar radiation was calculated too high. For the present simulations the shelf run
139 has been repeated with adequate solar radiation forcing.

140 River-induced horizontal transport due to the hydraulic gradient is incorporated (Große et
141 al., 2017; Kerimoglu et al., 2018). This component of the hydrodynamic horizontal transport
142 corresponds to the amount of freshwater discharge.

143 Within this study we use the term flushing time. It is the average time when a basin is filled
144 with laterally advected water. The flushing time depends on the specific basin: large basins
145 have usually higher flushing times than smaller basins. High flushing times correspond with
146 low water renewal times.

147 **2.1.3. The biogeochemical module**

148 The relevant biogeochemical processes and their parameterisations have been detailed in
149 Lorkowski et al. (2012). In former model setups TA was restored to prescribed values derived
150 from observations (Thomas et al., 2009) with a relaxation time of two weeks (Kühn et al.,
151 2010; Lorkowski et al., 2012). The changes in TA treatment for the study at hand is described

152 below. Results from the Northwest-European Shelf model application (Lorkowski et al.,
153 2012) were used as boundary conditions for the recent biogeochemical simulations at the
154 southern and northern boundaries (Fig. 1).

155 The main model extension was the introduction of a prognostic treatment of TA in order to
156 study the impact of biogeochemical and physical driven changes of TA onto the carbonate
157 system and especially on acidification (Pätsch et al., 2018). The physical part contains
158 advective and mixing processes as well as dilution by riverine freshwater input. The pelagic
159 biogeochemical part is driven by planktonic production and respiration, formation and
160 dissolution of calcite, pelagic and benthic degradation and remineralisation, and also by
161 atmospheric deposition of reduced and oxidised nitrogen. All these processes impact TA. In
162 this model version benthic denitrification has no impact on pelagic TA concentrations. Other
163 benthic anaerobic processes are not considered. Only the carbonate ions from benthic
164 calcite dilution increase pelagic TA concentrations. Aerobic remineralisation releases
165 ammonium and phosphate, which enter the pelagic system across the benthic-pelagic
166 interface and alter the pelagic TA concentration. The theoretical background to this has been
167 outlined by Wolf-Gladrow et al. (2007).

168 The years 2001 to 2009 were simulated with 3 spin up years in 2000. Two different scenarios
169 (A and B) were conducted. Scenario A is the reference scenario without implementation of
170 any Wadden Sea processes. For scenario B we used the same model configuration as for
171 scenario A and additionally implemented Wadden Sea export rates of TA and DIC as
172 described in section 2.3.1. The respective Wadden Sea export rates (Fig. 2) are calculated by
173 the temporal integration of the product of `wad_sta` and `wad_exc` over one month (see
174 section 2.3.1, equation 2).

175 **2.2. External sources and boundary conditions**

176 ***2.2.1. Freshwater discharge***

177 Daily data of freshwater fluxes from 16 rivers were used (Fig. 1). For the German Bight and
178 the other continental rivers daily observations of runoff provided by Pätsch & Lenhart (2008)
179 were incorporated. The discharges of the rivers Elbe, Weser and Ems were increased by
180 21 %, 19 % and 30 % in order to take additional drainage into account that originated from
181 the area downstream of the respective points of observation (Radach and Pätsch, 2007). The

182 respective tracer loads were increased accordingly. The data of Neal (2002) were
183 implemented for the British rivers for all years with daily values for freshwater. The annual
184 amounts of freshwater of the different rivers are shown in the appendix (Table A1). Riverine
185 freshwater discharge was also considered for the calculation of the concentrations of all
186 biogeochemical tracers in the model.

187 **2.2.2. River input**

188 **Data sources**

189 River load data for the main continental rivers were taken from the report by Pätsch &
190 Lenhart (2008) that was kept up to date continuously so that data for the years 2007 – 2009
191 were also available (https://wiki.cen.uni-hamburg.de/ifm/ECOHAM/DATA_RIVER). They
192 calculated daily loads of nutrients and organic matter based on data provided by the
193 different river authorities. Additionally, loads of the River Eider were calculated according to
194 Johannsen et al. (2008).

195 Up to now, all ECOHAM applications used constant riverine DIC concentrations. TA was not
196 used. For the study at hand we introduced time varying riverine TA and DIC concentrations.
197 New data of freshwater discharge were introduced, as well as TA and DIC loads for the
198 British rivers (Neal, 2002). Monthly mean concentrations of nitrate, TA and DIC were added
199 for the Dutch rivers (www.waterbase.nl) and for the German river Elbe (Amann et al., 2015).
200 The Dutch river data were observed in the years 2007 – 2009. The river Elbe data were taken
201 in the years 2009 – 2011. These concentration data were prescribed for all simulation years
202 as mean annual cycle.

203 The data sources and positions of the river mouths of all 16 rivers are shown in Table A2 and
204 in Fig. 1. The respective riverine concentrations of TA and DIC are given in Table A3.
205 Schwichtenberg (2013) describes the river data in detail.

206 A few small flood gates (“Siel”) and rivers transport fresh water from the recharge areas into
207 the intertidal areas (Streif, 1990). The recharge areas for these inlets differ considerably
208 from each other, leading to different relative contributions for the fresh water input.
209 Whereas the catchments of Schweiburger Siel (22.2 km²) and the Hooksier Binnentief are
210 only of minor importance, the Vareler Siel, the Eckenwarder Siel, and the Maade Siel are of

211 medium importance, and the highest contribution may originate from the Wangersiel, the
212 Dangaster Siel, and the Jade-Wapeler Siel (Lipinski, 1999).

213

214 **Effective river input**

215 In order to analyse the net effect on concentrations in the sea due to river input, the
216 effective river input (Riv_{eff} [Gmol yr⁻¹]) is introduced:

217

$$Riv_{eff} = \frac{\Delta C|_{riv}}{\rho \cdot yr} \cdot V \cdot C \quad (1)$$

218

219 with $\Delta C|_{riv}$ [$\mu\text{mol kg}^{-1}$]: the concentration change in the river mouth cell due to river load riv
220 and the freshwater flux from the river. V [l] is the volume of the river mouth cell, ρ [kg l^{-1}]
221 density of water, yr is one year, C [10^{-15}l^{-1}] is a constant.

222 Bulk alkalinity discharged by rivers is quite large but most of the rivers entering the North
223 Sea (here the German Bight) have lower TA concentrations than the sea water. In case of
224 identical concentrations, the effective river load Riv_{eff} is zero. The TA related molecules enter
225 the sea, and in most cases, they are leaving it via transport. In case of tracing or budgeting
226 both the real TA river discharge and the transport must be recognized. In order to
227 understand TA concentration changes in the sea Riv_{eff} is appropriate.

228

229 **2.2.3. Meteorological forcing**

230 The meteorological forcing was provided by NCEP Reanalysis (Kalnay et al., 1996) and
231 interpolated on the model grid field. It consisted of six-hourly fields of air temperature,
232 relative humidity, cloud coverage, wind speed, atmospheric pressure, and wind stress for
233 every year. 2-hourly and daily mean short wave radiation were calculated from astronomic
234 insolation and cloudiness with an improved formula (Lorkowski et al., 2012).

235 **2.3. The Wadden Sea**

236 **2.3.1. Implementation of Wadden Sea dynamics**

237 For the present study the exchange of TA and DIC between North Sea and Wadden Sea was
238 implemented into the model by defining sinks and sources of TA and DIC for some of the
239 south-eastern cells of the North Sea grid (Fig. 1). The cells with adjacent Wadden Sea were
240 separated into three exchange areas: The East Frisian, the North Frisian Wadden Sea and the
241 Jade Bay, marked by “E”, “N” and “J” (Fig. 1, right side).

242 Two parameters were determined in order to quantify the TA and DIC exchange between
243 the Wadden Sea and the North Sea.

- 244 1. Concentration changes of pelagic TA and DIC in the Wadden Sea during one tide, and
- 245 2. Water mass exchange between the back-barrier islands and the open sea during one
246 tide

247 Measured concentrations of TA and DIC (Winde, 2013; Winde et al., 2014) as well as
248 modelled water mass exchange rates of the export areas by Grashorn (2015) served as bases
249 for the calculated exchange. Details on flux calculations and measurements are described
250 below. The daily Wadden Sea exchange of TA and DIC was calculated as:

$$wad_flu = \frac{wad_sta * wad_exc}{vol} \quad (2)$$

251 Differences in measured concentrations in the Wadden Sea during rising and falling water
252 levels, as described in section 2.3.2, were temporally interpolated and summarized as
253 wad_sta [mmol m⁻³]. Modelled daily Wadden Sea exchange rates of water masses (tidal
254 prisms during falling water level) were defined as wad_exc [m³ d⁻¹], and the volume of the
255 corresponding North Sea grid cell was vol [m³]. wad_flu [mmol m⁻³ d⁻¹] were the daily
256 concentration changes of TA and DIC in the respective North Sea grid cells.

257 In fact, some amounts of the tidal prisms return without mixing with North Sea water, and
258 calculations of Wadden Sea – North Sea exchange should therefore consider flushing times
259 in the respective back-barrier areas. Since differences in measured concentrations between
260 rising and falling water levels were used, this effect is already assumed to be represented in
261 the data. This approach enabled the use of tidal prisms without consideration of any flushing
262 times.

263 **2.3.2. Wadden Sea - measurements**

264 The flux calculations for the Wadden Sea – North Sea exchange were carried out in tidal
265 basins of the East and North Frisian Wadden Sea (Spiekeroog Island, Sylt-Rømø) as well as in
266 the Jade Bay. For the present study seawater samples representing tidal cycles during
267 different seasons (Winde, 2013). The mean concentrations of TA and DIC during rising and
268 falling water levels and the respective differences (Δ TA and Δ DIC) are given in Table 1.
269 Measurements in August 2002 were taken from Moore et al. (2011). The Δ -values were used
270 as *wad_sta* and were linearly interpolated between the times of observations for the
271 simulations. In this procedure, the linear progress of the Δ -values does not represent the
272 natural behaviour perfectly, especially if only few data are available. As a consequence,
273 possible short events of high TA and DIC export rates that occurred in periods outside the
274 observation periods may have been missed.

275 Due to the low number of concentration measurements a statistical analysis of uncertainties
276 of Δ TA and Δ DIC was not possible. They were measured with a lag of 2 hours after low tide
277 and high tide. This was done in order to obtain representative concentrations of rising and
278 falling water levels. As a consequence, only 2 - 3 measurements for each location and season
279 were considered for calculations of Δ TA and Δ DIC.

280 **2.3.3. Wadden Sea – modelling the exchange rates**

281 Grashorn (2015) performed the hydrodynamic computations of exchanged water masses
282 (*wad_exc*) with the model FVCOM (Chen et al., 2003) by adding up the cumulative seaward
283 transport during falling water level (tidal prisms) between the back-barrier islands that were
284 located near the respective ECOHAM cells with adjacent Wadden Sea area. These values are
285 given in Table 2 for each ECOHAM cell in the respective export areas. The definition of the
286 first cell N1 and the last cell E4 is in accordance to the clockwise order in Fig. 1 (right side).
287 The mean daily runoff of all N-, J- and E-positions was $8.1 \text{ km}^3 \text{ d}^{-1}$, $0.8 \text{ km}^3 \text{ d}^{-1}$ and $2.3 \text{ km}^3 \text{ d}^{-1}$
288 respectively.

289 **2.3.4. Additional Sampling of DIC and TA**

290 DIC and TA concentrations for selected freshwater inlets sampled in October 2010 and May
291 2011 are presented in Table 3. Sampling and analyses took place as described by Winde et
292 al. (2014) and are here reported for completeness and input for discussion only. The autumn
293 data are deposited under doi:10.1594/PANGEA.841976. The samples for TA measurements

294 were filled without headspace into pre-cleaned 12 ccm Exetainer®, filled with 0.1 ml
295 saturated HgCl₂ solution. The samples for DIC analysis were completely filled into 250 ccm
296 ground-glass-stoppered bottles, and then poisoned with 100 µl of a saturated HgCl₂ solution.
297 The DIC concentrations were determined at IOW by coulometric titration according to
298 Johnson et al. (1993), using reference material provided by A. Dickson (University of
299 California, San Diego; Dickson et al., 2003) for the calibration (batch 102). TA was measured
300 by potentiometric titration using HCl using a Schott titri plus equipped with an IOline
301 electrode A157. Standard deviations for DIC and TA measurements were better than +/-2
302 and +/-10 µmol kg⁻¹, respectively.

303

304 **2.4. Statistical analysis**

305 A statistical overview of the simulation results in comparison to the observations (Salt et al.,
306 2013) is given in Table 4 and 5. In the validation area (magenta box in Fig. 1) observations of
307 10 different stations were available, each with four to six measurements at different depths
308 (51 measured points). Measured TA and DIC concentrations of each point were compared
309 with modelled TA and DIC concentrations in the respective grid cells, respectively. The
310 standard deviations (Stdv), the root means square errors (RMSE), and correlation
311 coefficients (r) were calculated for each simulation. In addition to the year 2008, which we
312 focus on in this study, observations were performed at the same positions in summer 2005
313 and 2001. These data are also statistically compared with the model results.

314 **3. Results**

315 **3.1. Model validation - TA concentrations in summer 2008**

316 The results of scenarios A and B were compared with observations of TA in August 2008 (Salt
317 et al., 2013) for surface water. The observations revealed high TA concentrations in the
318 German Bight (east of 7° E and south of 55° N) and around the Danish coast (around 56° N)
319 as shown in Fig. 3a. The observed concentrations in these areas ranged between 2350 and
320 2387 µmol TA kg⁻¹. These findings were in accordance with observed TA concentrations in
321 August / September 2001 (Thomas et al., 2009). TA concentrations in other parts of the
322 observation domain ranged between 2270 µmol TA kg⁻¹ near the British coast (53° N – 56° N)
323 and 2330 µmol TA kg⁻¹ near the Dutch coast and the Channel. In the validation box the

324 overall average and the standard deviation of all observed TA concentrations (Stdv) was
325 2334 and 33 $\mu\text{mol TA kg}^{-1}$, respectively.

326 In scenario A the simulated surface TA concentrations showed a more homogeneous pattern
327 than observations with maximum values of 2396 $\mu\text{mol TA kg}^{-1}$ at the western part of the
328 Dutch coast and even higher (2450 $\mu\text{mol TA kg}^{-1}$) in the river mouth of the Wash estuary at
329 the British coast. Minimum values of 2235 and 2274 $\mu\text{mol TA kg}^{-1}$ were simulated at the
330 mouths of the rivers Elbe and Firth of Forth. The modelled TA concentration ranged from
331 2332 to 2351 $\mu\text{mol TA kg}^{-1}$ in the German Bight and in the Jade Bay. Strongest
332 underestimations in relation to observations are located in a band close to the coast
333 stretching from the East Frisian Islands to 57° N at the Danish coast (Fig. 4a). The deviation of
334 simulation results of scenario A from observations in the validation box was represented by
335 a RMSE of 28 $\mu\text{mol TA kg}^{-1}$. The standard deviation was 7 $\mu\text{mol TA kg}^{-1}$ and the correlation
336 amounted to $r = 0.77$ (Table 4). In the years 2005 and 2001 similar statistical values are
337 found, but the correlation coefficient was smaller.

338 The scenario B was based on a Wadden Sea export of TA and DIC as described above. The
339 major difference in TA concentrations of this scenario compared to A occurred east of 6.5° E.
340 Surface TA concentrations there peaked in the Jade Bay (2769 $\mu\text{mol TA kg}^{-1}$) and were
341 elevated off the North Frisian and Danish coasts from 54.2° to 56° N ($> 2400 \mu\text{mol TA kg}^{-1}$).
342 Strongest underestimations in relation to observations are noted off the Danish coast
343 between 56° and 57° N (Fig. 4b). In the German Bight the model overestimated the
344 observations slightly, while at the East Frisian Islands the model underestimates TA. When
345 approaching the Dutch Frisian Islands the simulation overestimates TA compared to
346 observations and strongest overestimations can be seen near the river mouth of River Rhine.
347 Compared to scenario A the simulation of scenario B was closer to the observations in terms
348 of RMSE (18 $\mu\text{mol TA kg}^{-1}$) and the standard deviation (Stdv = 22 $\mu\text{mol TA kg}^{-1}$). Also, the
349 correlation ($r = 0.86$) improved (Table 4). In the years 2001 and 2005 the observed mean
350 values are slightly overestimated by the model. The statistical values for 2001 are better
351 than for 2005, where scenario A better compares with the observations.

352

353 **3.2. Model validation - DIC concentrations in summer 2008**

354 Analogously to TA the simulation results were compared with surface observations of DIC
355 concentrations in summer 2008 (Salt et al., 2013). They also revealed high values in the
356 German Bight (east of 7° E and south of 55° N) and around the Danish coast (near 56° N)
357 which is shown in Fig. 5. The observed DIC concentrations in these areas ranged between
358 2110 and 2173 $\mu\text{mol DIC kg}^{-1}$. Observed DIC concentrations in other parts of the model
359 domain ranged between 2030 and 2070 $\mu\text{mol DIC kg}^{-1}$ in the north western part and 2080 -
360 2117 $\mu\text{mol DIC kg}^{-1}$ at the Dutch coast. In the validation box the overall average and the
361 standard deviation of all observed DIC concentrations were 2108 and 25.09 $\mu\text{mol DIC kg}^{-1}$,
362 respectively.

363 The DIC concentrations in scenario A ranged between 1935 and 1977 $\mu\text{mol DIC kg}^{-1}$ at the
364 North Frisian and Danish coast (54.5° N - 55.5° N) and 1965 $\mu\text{mol DIC kg}^{-1}$ in the Jade Bay.
365 Maxima of up to 2164 $\mu\text{mol DIC kg}^{-1}$ were modelled at the western part of the Dutch coast
366 north of the mouth of River Rhine (Fig. 5). The DIC concentrations in the German Bight
367 showed a heterogeneous pattern in the model, and sometimes values decreased from west
368 to east, which contrasts the observations (Fig. 5a). This may be the reason for the negative
369 correlation coefficient $r = -0.64$ between model and observations (Table 5). The significant
370 deviation from observation of results from scenario A is also indicated by the RMSE of
371 43 $\mu\text{mol DIC kg}^{-1}$, and a standard deviation of 14 $\mu\text{mol DIC kg}^{-1}$. In 2001 and 2005 the
372 simulation results of this scenario A are better, which is expressed in positive correlation
373 coefficients and small RMSE values.

374 In scenario B the surface DIC concentrations at the Wadden Sea coasts increased: The North
375 Frisian coast shows concentrations of up to 2200 $\mu\text{mol DIC kg}^{-1}$ while the German Bight has
376 values of 2100 – 2160 $\mu\text{mol DIC kg}^{-1}$, and Jade Bay concentrations were higher than
377 2250 $\mu\text{mol DIC kg}^{-1}$. The other areas are comparable to scenario A. In scenario B the RMSE in
378 the validation box decreased to 26 $\mu\text{mol DIC kg}^{-1}$ in comparison to scenario A. The standard
379 deviation decreased to 9.1 $\mu\text{mol DIC kg}^{-1}$, and the correlation improved to $r = 0.55$ (Table 5).
380 The average values are close to the observed ones for all years, even though in 2005 a large
381 RMSE was found.

382 The comparison between observations and simulation results of scenario A (Fig. 4c) clearly
383 show model underestimations in the south-eastern area and are strongest in the inner
384 German Bight towards the North Frisian coast ($> 120 \mu\text{mol DIC kg}^{-1}$). Scenario B also models
385 values lower than observations in the south-eastern area (Fig. 4d), but the agreement
386 between observation and model results is reasonable. Only off the Danish coast near 6.5° E ,
387 56° N the model underestimates DIC by $93 \mu\text{mol DIC kg}^{-1}$.

388 ***3.3. Hydrodynamic conditions and flushing times***

389 The calculations of Wadden Sea TA export in Thomas et al. (2009) were based on several
390 assumptions concerning riverine input of bulk TA and nitrate, atmospheric deposition of
391 NO_x , water column inventories of nitrate and the exchange between the Southern Bight and
392 the adjacent North Sea (Lenhart et al., 1995). The latter was computed by considering that
393 the water in the Southern Bight is flushed with water of the adjacent open North Sea at time
394 scales of six weeks. For the study at hand, flushing times in the validation area in summer
395 and winter are presented for the years 2001 to 2009 in Fig. 6. Additionally, monthly mean
396 flow patterns of the model area are presented for June, July and August for the years 2003
397 and 2008, respectively (Fig. 7). They were chosen to highlight the pattern in summer 2003
398 with one of the highest flushing times (lowest water renewal times), and that in 2008
399 corresponding to one of the lowest flushing times (highest water renewal times).

400 The flushing times were determined for the three areas 1 – validation area, 2 – western part
401 of the validation area, 3 – eastern part of the validation area. They were calculated by
402 dividing the total volume of the respective areas 1 – 3 by the total inflow into the areas
403 $\text{m}^3 (\text{m}^3 \text{ s}^{-1})^{-1}$. Flushing times (rounded to integer values) were consistently higher in summer
404 than in winter, meaning that highest inflow occurred in winter. Summer flushing times in the
405 whole validation area ranged from 54 days in 2008 to 81 days in 2003 and 2006, whereas the
406 winter values in the same area ranged from 32 days in 2008 to 51 days in 2003 and 2009.
407 The flushing times in the western and eastern part of the validation area were smaller due to
408 the smaller box sizes. Due to the position, flushing times in the western part were
409 consistently shorter than in the eastern part. These differences ranged from 5 days in winter
410 2002 to 14 days in summer 2006 and 2008. The interannual variabilities of all areas were
411 higher in summer than in winter.

412 The North Sea is mainly characterised by an anti-clockwise circulation pattern (Otto et al.,
413 1990; Pätsch et al., 2017). This can be observed for the summer months in 2008 (Fig. 7).
414 More disturbed circulation patterns in the south-eastern part of the model domain occurred
415 in June 2003: In the German Bight and in the adjacent western area two gyres with reversed
416 rotating direction are dominant. In August 2003 the complete eastern part shows a
417 clockwise rotation which is due to the effect of easterly winds as opposed to prevalent
418 westerlies. In this context such a situation is called meteorological blocking situation.

419 **3.4. Seasonal and interannual variability of TA and DIC concentrations**

420 The period from 2001 to 2009 was simulated for the scenarios A and B. For both scenarios
421 monthly mean surface concentrations of TA were calculated in the validation area and are
422 shown in Fig. 8a and 8b. The highest TA concentration in scenario A was $2329 \mu\text{mol TA kg}^{-1}$
423 and occurred in July 2003. The lowest TA concentrations in each year were about 2313 to
424 $2318 \mu\text{mol TA kg}^{-1}$ and occurred in February and March. Scenario B showed generally higher
425 values: Summer concentrations were in the range of 2348 to $2362 \mu\text{mol TA kg}^{-1}$ and the
426 values peaked in 2003. The lowest values occurred in the years 2004 – 2008. Also, winter
427 values were higher in scenario B than in scenario A: They range from 2322 to
428 $2335 \mu\text{mol TA kg}^{-1}$.

429

430 Corresponding to TA, monthly mean surface DIC concentrations in the validation area are
431 shown in Fig. 8c and 8d. In scenario A the concentrations increased from October to
432 February and decreased from March to August (Fig. 8c). In scenario B the time interval with
433 increasing concentrations was extended into March. Maximum values of 2152 to
434 $2172 \mu\text{mol DIC kg}^{-1}$ in scenario A occur in February and March of each model year, and
435 minimum values of 2060 to $2080 \mu\text{mol DIC kg}^{-1}$ in August. Scenario B shows generally higher
436 values: Highest values in February and March are 2161 to $2191 \mu\text{mol DIC kg}^{-1}$. Lowest values
437 in August range from 2095 to $2112 \mu\text{mol DIC kg}^{-1}$. The amplitude of the annual cycle is
438 smaller in scenario B, because the Wadden Sea export shows highest values in summer
439 (Fig. 2).

440 The pattern of the monthly TA and DIC concentrations of the reference scenario A differ
441 drastically in that TA does not show a strong seasonal variability, whereas DIC does vary

442 significantly. In case of DIC this is due to the biological drawdown during summer. On the
443 other hand, the additional input (scenario B) from the Wadden Sea in summer creates a
444 strong seasonality for TA and instead flattens the variations in DIC.

445 **4. Discussion**

446

447 Thomas et al. (2009) estimated the contribution of shallow intertidal and subtidal areas to
448 the alkalinity budget of the SE North Sea. That estimate (by closure of mass fluxes) was
449 about 73 Gmol TA yr⁻¹ originating from the Wadden Sea fringing the southern and eastern
450 coast. These calculations were based on observations from the CANOBA dataset in 2001 and
451 2002. The observed high TA concentrations in the south-eastern North Sea were also
452 encountered in August 2008 (Salt et al., 2013) and these measurements were used for the
453 main model validation in this study. Our simulations result in 39 Gmol TA yr⁻¹ as export from
454 the Wadden Sea into the North Sea. Former modelling studies of the carbonate system of
455 the North Sea (Artioli et al., 2012; Lorkowski et al., 2012) did not consider the Wadden Sea
456 as a source of TA and DIC, and good to reasonable agreement to observations from the
457 CANOBA dataset was only achieved in the open North Sea in 2001 / 2002 (Thomas et al.,
458 2009). Subsequent simulations that included TA export from aerobic and anaerobic
459 processes in the sediment improved the agreement between data and models (Pätsch et al.,
460 2018). When focusing on the German Bight, however, the observed high TA concentrations
461 in summer measurements east of 7° E could not be simulated satisfactorily.

462 The present study confirms the Wadden Sea as an important TA source for the German Bight
463 and quantifies the annual Wadden Sea TA export rate to 39 Gmol TA yr⁻¹. Additionally, the
464 contributions by most important rivers have been more precisely quantified and narrow
465 down uncertainties in the budgets of TA and DIC in the German Bight. All steps that were
466 required to calculate the budget including uncertainties are discussed in the following.

467

468 ***4.1. Uncertainties of Wadden Sea – German Bight exchange rates of TA and DIC***

469 The Wadden Sea is an area of effective benthic decomposition of organic material (Böttcher
470 et al., 2004; Billerbeck et al., 2006; Al-Rai et al., 2009; van Beusekom et al., 2012) originating
471 both from land and from the North Sea (Thomas et al., 2009). In general, anaerobic

472 decomposition of the organic matter generates TA and increases the CO₂ buffer capacity of
473 seawater. On longer time scales TA can only be generated by processes that involve
474 permanent loss of anaerobic remineralisation products (Hu and Cai, 2011). A second
475 precondition is the nutrient availability to produce organic matter, which in turn serves as
476 necessary component of anaerobic decomposition (Gustafsson et al., 2019). The Wadden
477 Sea export rates of TA and DIC modelled in the present study are based on concentration
478 measurements during tidal cycles in the years 2002 and 2009 to 2011 (Table 1), and on
479 calculated tidal prisms of two day-periods that are considered to be representative of annual
480 mean values. This approach introduces uncertainties with respect to the true amplitudes of
481 concentrations differences in the tidal cycle and in seasonality due to the fact that
482 differences in concentrations during falling and rising water levels were linearly interpolated.
483 These interpolated values are based on four to five measurements in the three export areas
484 and were conducted in different years. Consequently, the approach does not reproduce the
485 exact TA and DIC concentrations in the years 2001 to 2009, because only meteorological
486 forcing, river loads and nitrogen deposition were specified for these particular years. The
487 simulation of scenario B thus only approximates Wadden Sea export rates. More
488 measurements distributed with higher resolution over the annual cycle would clearly
489 improve our estimates. Nevertheless, the implementation of Wadden Sea export rates here
490 results in improved reproduction of observed high TA concentrations in the German Bight in
491 summer in comparison to the reference run A (Fig. 3).

492 We calculated the sensitivity of our modelled annual TA export rates on uncertainties of the
493 Δ -values of Table 1. As the different areas North- and East Frisian Wadden Sea and Jade Bay
494 has different exchange rates of water, for each region the uncertainty of 1 $\mu\text{mol kg}^{-1}$ in ΔTA
495 at all times has been calculated. The East Frisian Wadden Sea export would differ by
496 0.84 Gmol TA yr⁻¹, the Jade Bay export by 0.09 Gmol TA yr⁻¹ and the North Frisian export by
497 3 Gmol TA yr⁻¹.

498 Primary processes that contribute to the TA generation in the Wadden Sea are
499 denitrification, sulphate reduction, or processes that are coupled to sulphate reduction and
500 other processes (Thomas et al., 2009). In our model, the implemented benthic denitrification
501 does not generate TA (Seitzinger & Giblin, 1996), because modelled benthic denitrification
502 does not consume nitrate (Pätsch & Kühn, 2008). Benthic denitrification is coupled to

503 nitrification in the upper layer of the sediment (Raaphorst et al., 1990), giving reason for
504 neglecting TA generation by this process in the model. The modelled production of N_2 by
505 benthic denitrification falls in the range of 20 – 25 Gmol N yr^{-1} in the validation area, which
506 would result in a TA production of about 19 – 23 Gmol TA yr^{-1} (Brenner et al., 2016). In the
507 model nitrate uptake by phytoplankton produces about 40 Gmol TA yr^{-1} , which partly
508 compensates the missing TA generation by benthic denitrification. This amount of nitrate
509 would not fully be available for primary production if parts of it would be consumed by
510 denitrification. Different from this, the TA budget of Thomas et al. (2009) included estimates
511 for the entire benthic denitrification as a TA generating process.

512 Sulphate reduction (not modelled here) also contributes to alkalinity generation. On longer
513 time scales the net effect is vanishing as the major part of the reduced components are
514 immediately re-oxidised in contact with oxygen. Iron- and sulphate- reduction generates TA
515 but only their reaction product iron sulphide (essentially pyrite) conserves the reduced
516 components from re-oxidation. As the formation of pyrite consumes TA, the TA contribution
517 of iron reduction in the North Sea is assumed to be small and to balance that of pyrite
518 formation (Brenner et al., 2016).

519 Atmospheric nitrogen deposition is taken into account in the simulations. Oxidised N-species
520 (NO_x) dominate reduced species (NH_y) slightly in the validation area during 6 out of 9
521 simulation years. This implies that the deposition of dissolved inorganic nitrogen decreases
522 TA in 6 of 9 years. The average decrease within 6 years is about 0.4 Gmol TA yr^{-1} , whereas
523 the average increase within 3 years is only 0.1 Gmol TA yr^{-1} . Thomas et al. (2009) also
524 assumed a dominance of oxidised species and consequently defined a negative contribution
525 to the TA budget.

526 Dissolution of biogenic carbonates may be an efficient additional enhancement of the CO_2
527 buffer capacity (that is: source of TA), since most of the tidal flat surface sediments contain
528 carbonate shell debris (Hild, 1997). On the other hand, shallow oxidation of biogenic
529 methane formed in deep and shallow tidal flat sediments (not modelled) (Höpner &
530 Michaelis, 1994; Neira & Rackemann, 1996; Böttcher et al., 2007) has the potential to lower
531 the buffer capacity, thus counteracting or balancing the respective effect of carbonate
532 dissolution. The impact of methane oxidation on the developing TA / DIC ratio in surface

533 sediments, however, is complex and controlled by a number of superimposing
534 biogeochemical processes (e.g., Akam et al., 2020).

535 The net effect of evaporation and precipitation in the Wadden Sea also has to be considered
536 in budgeting TA. Although these processes are balanced in the North Sea (Schott, 1966),
537 enhanced evaporation can occur in the Wadden Sea due to increased heating during low
538 tide around noon. Onken & Riethmüller (2010) estimated an annual negative freshwater
539 budget in the Hörnum Basin based on long-term hydrographic time series from observations
540 in a tidal channel. From this data a mean salinity difference between flood and ebb currents
541 of approximately -0.02 is calculated. This would result in an increased TA concentration of
542 $1 \mu\text{mol TA kg}^{-1}$, which is within the range of the uncertainty of measurements. Furthermore,
543 the enhanced evaporation estimated from subtle salinity changes interferes with potential
544 input of submarine groundwater into the tidal basins, that been identified by Moore et al.
545 (2011), Winde et al. (2014), and Santos et al. (2015). The magnitude of this input is difficult
546 to estimate at present, for example from salinity differences between flood and ebb tides,
547 because the composition of SGD passing the sediment-water interfacial mixing zone has to
548 be known. Although first characteristics have been reported (Moore et al., 2011; Winde et
549 al., 2014; Santos et al., 2015), the quantitative effect of additional DIC, TA, and nutrient input
550 via both fresh and recirculated SGD into the Wadden Sea remains unclear.

551 An input of potential significance are small inlets that provide fresh water as well as DIC and
552 TA (Table 3). The current data base for seasonal dynamics of this source, however, is limited
553 and, therefore, this source cannot yet be considered quantitatively in budgeting approaches.

554

555 **4.2 TA / DIC ratios over the course of the year**

556

557

558 Ratios of TA and DIC generated in the tidal basins (Table 1) give some indication of the
559 dominant biogeochemical mineralisation and re-oxidation processes occurring in the
560 sediments of individual Wadden Sea sectors, although these processes have not been
561 explicitly modelled here (Chen & Wang, 1999; Zeebe & Wolf-Gladrow, 2001; Thomas et al.
562 2009; Sippo et al., 2016; Wurgaft et al., 2019; Akam et al., 2020). Candidate processes are
563 numerous and the export ratios certainly express various combinations, but the most

564 quantitatively relevant likely are aerobic degradation of organic material (resulting in a
565 reduction of TA due to nitrification of ammonia to nitrate with a TA / DIC ratio of -0.16),
566 denitrification (TA / DIC ratio of 0.8, see Rassmann et al., 2020), and anaerobic processes
567 related to sulphate reduction of organoclastic material (TA / DIC ratio of 1, see Sippo et al.,
568 2016). Other processes are aerobic (adding only DIC) and anaerobic (TA / DIC ratio of 2)
569 oxidation of upward diffusing methane, oxidation of sedimentary sulphides upon
570 resuspension into an aerated water column (no effect on TA / DIC) followed by oxidation of
571 iron (consuming TA), and nitrification of ammonium (consuming TA, TA / DIC ratio is -2, see
572 Pätsch et al., 2018 and Zhai et al. 2017).

573 The TA / DIC export ratios of DIC and TA for the individual tidal basins in three Wadden Sea
574 sectors (East Frisian, Jade Bay and North Frisian) as calculated from observed Δ TA and Δ DIC
575 over tidal cycles in different seasons are depicted in Fig. 9. They may give an indication of
576 regionally and seasonally varying processes occurring in the sediments of the three study
577 regions. The ratios vary between 0.2 and 0.5 in the North Frisian Wadden Sea with slightly
578 more TA than DIC generated in spring, summer and autumn, and winter having a negative
579 ratio of -0.5. The winter ratio coincides with very small measured differences of DIC in
580 imported and exported waters (Δ DIC = -2 $\mu\text{mol kg}^{-1}$) and the negative TA / DIC ratio may thus
581 be spurious. The range of ratios in the other seasons is consistent with sulphate reduction
582 and denitrification as the dominant processes in the North Frisian tidal basins.

583 The TA / DIC ratios in the Jade Bay samples were consistently higher than those in the North
584 Frisian tidal basin and vary between 1 and 2 in spring and summer, suggesting a significant
585 contribution by organoclastic sulphate reduction and anaerobic oxidation of methane
586 (Al-Raei et al., 2009). The negative ratio of -0.4 in autumn is difficult to explain with
587 remineralisation or re-oxidation processes, but as with the fall ratio in Frisian tidal basin, it
588 coincides with a small change in Δ DIC (-3 $\mu\text{mol kg}^{-1}$) at positive Δ TA (8 $\mu\text{mol kg}^{-1}$). Taken at
589 face value, the resulting negative ratio of -0.4 implicates a re-oxidation of pyrite, normally at
590 timescales of early diagenesis thermodynamically stable (Hu and Cai, 2011), possibly
591 promoted by increasing wind forces and associated aeration and sulphide oxidation of
592 anoxic sediment layers (Kowalski et al., 2013). The DIC export rate from Jade Bay had its
593 minimum in autumn, consistent with a limited supply and mineralisation of organic matter,
594 possibly modified by seasonally changing impacts from small tidal inlets (Table 3).

595 The TA / DIC ratio of the East Frisian Wadden Sea is in the approximate range of those in
596 Jade Bay, but has one unusually high ratio in November caused by a significant increase in TA
597 of $14 \mu\text{mol kg}^{-1}$ at a low increase of $5 \mu\text{mol kg}^{-1}$ in DIC. Barring an analytical artefact, the
598 maximum ratio of 3 may reflect a short-term effect of iron reduction.

599 Based on these results, processes in the North Frisian Wadden Sea export area differ from
600 the East Frisian Wadden Sea and the Jade Bay areas. The DIC export rates suggest that
601 significant amounts of organic matter were degraded in North Frisian tidal basins, possibly
602 controlled by higher daily exchanged water masses in the North Frisian ($8.1 \text{ km}^3 \text{ d}^{-1}$) than in
603 the East Frisian Wadden Sea ($2.3 \text{ km}^3 \text{ d}^{-1}$) and in the Jade Bay ($0.8 \text{ km}^3 \text{ d}^{-1}$) (compare
604 Table 2). On the other hand, TA export rates of the North Frisian and the East Frisian
605 Wadden Sea were in the same range.

606 Regional differences in organic matter mineralisation in the Wadden Sea have been
607 discussed by van Beusekom et al. (2012) and Kowalski et al. (2013) in the context of
608 connectivity with the open North Sea and influences of eutrophication and sedimentology.
609 They suggested that the organic matter turnover in the entire Wadden Sea is governed by
610 organic matter import from the North Sea, but that regionally different eutrophication
611 effects as well as sediment compositions modulate this general pattern. The reason for
612 regional differences may be related to the shape and size of the individual tidal basins. van
613 Beusekom et al. (2012) found that wider tidal basins with a large distance between barrier
614 islands and mainland, as is the case in the North Frisian Wadden Sea, generally have a lower
615 eutrophication status than narrower basins predominating in the East Frisian Wadden Sea.
616 Together with the high-water exchange rate the accumulation of organic matter is reduced
617 in the North Frisian Wadden Sea and the oxygen demand per volume is lower than in the
618 more narrow eutrophicated basins. Therefore, aerobic degradation of organic matter
619 dominated in the North Frisian Wadden Sea, where the distance between barrier islands and
620 mainland is large. This leads to less TA production (in relation to DIC production) than in the
621 East Frisian Wadden Sea, where anaerobic degradation of organic matter dominated in more
622 restricted tidal basins.

623

624 **4.3. TA budgets and variability of TA inventory in the German Bight**

625 Modelled TA and DIC concentrations in the German Bight have a high interannual and
626 seasonal variability (Fig. 8). The interannual variability of the model results are mainly driven
627 by the physical prescribed environment. Overall, the TA variability is more sensitive to
628 Wadden Sea export rates than DIC variability, because the latter is dominated by biological
629 processes. However, the inclusion of Wadden Sea DIC export rates improved
630 correspondence with observed DIC concentrations in the near-coastal North Sea.

631 It is a logical step to attribute the TA variability to variabilities of the different sources. In
632 order to calculate a realistic budget, scenario B was considered. Annual and seasonal
633 budgets of TA sources and sinks in this scenario are shown in Table 6. Note that Riv_{eff} is not
634 taken into account for the budget calculations. This is explained in the Method Section 2.2.2
635 “River Input”.

636 Comparing the absolute values of all sources and sinks of the mean year results in a relative
637 ranking of the processes. 41 % of all TA inventory changes in the validation area were due to
638 river loads, 37 % were due to net transport, 16 % were due to Wadden Sea export rates, 6 %
639 were due to internal processes. River input ranged from 78 to 152 Gmol TA yr⁻¹ and had the
640 highest absolute variability of all TA sources in the validation area. This is mostly due to the
641 high variability of annual freshwater discharge, which is indicated by low (negative) values of
642 Riv_{eff} . The latter values show that the riverine TA loads together with the freshwater flux
643 induce a small dilution of TA in the validation area for each year. Certainly, this ranking
644 depends mainly on the characteristics of the Elbe estuary. Due to the high concentration of
645 TA in rivers Rhine and Meuse (Netherlands) they had an effective river input of
646 +24 Gmol TA yr⁻¹ in 2008, which constitutes a much greater impact on TA concentration
647 changes than the Elbe river. In a sensitivity test, we switched off the TA loads of rivers Rhine
648 and Meuse for the year 2008 and found that the net flow of -71 Gmol TA yr⁻¹ decreased to
649 -80 Gmol TA yr⁻¹, which indicates that water entering the validation box from the western
650 boundary is less TA-rich in the test case than in the reference run.

651 At seasonal time scales (Table 6 lower part) the net transport dominated the variations from
652 October to March, while internal processes play a more important role from April to June
653 (28 %). The impact of effective river input was less than 5 % in every quarter. The Wadden
654 Sea TA export rates had an impact of 36 % on TA mass changes in the validation area from

655 July to September. Note that these percentages are related to the sum of the absolute
656 values of the budgeting terms.

657 Summing up the sources and sinks, Wadden Sea exchange rates, internal processes and
658 effective river loads resulted in highest sums in 2002 and 2003 (51 and 52 Gmol TA yr⁻¹) and
659 lowest in 2009 (44 Gmol TA yr⁻¹). For the consideration of TA variation we excluded net
660 transport and actual river loads, because these fluxes are diluted and do not necessarily
661 change the TA concentrations. In agreement with this, the highest TA concentrations were
662 simulated in summer 2003 (Fig. 8). The high interannual variability of summer
663 concentrations was driven essentially by hydrodynamic differences between the years.
664 Flushing times and their interannual variability were higher in summer than in winter (Fig. 6)
665 of every year. High flushing times or less strong circulation do have an accumulating effect
666 on exported TA in the validation area. To understand the reasons of the different flushing
667 times monthly stream patterns were analysed (Fig. 7). Distinct anticlockwise stream patterns
668 defined the hydrodynamic conditions in every winter. Summer stream patterns were in most
669 years weaker, especially in the German Bight (compare Fig. 7, June 2003). In August 2003 the
670 eastern part of the German Bight shows a clockwise rotation, which transports TA-enriched
671 water from July back to the Wadden-Sea area for further enrichment. This could explain the
672 highest concentrations in summer 2003.

673 Thomas et al. (2009) estimated that 73 Gmol TA yr⁻¹ were produced in the Wadden Sea.
674 Their calculations were based on measurements in 2001 and 2002. The presented model
675 was validated with data measured in August 2008 (Salt et al., 2013) at the same positions.
676 High TA concentrations in the German Bight were observed in summer 2001 and in summer
677 2008. Due to the scarcity of data, the West Frisian Wadden Sea was not considered in the
678 simulations, but, as the western area is much larger than the eastern area, the amount of
679 exported TA from that area can be assumed to be in the same range as from the East Frisian
680 Wadden Sea (10 to 14 Gmol TA yr⁻¹). With additional export from the West Frisian Wadden
681 Sea, the maximum overall Wadden Sea export may be as high as 53 Gmol TA yr⁻¹. Thus, the
682 TA export from the Wadden Sea calculated in this study is 20 to 34 Gmol TA yr⁻¹ lower than
683 that assumed in the study of Thomas et al. (2009). This is mainly due to the flushing time
684 that was assumed by Thomas et al. (2009). They considered the water masses to be flushed
685 within six weeks (Lenhart et al., 1995). Flushing times calculated in the present study were

686 significantly longer and more variable in summer. Since the Wadden Sea export calculated
687 by Thomas et al. (2009) was defined as a closing term for the TA budget, underestimated
688 summerly flushing times led to an overestimation of the exchange with the adjacent North
689 Sea.

690 Table 4 shows that our scenario B underestimates the observed TA concentration by about
691 $5.1 \mu\text{mol kg}^{-1}$ in 2008. Scenario A has lower TA concentration than scenario B in the
692 validation area. The difference is about $11 \mu\text{mol kg}^{-1}$. This means that the Wadden Sea
693 export of $39 \text{ Gmol TA yr}^{-1}$ results in a concentration difference of $11 \mu\text{mol kg}^{-1}$. Assuming
694 linearity, the deviation between scenario B and the observations ($5.1 \mu\text{mol kg}^{-1}$) would be
695 compensated by an additional Wadden Sea export of about $18 \text{ Gmol TA yr}^{-1}$. If we assume
696 that the deviation between observation and scenario B is entirely due to uncertainties or
697 errors in the Wadden Sea export estimate, then the uncertainty of this export is
698 $18 \text{ Gmol TA yr}^{-1}$.

699 Another problematic aspect in the TA export estimate by Thomas et al. (2009) is the fact that
700 their TA budget merges the sources of anaerobic TA generation from sediment and from the
701 Wadden Sea into a single source “anaerobic processes in the Wadden Sea”. Burt et al. (2014)
702 found a sediment TA generation of $12 \text{ mmol TA m}^{-2} \text{ d}^{-1}$ at one station in the German Bight
703 based on Ra-measurements. This fits into the range of microbial gross sulphate reduction
704 rates reported by Al-Raei et al. (2009) in the back-barrier tidal areas of Spiekeroog island,
705 and by Brenner et al. (2016) at the Dutch coast. Within the latter paper, the different
706 sources of TA from the sediment were quantified. The largest term was benthic calcite
707 dissolution, which would be cancelled out in terms of TA generation assuming a steady-state
708 compensation by biogenic calcite production. Extrapolating the southern North Sea TA
709 generation (without calcite dissolution) from the data for one station of Brenner et al. (2016)
710 results in an annual TA production of 12.2 Gmol in the German Bight (Area = 28.415 km^2).
711 This is likely an upper limit of sediment TA generation, as the measurements were done in
712 summer when seasonal fluxes are maximal. This calculation reduces the annual Wadden Sea
713 TA generation estimated by Thomas et al. (2009) from 73 to 61 Gmol , which is still higher
714 than our present estimate. In spite of the unidentified additional TA-fluxes, both the
715 estimate by Thomas et al. (2009) and our present model-based quantification confirm the

716 importance of the Wadden-Sea export fluxes of TA on the North Sea carbonate system at
717 present and in the future.

718 ***4.4 The impact of exported TA and DIC on the North Sea and influences on export*** 719 ***magnitude***

720 Observed high TA and DIC concentrations in the SE North Sea are mainly caused by TA and
721 DIC export from the Wadden Sea (Fig. 3-5). TA concentrations could be better reproduced
722 than DIC concentrations in the model experiments, which was mainly due to the higher
723 sensitivity of DIC to modelled biology. Nevertheless, from a present point of view the
724 Wadden Sea is the main driver of TA concentrations in the German Bight. Future forecast
725 studies of the evolution of the carbonate system in the German Bight will have to specifically
726 focus on the Wadden Sea and on processes occurring there. In this context the Wadden Sea
727 evolution during future sea level rise is the most important factor. The balance between
728 sediment supply from the North Sea and sea level rise is a general precondition for the
729 persistence of the Wadden Sea (Flemming and Davis, 1994; van Koningsveld et al., 2008). An
730 accelerating sea level rise could lead to a deficient sediment supply from the North Sea and
731 shift the balance at first in the largest tidal basins and at last in the smallest basins. (CPSL,
732 2001; van Goor et al., 2003). The share of intertidal flats as potential sedimentation areas is
733 larger in smaller tidal basins (van Beusekom et al., 2012), whereas larger basins have a larger
734 share of subtidal areas. Thus, assuming an accelerating sea level rise, large tidal basins will
735 turn into lagoons, while tidal flats may still exist in smaller tidal basins. This effect could
736 decrease the overall Wadden Sea export rates of TA, because sediments would no longer be
737 exposed to the atmosphere and the products of sulphate reduction would re-oxidise in the
738 water column. Moreover, benthic-pelagic exchange in the former intertidal flats would be
739 more diffusive and less advective than today due to a lowering of the hydraulic gradients
740 during ebb tides, when parts of the sediment become unsaturated with water. This would
741 decrease TA export into the North Sea. Caused by changes in hydrography and sea level the
742 sedimentological composition may also change. If sediments become more sandy, aerobic
743 degradation of organic matter is likely to become more important (de Beer et al., 2005). In
744 fine grained silt diffusive transport plays a key role, while in the upper layer of coarse (sandy)
745 sediments advection is the dominant process. Regionally, the North Frisian Wadden Sea will

746 be more affected by rising sea level because there the tidal basins are larger than the tidal
747 basins in the East Frisian Wadden Sea and even larger than the inner Jade Bay.

748 The Wadden Sea export of TA and DIC is driven by the turnover of organic material.
749 Decreasing anthropogenic eutrophication can lead to decreasing phytoplankton biomass and
750 production (Cadée & Hegeman, 2002; van Beusekom et al., 2009). Thus, the natural
751 variability of the North Sea primary production becomes more important in determining the
752 organic matter turnover in the Wadden Sea (McQuatters-Gollop et al., 2007; McQuatters-
753 Gollop & Vermaat, 2011). pH values in Dutch coastal waters decreased from 1990 to 2006
754 drastically. Changes in nutrient variability were identified as possible drivers (Provoost et al.,
755 2010), which is consistent with model simulations by Borges and Gypens (2010). Moreover,
756 despite the assumption of decreasing overall TA export rates from the Wadden Sea the
757 impact of the North Frisian Wadden Sea on the carbonate system of the German Bight could
758 potentially adjust to a change of tidal prisms and thus a modulation in imported organic
759 matter. If less organic matter is remineralised in the North Frisian Wadden Sea, less TA and
760 DIC will be exported into the North Sea.

761 In the context of climate change, processes that have impact on the freshwater budget of
762 tidal mud flats will gain in importance. Future climate change will have an impact in coastal
763 hydrology due to changes in ground water formation rates (Faneca Sánchez et al., 2012;
764 Sulzbacher et al., 2012), that may change both surface and subterranean run-off into the
765 North Sea. An increasing discharge of small rivers and groundwater into the Wadden Sea is
766 likely to increase DIC, TA, and possibly nutrient loads and may enhance the production of
767 organic matter. Evaporation could also increase due to increased warming and become a
768 more important process than today (Onken & Riethmüller, 2010), as will methane cycling
769 change due to nutrient changes, sea level and temperature rise (e.g., Höpner and Michaelis,
770 1994; Akam et al., 2020).

771 Concluding, in the course of climate change the North Frisian Wadden Sea will be affected
772 first by sea level rise, which will result in decreased TA and DIC export rates due to less
773 turnover of organic matter there. This could lead to a decreased buffering capacity in the
774 German Bight for atmospheric CO₂. Overall, less organic matter will be remineralised in the
775 Wadden Sea.

776

777

778 **5 Conclusion and Outlook**

779

780 We present a budget calculation of TA sources in the German Bight and relate 16 % of the
781 annual TA inventory changes to TA exports from the Wadden Sea. The impact of riverine
782 bulk TA seems to be less important due to the comparatively low TA concentrations in the
783 Elbe estuary, a finding that has to be proven by future research.

784 The evolution of the carbonate system in the German Bight under future changes depends
785 on the development of the Wadden Sea. The amount of TA and DIC that is exported from
786 the Wadden Sea depends on the amount of organic matter and / or nutrient that are
787 imported from the North Sea and finally remineralised in the Wadden Sea. Decreasing
788 riverine nutrient loads led to decreasing phytoplankton biomass and production (Cadée &
789 Hegeman, 2002; van Beusekom et al., 2009), a trend that is expected to continue in the
790 future (European Water Framework Directive). However, altered natural dynamics of
791 nutrient cycling and productivity can override the decreasing riverine nutrient loads (van
792 Beusekom et al., 2012), but these will not generate TA in the magnitude of denitrification of
793 river-borne nitrate.

794 Sea level rise in the North Frisian Wadden Sea will potentially be more affected by a loss of
795 intertidal areas than the East Frisian Wadden Sea (van Beusekom et al., 2012). This effect will
796 likely reduce the turnover of organic material in this region of the Wadden Sea, which may
797 decrease TA production and transfer into the southern North Sea.

798 Thomas et al. (2009) estimated that the Wadden Sea facilitates approximately 7 – 10% of the
799 annual CO₂ uptake of the North Sea. This is motivation for model studies on the future role
800 of the Wadden Sea in the CO₂ balance of the North Sea under regional climate change.

801 Future research will also have to address the composition and amount of submarine ground
802 water discharge, as well as the magnitude and seasonal dynamics in discharge and
803 composition of small water inlets at the coast, which are in this study only implicitly included
804 and in other studies mostly ignored due to a lacking data base.

805 **Data availability**

806 The river data are available at https://wiki.cen.uni-hamburg.de/ifm/ECOHAM/DATA_RIVER
807 and www.waterbase.nl. Meteorological data are stored at <https://psl.noaa.gov/>. The North
808 Sea TA and DIC data are stored at <https://doi.org/10.1594/PANGAEA.438791> (2001),
809 <https://doi.org/10.1594/PANGAEA.441686> (2005). The data of the North Sea cruise 2008
810 have not been published, yet, but can be requested via the CODIS data portal
811 (<http://www.nioz.nl/portals-en>; registration required). Additional Wadden Sea TA and DIC
812 data are deposited under doi:10.1594/PANGAEA.841976.

813

814 **Author contributions**

815 The scientific concept for this study was originally developed by JP and MEB. FS wrote the
816 basic manuscript as part of his PhD thesis. VW provided field analytical data, as part of her
817 PhD thesis. JP developed the original text further with contributions from all co-authors.

818 **Competing interests**

819 The authors declare that they have no conflict of interest.

820

821 **Acknowledgements**

822 The authors appreciate the two constructive reviews, which greatly helped to improve the
823 manuscript, and the editorial handling by Jack Middelburg. I. Lorkowski, W. Kühn, and F.
824 Große are acknowledged for stimulating discussions, S. Grashorn for providing tidal prisms
825 and P. Escher for laboratory support. This work was financially supported by BMBF during
826 the Joint Research Project BIOACID (TP 5.1, 03F0608L and TP 3.4.1, 03F0608F), with further
827 support from Leibniz Institute for Baltic Sea Research. We also acknowledge the support by
828 the Cluster of Excellence 'CliSAP' (EXC177), University of Hamburg, funded by the German
829 Science Foundation (DFG) and the support by the German Academic Exchange service
830 (DAAD, MOPGA-GRI, #57429828) with funds of the German Federal Ministry of Education
831 and Research (BMBF). We used NCEP Reanalysis data provided by the NOAA/OAR/ESRL
832 PSL, Boulder, Colorado, USA, from their Web site at <https://psl.noaa.gov/>.

833

834

835

836 **Tables**

837 **Table 1: Mean TA and DIC concentrations [$\mu\text{mol l}^{-1}$] during rising and falling water levels**
 838 **and the respective differences (Δ -values) that were used as wad_sta in (1). Areas are the**
 839 **North Frisian (N), the East Frisian (E) Wadden Sea and the Jade Bay (J).**

Area	Date	TA (rising)	TA (falling)	Δ TA	DIC (rising)	DIC (falling)	Δ DIC
N	29.04.2009	2343	2355	12	2082*	2106	24
	17.06.2009	2328	2332	4	2170	2190	20
	26.08.2009	2238	2252	14	2077	2105	28
	05.11.2009	2335	2333	-2	2205	2209	4
J	20.01.2010	2429	2443	14	2380	2392	12
	21.04.2010	2415	2448	33	2099	2132	33
	26.07.2010	2424	2485	61	2159	2187	28
	09.11.2010	2402	2399	-3	2302	2310	8
E	03.03.2010	2379	2393	14	2313	2328	15
	07.04.2010	2346	2342	-4	2068	2082	14
	17./18.05.2011	2445	2451	6	2209	2221	12
	20.08.2002	2377	2414	37	2010	2030	20
	01.11.2010	2423	2439	16	2293	2298	5

840 *: This value was estimated.

841

842 **Table 2: Daily Wadden Sea runoff to the North Sea at different export areas.**

Position	wad_exc [$10^6 \text{ m}^3 \text{ d}^{-1}$]
N1	273
N2	1225
N3	1416
N4	1128
N5	4038
N6	18
J1 - J3	251
E1	380
E2	634
E3	437
E4	857

843

844

845

846 **Table 3: Examples for the carbonate system composition of small fresh water inlets**
 847 **draining into the Jade Bay and the backbarrier tidal area of Spiekeroog Island, given in**
 848 **($\mu\text{mol kg}^{-1}$). Autumn results (A) (October 31st, 2010) are taken from Winde et al. (2014);**
 849 **spring sampling (S) took place on May 20th, 2011.**

Site	Position	DIC(A)	TA(A)	DIC(S)	TA(S)
Neuharlingersiel	53°41.944 N 7°42.170 E	2319	1773	1915	1878
Harlesiel	53°42.376 N 7°48.538 E	3651	3183	1939	1983
Wanger- /Horumersiel	53°41.015 N 8°1.170 E	5405	4880	6270	6602
Hooksiel	53°38.421 N 8°4.805 E	2875	3105	3035	3302
Maade	53°33.534 N 8°7.082 E	5047	4448	5960	6228
Mariensiel	53°30.895 N 8°2.873 E	6455	5904	3665	3536
Dangaster Siel	53°26.737N 8°6.577 E	1868	1246	1647	1498
Wappellersiel	53°23.414 N 8°12.437 E	1373	630	1358	1152
Schweiburger Siel	53°24.725 N 8°16.968 E	4397	3579	4656	4493
Eckenwarder Siel	53°31.249 N 8°16.527 E	6542	6050	2119	4005

850

851

852

853

854

855 **Table 4: Averages ($\mu\text{mol kg}^{-1}$), standard deviations ($\mu\text{mol kg}^{-1}$), RMSE ($\mu\text{mol kg}^{-1}$), and**
856 **correlation coefficients r for the observed TA concentrations and the corresponding**
857 **scenarios A and B within the validation area.**

TA	Average	Stdv	RMSE	r
Obs 2008	2333.52	32.51		
Obs 2005	2332.09	21.69		
Obs 2001	2333.83	33.19		
Sim A 2008	2327.64	6.84	27.97	0.77
Sim A 2005	2322.16	5.21	22.05	0.45
Sim A 2001	2329.79	5.32	31.89	0.24
Sim B 2008	2338.60	22.09	18.34	0.86
Sim B 2005	2339.48	26.81	31.81	0.18
Sim B 2001	2342.96	17.28	30.07	0.47

858

859

860

861

862

863

864

865

866

867

868

869

870

871 **Table 5: Averages ($\mu\text{mol kg}^{-1}$), standard deviations ($\mu\text{mol kg}^{-1}$), RMSE ($\mu\text{mol kg}^{-1}$), and**
872 **correlation coefficients r for the observed DIC concentrations and the corresponding**
873 **scenarios A and B within the validation area.**

874

DIC	Average	Stdv	RMSE	r
Obs 2008	2107.05	24.23		
Obs 2005	2098.20	33.42		
Obs 2001	2105.49	25.21		
Sim A 2008	2080.93	14.24	43.48	-0.64
Sim A 2005	2083.53	21.94	26.97	0.73
Sim A 2001	2077.53	17.61	38.89	0.22
Sim B 2008	2091.15	9.25	25.87	0.55
Sim B 2005	2101.26	10.97	33.96	0.10
Sim B 2001	2092.69	11.71	25.33	0.48

875

876

877

878

879

880

881

882

883

884

885 **Table 6: Annual TA budgets in the validation area of the years 2001 to 2009, annual**
886 **averages and seasonal budgets of January to March, April to June, July to September and**
887 **October to December [Gmol]. Net Flow is the annual net TA transport across the**
888 **boundaries of the validation area. Negative values indicate a net export from the**
889 **validation area to the adjacent North Sea. Δ content indicates the difference of the TA**
890 **contents between the last and the first time steps of the simulated year or quarter.**

	Wadden Sea export Gmol/yr	internal processes Gmol/yr	river loads Gmol/yr	Riv _{eff} Gmol/yr	net flow Gmol/yr	Δ content Gmol
2001	39	13	87	-5	38	177
2002	39	19	152	-7	-223	-13
2003	39	16	91	-3	-98	48
2004	39	13	78	-5	-8	122
2005	39	12	89	-5	-98	42
2006	39	12	88	-4	-56	83
2007	39	12	110	-5	-132	29
2008	39	14	93	-5	-71	75
2009	39	10	83	-5	-151	-19
Average	Gmol/yr 39	Gmol/yr 14	Gmol/yr 101	Gmol/yr -5	Gmol/yr -89	Gmol 65
t = 3 mon	Gmol/t	Gmol/t	Gmol/t	Gmol/t	Gmol/t	Gmol
Jan - Mar	7	-1	38	-1	-49	-5
Apr - Jun	10	15	23	-2	6	54
Jul - Sep	17	-2	15	-2	13	43
Oct - Dec	4	1	25	0	-56	-26

891 **6. Figure Captions**

892

893 Figure 1: Upper panel: Map of the south-eastern North Sea and the bordering land. Lower
894 panel: Model domains of ECOHAM (red) and FVCOM (blue), positions of rivers 1 – 16 (left,
895 see Table 2) and the Wadden Sea export areas grid cells (right). The magenta edges identify
896 the validation area, western and eastern part separated by the magenta dashed line.

897 Figure 2: Monthly Wadden Sea export of DIC and TA [Gmol mon^{-1}] at the North Frisian
898 coast (N), East Frisian coast (E) and the Jade Bay in scenario B. The export rates were
899 calculated for DIC and TA based on measured concentrations and simulated water fluxes.

900 Figure 3: Surface TA concentrations [$\mu\text{mol TA kg}^{-1}$] in August 2008 observed (a) and
901 simulated with scenario A (b) and B (c). The black lines indicate the validation box.

902 Figure 4: Differences between TA surface summer observations and results from
903 scenario A (a) and B (b) and the differences between DIC surface observations and results
904 from scenario A (c) and B (d), all in $\mu\text{mol kg}^{-1}$. The black lines indicate the validation box.

905 Figure 5: Surface DIC concentrations [$\mu\text{mol DIC kg}^{-1}$] in August 2008 observed (a) and
906 simulated with scenario A (b) and B (c). The black lines indicate the validation box.

907 Figure 6: Flushing times in the validation area in summer (June to August) and winter
908 (January to March). The whole validation area is represented in blue, green is the western
909 part of the validation area (4.5° E to 7° E) and red is the eastern part (east of 7° E).

910 Figure 7: Monthly mean simulated streamlines for summer months 2003 and 2008.

911 Figure 8: Simulated monthly mean concentrations of TA (scenario A (a), scenario B (b))
912 [$\mu\text{mol TA kg}^{-1}$] and DIC (scenario A (c), scenario B (d)) [$\mu\text{mol DIC kg}^{-1}$] in the validation area
913 for the years 2001-2009.

914 Figure 9: Temporally interpolated TA/DIC ratio of the export rates in the North Frisian, East
915 Frisian, and Jade Bay. These ratios are calculated using the Δ -values of Table 1.

916

917

918 **7. References**

919

920 Akam, S.A., Coffin, R.B., Abdulla, H.A.N., and Lyons T.W.: Dissolved inorganic carbon pump in
921 methane-charged shallow marine sediments: State of the art and new model perspectives.
922 *Frontiers in Marine Sciences* 7, 206, DOI: 10.3389/FMARS.2020.00206, 2020.

923 Al-Raei, A.M., Bosselmann, K., Böttcher, M.E., Hespeneide, B., and Tauber, F.: Seasonal
924 dynamics of microbial sulfate reduction in temperate intertidal surface sediments: Controls
925 by temperature and organic matter. *Ocean Dynamics* 59, 351-370, 2009.

926 Amann, T., Weiss, A., and Hartmann, J.: Inorganic Carbon Fluxes in the Inner Elbe Estuary,
927 Germany, *Estuaries and Coasts* 38(1), 192-210, doi:10.1007/s12237-014-9785-6, 2015.

928

929 Artioli, Y., Blackford, J. C., Butenschön, M., Holt, J. T., Wakelin, S. L., Thomas, H., Borges, A.
930 V., and Allen, J. I.: The carbonate system in the North Sea: Sensitivity and model validation,
931 *Journal of Marine Systems*, 102-104, 1-13, doi:10.1016/j.jmarsys.2012.04.006, 2012.

932

933 Backhaus, J.O.: A three-dimensional model for the simulation of shelf sea dynamics, *Ocean*
934 *Dynamics*, 38(4), 165–187, doi:10.1016/0278-4343(84)90044-X, 1985.

935

936 Backhaus, J.O., and Hainbucher, D.: A finite difference general circulation model for shelf
937 seas and its application to low frequency variability on the North European Shelf, Elsevier
938 *Oceanography Series*, 45, 221–244, doi:10.1016/S0422-9894(08)70450-1, 1987.

939

940 Ben-Yaakov, S.: pH BUFFERING OF PORE WATER OF RECENT ANOXIC MARINE SEDIMENTS,
941 *Limnology and Oceanography*, 18, doi: 10.4319/lo.1973.18.1.0086, 1973.

942

943 Berner, R. A., Scott, M. R., and Thomlinson, C.: Carbonate alkalinity in the pore waters of
944 anoxic marine sediments. *Limnology & Oceanography*, 15, 544–549,
945 doi:10.4319/lo.1970.15.4.0544, 1970.

946

947 Billerbeck, M., Werner, U., Polerecky, L., Walpersdorf, E., de Beer, D., and Hüttel, M.:
948 Surficial and deep pore water circulation governs spatial and temporal scales of nutrient
949 recycling in intertidal sand flat sediment. *Mar Ecol Prog Ser* 326, 61-76, 2006.
950

951 Böttcher, M.E., Al-Raei, A.M., Hilker, Y., Heuer, V., Hinrichs, K.-U., and Segl, M.: Methane and
952 organic matter as sources for excess carbon dioxide in intertidal surface sands:
953 Biogeochemical and stable isotope evidence. *Geochimica et Cosmochim Acta* 71, A111,
954 2007.
955

956 Böttcher, M.E., Hespeneide, B., Brumsack, H.-J., and Bosselmann, K.: Stable isotope
957 biogeochemistry of the sulfur cycle in modern marine sediments: I. Seasonal dynamics in a
958 temperate intertidal sandy surface sediment. *Isotopes Environ. Health Stud.* 40, 267-283,
959 2004.
960

961 Borges, A. V.: Present day carbon dioxide fluxes in the coastal ocean and possible feedbacks
962 under global change, In *Oceans and the atmospheric carbon content* (P.M. da Silva Duarte &
963 J.M. Santana Casiano Eds), Chapter 3, 47-77, doi:10.1007/978-90-481-9821-4, 2011.
964

965 Borges, A. V. and Gypens, N.: Carbonate chemistry in the coastal zone responds more
966 strongly to eutrophication than to ocean acidification. *Limn. Oceanogr.* 55(1): 346-353, 2010.
967

968 Brasse, J., Reimer, A., Seifert, R., and Michaelis, W.: The influence of intertidal mudflats on
969 the dissolved inorganic carbon and total alkalinity distribution in the German Bight,
970 southeastern North Sea, *J. Sea Res.* 42, 93-103, doi: 10.1016/S1385-1101(99)00020-9, 1999.
971

972 Brenner, H., Braeckman, U., Le Guitton, M., and Meysman, F. J. R.: The impact of
973 sedimentary alkalinity release on the water column CO₂ system in the North Sea,
974 *Biogeosciences*, 13(3), 841-863, doi:10.5194/bg-13-841-2016, 2016.
975

976 Burt, W. J., Thomas, H., Pätsch, J., Omar, A. M., Schrum, C., Daewel, U., Brenner, H., and de
977 Baar, H. J. W.: Radium isotopes as a tracer of sediment-water column exchange in the North
978 Sea, *Global Biogeochemical Cycles* 28, pp 19, doi:10.1002/2014GB004825, 2014.

979

980 Burt, W. J., Thomas, H., Hagens, M., Pätsch, J., Clargo, N. M., Salt, L. A., Winde, V., and
981 Böttcher, M. E.: Carbon sources in the North Sea evaluated by means of radium and stable
982 carbon isotope tracers, *Limnology and Oceanography*, 61(2), 666-683,
983 doi:10.1002/lno.10243, 2016.

984

985 Cadée, G. C., and Hegeman, J.: Phytoplankton in the Marsdiep at the end of the 20th century;
986 30 years monitoring biomass, primary production, and Phaeocystis blooms, *J. Sea Res.* 48,
987 97-110, doi:10.1016/S1385-1101(02)00161-2, 2002.

988

989 Cai, W.-J., Hu, X., Huang, W.-J., Jiang, L.-Q., Wang, Y., Peng, T.-H., and Zhang, X.: Surface
990 ocean alkalinity distribution in the western North Atlantic Ocean margins, *Journal of*
991 *Geophysical Research*, 115, C08014, doi:10.1029/2009JC005482, 2010.

992

993 Carvalho, A. C. O., Marins, R. V., Dias, F. J. S., Rezende, C. E., Lefèvre, N., Cavalcante, M. S.,
994 and Eschrique, S. A.: Air-sea CO₂ fluxes for the Brazilian northeast continental shelf in a
995 climatic transition region, *Journal of Marine Systems*, 173, 70-80,
996 doi:10.1016/j.jmarsys.2017.04.009, 2017.

997

998 Chambers, R. M., Hollibaugh, J. T., and Vink, S. M.: Sulfate reduction and sediment
999 metabolism in Tomales Bay, California, *Biogeochemistry*, 25, 1–18, doi:10.1007/BF00000509,
1000 1994.

1001

1002 Chen, C.-T. A., and Wang, S.-L.: Carbon, alkalinity and nutrient budgets on the East China Sea
1003 continental shelf. *Journal of Geophysical Research*, 104, 20,675–20,686,
1004 doi:10.1029/1999JC900055, 1999.

1005

1006 Chen, C., Liu, H., and Beardsley, R. C.: An Unstructured Grid, Finite-Volume, Three-
1007 Dimensional, Primitive Equations Ocean Model: Application to Coastal Ocean and Estuaries, *J*
1008 *Atmos Oceanic Technol*, 20 (1), 159-186,
1009 doi:10.1175/1520-0426(2003)020<0159:AUGFVT>2.0.CO;2, 2003.

1010

1011 CPSL. Final Report of the Trilateral Working Group on Coastal Protection and Sea Level Rise.
1012 Wadden Sea Ecosystem No. 13. Common Wadden Sea Secretariat, Wilhelmshaven,
1013 Germany. 2001.
1014
1015 de Beer, D., Wenzhöfer, F., Ferdelman, T.G., Boehme, S., Huettel, M., van Beusekom, J.,
1016 Böttcher, M.E., Musat, N., Dubilier, N.: Transport and mineralization rates in North Sea sandy
1017 intertidal sediments (Sylt-Rømø Basin, Waddensea). *Limnol. Oceanogr.* 50, 113-127, 2005.
1018
1019 Dickson, A.G., Afghan, J.D., Anderson, G.C.: Reference materials for oceanic CO₂ analysis: a
1020 method for the certification of total alkalinity. *Marine Chemistry* 80, 185-197, 2003.
1021
1022 Dollar, S. J., Smith, S. V., Vink, S. M., Obrebski, S., and Hollibaugh, J.T.: Annual cycle of
1023 benthic nutrient fluxes in Tomales Bay, California, and contribution of the benthos to total
1024 ecosystem metabolism, *Marine Ecology Progress Series*, 79, 115–125,
1025 doi:10.3354/meps079115, 1991.
1026
1027 Duarte, C. M., Hendriks, I. E., Moore, T. S., Olsen, Y. S., Steckbauer, A., Ramajo, L.,
1028 Carstensen, J., Trotter, J. A., and McCulloch, M. Is Ocean Acidification an Open-Ocean
1029 Syndrome? Understanding Anthropogenic Impacts on Seawater pH. *Estuaries and Coasts*
1030 36(2): 221-236. 2013.
1031
1032 Ehlers, J.: Geomorphologie und Hydrologie des Wattenmeeres. In: Lozan, J.L., Rachor, E., Von
1033 Westernhagen, H., Lenz, W. (Eds.), *Warnsignale aus dem Wattenmeer*. Blackwell
1034 Wissenschaftsverlag, Berlin, pp. 1–11. 1994.
1035
1036 Faneca Sánchez, M., Gunnink, J. L., van Baaren, E. S., Oude Essink, G. H. P., Siemon, B.,
1037 Auken, E., Elderhorst, W., de Louw, P. G. B.: Modelling climate change effects on a Dutch
1038 coastal groundwater system using airborne electromagnetic measurements. *Hydrol. Earth*
1039 *Syst. Sci.* 16(12), 4499-4516, 2012.
1040
1041 Flemming, B. W., and Davis, R. A. J.: Holocene evolution, morphodynamics and

1042 sedimentology of the Spiekeroog barrier island system (southern North Sea). *Senckenb.*
1043 *Marit.* 25, 117-155, 1994.

1044

1045 Große, F., Kreuz, M., Lenhart, H.-J., Pätsch, J., and Pohlmann, T.: A Novel Modeling Approach
1046 to Quantify the Influence of Nitrogen Inputs on the Oxygen Dynamics of the North Sea,
1047 *Frontiers in Marine Science* 4(383), pp 21, doi:10.3389/fmars.2017.00383, 2017.

1048

1049 Grashorn, S., Lettmann, K. A., Wolff, J.-O., Badewien, T. H., and Stanev, E. V.: East Frisian
1050 Wadden Sea hydrodynamics and wave effects in an unstructured-grid model, *Ocean*
1051 *Dynamics* 65(3), 419-434, doi:10.1007/s10236-014-0807-5, 2015.

1052

1053 Gustafsson, E., Hagens, M., Sun, X., Reed, D. C., Humborg, C., Slomp, C. P., Gustafsson, B. G.:
1054 Sedimentary alkalinity generation and long-term alkalinity development in the Baltic Sea.
1055 *Biogeosciences* 16(2): 437-456, 2019.

1056 HASEC: OSPAR Convention for the Protection of the Marine Environment of the North-East
1057 Atlantic. Meeting of the Hazardous Substances and Eutrophication Committee (HASEC), Oslo
1058 27 February – 2 March 2012.

1059

1060 Hild, A.: Geochemie der Sedimente und Schwebstoffe im Rückseitenwatt von Spiekeroog
1061 und ihre Beeinflussung durch biologische Aktivität. *Forschungszentrum Terramare Berichte*
1062 5, 71 pp., 1997.

1063 Höpner, T., and Michaelis, H.: Sogenannte ‚Schwarze Flecken‘ – ein Eutrophierungssymptom
1064 des Wattenmeeres. In: L. Lozán, E. Rachor, K. Reise, H. von Westernhagen und W. Lenz.
1065 *Warnsignale aus dem Wattenmeer*. Berlin: Blackwell, 153-159, 1997.

1066

1067 Hoppema, J. M. J.; The distribution and seasonal variation of alkalinity in the southern bight
1068 of the North Sea and in the western Wadden Sea, *Netherlands Journal of Sea Research*, 26
1069 (1), 11-23, doi: 10.1016/0077-7579(90)90053-J, 1990.

1070

1071 Hu, X. and Cai, W.-J.: An assessment of ocean margin anaerobic processes on oceanic
1072 alkalinity budget. *Global Biogeochemical Cycles* 25: 1-11, 2011.

1073

1074 Johannsen, A., Dähnke, K., and Emeis, K.-C.: Isotopic composition of nitrate in five German
1075 rivers discharging into the North Sea, *Organic Geochemistry*, 39, 1678-1689
1076 doi:10.1016/j.orggeochem.2008.03.004, 2008.

1077

1078 Johnson, K.M., Wills, K.D., Buttler, D.B., Johnson, W.K., and Wong, C.S.: Coulometric total
1079 carbon dioxide analysis for marine studies: maximizing the performance of an automated
1080 gas extraction system and coulometric detector. *Marine Chemistry* 44, 167-187, 1993.

1081

1082 Kalnay, E., Kanamitsu, M., Kistler, R., Collins, W., Deaven, D., Gandin, L., Iredell, M., Saha S.,
1083 White, G., Woollen, J., Zhu, Y., Chelliah, M., Ebisuzaki, W., Higgins, W., Janowiak, J., Mo, K.C.,
1084 Ropelewski, C., Wang, J., Leetmaa, A., Reynolds, R., Jenne, R., and Joseph, D.: The
1085 NCEP/NCAR 40-year reanalysis project, *Bulletin of The American Meteorological Society*,
1086 77(3), 437–471, doi: 10.1175/1520-0477(1996)077<0437:TNYRP>2.0.CO;2, 1996.

1087

1088 Kempe, S. and Pegler, K.: Sinks and sources of CO₂ in coastal seas: the North Sea, *Tellus* 43 B,
1089 224-235, doi: 10.3402/tellusb.v43i2.15268, 1991.

1090

1091 Kerimoglu, O., Große, F., Kreuz, M., Lenhart, H.-J., and van Beusekom, J. E. E.: A model-based
1092 projection of historical state of a coastal ecosystem: Relevance of phytoplankton
1093 stoichiometry, *Science of The Total Environment* 639, 1311-1323,
1094 doi:10.1016/j.scitotenv.2018.05.215, 2018.

1095

1096 Kohlmeier, C., and Ebenhöf, W.: Modelling the biogeochemistry of a tidal flat ecosystem
1097 with EcoTiM, *Ocean Dynamics*, 59(2), 393-415, doi: 10.1007/s10236-009-0188-3, 2009.

1098

1099 Kowalski, N., Dellwig, O., Beck, M., Gräwe, U., Pierau, N., Nägler, T., Badewien, T., Brumsack,
1100 H.-J., van Beusekom, J.E., and Böttcher, M. E. Pelagic molybdenum concentration anomalies
1101 and the impact of sediment resuspension on the molybdenum budget in two tidal systems of
1102 the North Sea. *Geochimica et Cosmochimica Acta* 119, 198-211, 2013.

1103

1104 Kühn, W., Pätsch, J., Thomas, H., Borges, A. V., Schiettecatte, L.-S., Bozec, Y., and Prowe, A. E.

1105 F.: Nitrogen and carbon cycling in the North Sea and exchange with the North Atlantic-A
1106 model study, Part II: Carbon budget and fluxes, *Continental Shelf Research*, 30, 1701-1716,
1107 doi:10.1016/j.csr.2010.07.001, 2010.
1108

1109 Laruelle, G. G., Lauerwald, R., Pfeil, B., and Regnier, P.: Regionalized global budget of the CO₂
1110 exchange at the air-water interface in continental shelf seas, *Global Biogeochemical Cycles*,
1111 28 (11), 1199-1214, doi: 10.1002/2014gb004832, 2014.
1112

1113 Lenhart, H.-J., Radach, G., Backhaus, J. O., and Pohlmann, T.: Simulations of the North Sea
1114 circulation, its variability, and its implementation as hydrodynamical forcing in ERSEM, *Neth.*
1115 *J. Sea Res.*, 33, 271–299, doi:10.1016/0077-7579(95)90050-0, 1995.
1116

1117 Lettmann, K. A., Wolff, J.-O., and Badewien, T.H.: Modeling the impact of wind and waves on
1118 suspended particulate matter fluxes in the East Frisian Wadden Sea (southern North Sea),
1119 *Ocean Dynamics*, 59(2), 239-262, doi: 10.1007/s10236-009-0194-5, 2009.
1120

1121 Lipinski, M.: Nährstoffelemente und Spurenmetalle in Wasserproben der Hunte und Jade.
1122 Diploma thesis, C.v.O. University of Oldenburg, 82 pp., 1999.
1123

1124 Lorkowski, I., Pätsch, J., Moll, A., and Kühn, W.: Interannual variability of carbon fluxes in the
1125 North Sea from 1970 to 2006 – Competing effects of abiotic and biotic drivers on the gas-
1126 exchange of CO₂, *Estuarine, Coastal and Shelf Science*, 100, 38-57,
1127 doi:10.1016/j.ecss.2011.11.037, 2012.
1128

1129 Łukawska-Matuszewska, K. and Graca, B.: Pore water alkalinity below the permanent
1130 halocline in the Gdańsk Deep (Baltic Sea) - Concentration variability and benthic fluxes.
1131 *Marine Chemistry* 204: 49-61, 2017.
1132

1133 Mayer, B., Rixen, T., and Pohlmann, T.: The Spatial and Temporal Variability of Air-Sea CO₂
1134 Fluxes and the Effect of Net Coral Reef Calcification in the Indonesian Seas: A Numerical
1135 Sensitivity Study. *Frontiers in Marine Science* 5(116), 2018.
1136

1137 McQuatters-Gollop, A., Raitzos, D. E., Edwards, M., Pradhan, Y., Mee, L. D., Lavender, S. J.,
1138 and Attrill, M. J.: A long-term chlorophyll data set reveals regime shift in North Sea
1139 phytoplankton biomass unconnected to nutrient trends, *Limnology & Oceanography*, 52,
1140 635-648, doi:10.4319/lo.2007.52.2.0635, 2007.

1141

1142 McQuatters-Gollop, A., and Vermaat, J. E.: Covariance among North Sea ecosystem state
1143 indicators during the past 50 years e contrasts between coastal and open waters, *Journal of*
1144 *Sea Research*, 65, 284-292, doi:10.1016/j.seares.2010.12.004, 2011.

1145

1146 Moore, W.S., Beck, M., Riedel, T., Rutgers van der Loeff, M., Dellwig, O., Shaw, T.J.,
1147 Schnetger, B., and Brumsack, H.-J.: Radium-based pore water fluxes of silica, alkalinity,
1148 manganese, DOC, and uranium: A decade of studies in the German Wadden Sea, *Geochimica*
1149 *et Cosmochimica Acta*, 75, 6535 – 6555, doi:10.1016/j.gca.2011.08.037, 2011.

1150

1151 Neal, C.: Calcite saturation in eastern UK rivers, *The Science of the Total Environment*, 282-
1152 283, 311-326, doi:10.1016/S0048-9697(01)00921-4, 2002.

1153

1154 Neira, C., and Rackemann, M.: Black spots produced by buried macroalgae in intertidal sandy
1155 sediments of the Wadden Sea: Effects on the meiobenthos. *J. Sea Res.*, 36, 153 - 170, 1996.

1156

1157 Onken, R., and Riethmüller, R.: Determination of the freshwater budget of tidal flats from
1158 measurements near a tidal inlet, *Continental Shelf Research*, 30, 924-933,
1159 doi:10.1016/j.csr.2010.02.004, 2010.

1160

1161 Otto, L., Zimmerman, J.T.F., Furnes, G.K., Mork, M., Saetre, R., and Becker, G.: Review of the
1162 physical oceanography of the North Sea, *Netherlands Journal of Sea Research*, 26 (2-4), 161–
1163 238, doi:10.1016/0077-7579(90)90091-T, 1990.

1164

1165 Pätsch, J., and Kühn, W.: Nitrogen and carbon cycling in the North Sea and exchange with
1166 the North Atlantic – a model study Part I: Nitrogen budget and fluxes, *Continental Shelf*
1167 *Research*, 28, 767–787, doi: 10.1016/j.csr.2007.12.013, 2008.

1168

1169 Pätsch, J., and Lenhart, H.-J.: Daily Loads of Nutrients, Total Alkalinity, Dissolved Inorganic
1170 Carbon and Dissolved Organic Carbon of the European Continental Rivers for the Years
1171 1977–2006, Berichte aus dem Zentrum für Meeres- und Klimaforschung
1172 (https://wiki.cen.uni-hamburg.de/ifm/ECOHAM/DATA_RIVER), 2008.
1173

1174 Pätsch, J., Serna, A., Dähnke, K., Schlarbaum, T., Johannsen, A., and Emeis, K.-C.: Nitrogen
1175 cycling in the German Bight (SE North Sea) - Clues from modelling stable nitrogen isotopes.
1176 *Continental Shelf Research*, 30, 203-213, doi:10.1016/j.csr.2009.11.003, 2010.
1177

1178 Pätsch, J., Kühn, W., and Six, K. D.: Interannual sedimentary effluxes of alkalinity in the
1179 southern North Sea: model results compared with summer observations, *Biogeosciences*
1180 15(11), 3293-3309, doi: 10.5194/bg-15-3293-2018, 2018.
1181

1182 Pätsch, J., Burchard, H., Dieterich, C., Gräwe, U., Gröger, M., Mathis, M., Kapitza, H.,
1183 Bersch, M., Moll, A., Pohlmann, T., Su, J., Ho-Hagemann, H.T.M., Schulz, A., Elizalde, A., and
1184 Eden, C.: An evaluation of the North Sea circulation in global and regional models relevant
1185 for ecosystem simulations, *Ocean Modelling*, 116, 70-95,
1186 doi:10.1016/j.ocemod.2017.06.005, 2017.
1187

1188 Pohlmann, T.: Predicting the thermocline in a circulation model of the North Sea – Part I:
1189 model description, calibration and verification, *Continental Shelf Research*, 16(2), 131–146,
1190 doi:10.1016/0278-4343(95)90885-S, 1996.
1191

1192 Provoost, P., van Heuven, S., Soetaert, K., Laane, R. W. P. M., and Middelburg, J. J.: Seasonal
1193 and long-term changes in pH in the Dutch coastal zone, *Biogeoscience*, 7, 3869-3878,
1194 doi:10.5194/bg-7-3869-2010, 2010.
1195

1196 Raaphorst, W., Kloosterhuis H. T., Cramer, A., and Bakker, K. J. M.: Nutrient early diagenesis
1197 in the sandy sediments of the Dogger Bank area, North Sea: pore water results, *Neth. J. Sea.*
1198 *Res.*, 26(1), 25-52, doi: 10.1016/0077-7579(90)90054-K, 1990.
1199

1200 Radach, G. and Pätsch, J.: Variability of Continental Riverine Freshwater and Nutrient Inputs
1201 into the North Sea for the Years 1977-2000 and Its Consequences for the Assessment of
1202 Eutrophication, *Estuaries and Coasts* 30(1), 66-81, doi: 10.1007/BF02782968, 2007.
1203

1204 Rassmann, J., Eitel, E. M., Lansard, B., Cathalot, C., Brandily, C., Taillefert, M., and Rabouille,
1205 C.: Benthic alkalinity and dissolved inorganic carbon fluxes in the Rhône River prodelta
1206 generated by decoupled aerobic and anaerobic processes. *Biogeosciences*, 17, 13-33,
1207 doi:10.5194/bg-17-13-2020, 2020.

1208

1209 Reimer, S., Brasse, S., Doerffer, R., Dürselen, C. D., Kempe, S., Michaelis, W., and Seifert, R.:
1210 Carbon cycling in the German Bight: An estimate of transformation processes and transport,
1211 *Deutsche Hydr. Zeitschr.* 51, 313-329, doi: /10.1007/BF02764179, 1999.
1212

1213 Riedel, T., Lettmann, K., Beck, M., and Brumsack, H.-J.: Tidal variations in groundwater
1214 storage and associated discharge from an intertidal coastal aquifer. *Journal of Geophysical*
1215 *Research* 115, 1-10, 2010.

1216

1217 Rullkötter, J.: The back-barrier tidal flats in the southern North Sea—a multidisciplinary
1218 approach to reveal the main driving forces shaping the system, *Ocean Dynamics*, 59(2), 157-
1219 165, doi: 10.1007/s10236-009-0197-2, 2009.

1220

1221 Salt, L. A., Thomas, H., Prowe, A. E. F., Borges, A. V., Bozec, Y., and de Baar, H. J. W.:
1222 Variability of North Sea pH and CO₂ in response to North Atlantic Oscillation forcing, *Journal*
1223 *of Geophysical Research*, *Biogeosciences*, 118, pp 9, doi:10.1002/2013JG002306, 2013.
1224

1225 Santos, I. R., Eyre, B. D., and Huettel, M.: The driving forces of porewater and groundwater
1226 flow in permeable coastal sediments: A review, *Estuarine, Coastal and Shelf Science*, 98, 1-
1227 15, doi:10.1016/j.ecss.2011.10.024, 2012.

1228

1229 Santos, I. R., Beck, M., Brumsack, H.-J., Maher, D.T., Dittmar, T., Waska, H., and Schnetger,
1230 B.: Porewater exchange as a driver of carbon dynamics across a terrestrial-marine transect:

1231 Insights from coupled ^{222}Rn and pCO_2 observations in the German Wadden Sea, *Marine*
1232 *Chemistry*, 171, 10-20, doi:10.1016/j.marchem.2015.02.005, 2015.
1233

1234 Schott, F.: Der Oberflächensalzgehalt in der Nordsee, *Deutsche Hydr. Zeitschr.*, Reihe A Nr. 9,
1235 SUPPL. A9, pp 1-29, 1966.
1236

1237 Schwichtenberg, F.: Drivers of the carbonate system variability in the southern North Sea:
1238 River input, anaerobic alkalinity generation in the Wadden Sea and internal processes,
1239 (Doktorarbeit/PhS), Universität Hamburg, Hamburg, Germany, 161 pp, 2013.
1240

1241 Seibert, S.L., Greskowiak J., Prommer H., Böttcher M.E., Waska H., and Massmann G.:
1242 Modeling biogeochemical processes in a barrier island freshwater lens (Spiekeroog,
1243 Germany). *J. Hydrol.*, 575, 1133-1144, 2019.
1244

1245 Seitzinger, S., and Giblin, A.E.: Estimating denitrification in North Atlantic continental shelf
1246 sediments, *Biogeochemistry*, 35, 235–260, doi: 10.1007/BF02179829, 1996.
1247

1248 Shadwick, E. H., Thomas, H., Azetsu-Scott, K., Greenan, B. J. W., Head, E., and Horne, E.:
1249 Seasonal variability of dissolved inorganic carbon and surface water pCO_2 in the Scotian Shelf
1250 region of the Northwestern Atlantic, *Marine Chemistry*, 124 (1–4), 23-37,
1251 doi:10.1016/j.marchem.2010.11.004, 2011.
1252

1253 Sippo, J.Z., Maher, D.T., Tait, D.R., Holloway, C., Santos, I.R.: Are mangroves drivers or
1254 buffers of coastal acidification? Insights from alkalinity and dissolved inorganic carbon export
1255 estimates across a latitudinal transect. *Global Biogeochemical Cycles*, 30, 753-766, 2016.
1256

1257 Smith, S. V., and Hollibaugh, J. T.: Coastal metabolism and the oceanic organic carbon
1258 balance, *Reviews of Geophysics*, 31, 75–89, doi:10.1029/92RG02584, 1993.
1259

1260 Streif, H.: Das ostfriesische Wattenmeer. Nordsee, Inseln, Watten und Marschen. Gebrüder
1261 Borntraeger, Berlin, 1990.
1262

1263 Su, J. and Pohlmann, T.: Wind and topography influence on an upwelling system at the
1264 eastern Hainan coast. *Journal of Geophysical Research: Oceans* 114(C6), 2009.
1265

1266 Sulzbacher, H., Wiederhold, H., Siemon, B., Grinat, M., Igel, J., Burschil, T., Günther, T.,
1267 Hinsby, K.: Numerical modelling of climate change impacts on freshwater lenses on the
1268 North Sea Island of Borkum using hydrological and geophysical methods." *Hydrol. Earth Syst.*
1269 *Sci.* 16(10): 3621-3643, 2012.

1270

1271 Thomas, H., Bozec, Y., Elkalay, K., and de Baar, H. J. W.: Enhanced open ocean storage of CO₂
1272 from shelf sea pumping, *Science*, 304, 1005-1008, doi:10.1126/science.1095491, 2004.
1273

1274 Thomas, H., Schiettecatte, L.-S., Suykens, K., Kone, Y. J. M., Shadwick, E. H., Prowe, A. E. F.,
1275 Bozec, Y., De Baar, H. J. W., and Borges, A. V.: Enhanced ocean carbon storage from
1276 anaerobic alkalinity generation in coastal sediments, *Biogeosciences*, 6, 267-274,
1277 doi:10.5194/bg-6-267-2009, 2009.

1278

1279 van Beusekom, J. E. E., Carstensen, J., Dolch, T., Grage, A., Hofmeister, R., Lenhart, H.-J.,
1280 Kerimoglu, O., Kolbe, K., Pätsch, J., Rick, J., Rönn, L., and Ruitter, H.: Wadden Sea
1281 Eutrophication: Long-Term Trends and Regional Differences. *Frontiers in Marine Science*
1282 6(370), 2019

1283

1284 van Beusekom, J. E. E., Loebel, M., and Martens, P.: Distant riverine nutrient supply and local
1285 temperature drive the long-term phytoplankton development in a temperate coastal basin,
1286 *J. Sea Res.* 61, 26-33, doi:10.1016/j.seares.2008.06.005, 2009.

1287

1288 van Beusekom, J. E. E., Buschbaum, C., and Reise, K.: Wadden Sea tidal basins and the
1289 mediating role of the North Sea in ecological processes: scaling up of management? *Ocean &*
1290 *Coastal Management*, 68, 69-78, doi:10.1016/j.ocecoaman.2012.05.002, 2012.

1291

1292 van Goor, M. A., Zitman, T. J., Wang, Z. B., and Stive, M. J. F.: Impact of sea-level rise on the
1293 equilibrium state of tidal inlets, *Mar. Geol.* 202, 211-227, doi:10.1016/S0025-3227(03)00262-
1294 7, 2003.

1295

1296 van Koningsveld, M., Mulder, J. P. M., Stive, M. J. F., Van der Valk, L., and Van der Weck,
1297 A.W.: Living with sea-level rise and climate change: a case study of the Netherlands, *J. Coast.*
1298 *Res.* 24, 367-379, doi:10.2112/07A-0010.1, 2008.

1299

1300 Wang, Z. A., and Cai, W.-J.: Carbon dioxide degassing and inorganic carbon export from a
1301 marsh-dominated estuary (the Duplin River): A marsh CO₂ pump, *Limnology &*
1302 *Oceanography*, 49, 341–354, doi:10.4319/lo.2004.49.2.0341, 2004.

1303

1304 Winde, V.: Zum Einfluss von benthischen und pelagischen Prozessen auf das Karbonatsystem
1305 des Wattenmeeres der Nordsee. Dr.rer.nat. thesis, EMA University of Greifswald, 2012.

1306

1307 Winde, V., Böttcher, M. E., Escher, P., Böning, P., Beck, M., Liebezeit, G., and Schneider, B.:
1308 Tidal and spatial variations of $\delta^{13}\text{C}$ and aquatic chemistry in a temperate tidal basin during
1309 winter time, *Journal of Marine Systems*, 129, 396-404, doi:10.1016/j.jmarsys.2013.08.005,
1310 2014.

1311

1312 Wolf-Gladrow, D. A., Zeebe, R. E., Klaas, C., Kortzinger, A., and Dickson, A. G.: Total alkalinity:
1313 The explicit conservative expression and its application to biogeochemical processes, *Marine*
1314 *Chemistry*, 106, 287–300, doi:10.1016/j.marchem.2007.01.006, 2007.

1315

1316 Wurgaft E., Findlay A.J., Vigderovich H., Herut B., and Sivan O.: Sulfate reduction rates in the
1317 sediments of the Mediterranean continental shelf inferred from combined dissolved
1318 inorganic carbon and total alkalinity profiles. *Marine Chemistry*, 211,64-74, 2019.

1319

1320 Zhai, W.-D., Yan, X.-L., and Qi, D.: Biogeochemical generation of dissolved inorganic carbon
1321 and nitrogen in the North Branch of inner Changjiang Estuary in a dry season. *Estuarine,*
1322 *Coastal and Shelf Science* 197: 136-149, 2017.

1323

1324 Zeebe, R.E., and Wolf-Gladrow, D. 2001. CO₂ in seawater: Equilibrium, Kinetics, Isotopes.
1325 Elsevier Science Ltd., 2001.

1326

1327

1328

1329

1330

1331

1332

1333

1334

1335

1336

1337 **8. Appendix**

1338

1339 **Table A1: Annual riverine freshwater discharge [km³ yr⁻¹]. The numbering refers to Fig. 1.**

	2001	2002	2003	2004	2005	2006	2007	2008	2009
1) Elbe	23.05	43.38	23.95	19.56	25.56	26.98	26.61	24.62	24.28
2) Ems	3.47	4.48	3.15	3.52	2.99	2.54	4.32	3.32	2.58
3) Noordzeekanaal	3.21	2.98	2.49	3.05	3.03	2.96	1.55	3.05	2.46
4) IJsselmeer (east)	9.55	9.94	6.27	7.97	7.35	7.30	9.10	8.23	6.59
5) IJsselmeer (west)	9.55	9.94	6.27	7.97	7.35	7.30	9.10	8.23	6.59
6) Nieuwe Waterweg	50.37	51.33	34.72	42.91	41.61	44.21	49.59	49.76	44.69
7) Haringvliet	33.10	35.18	17.92	10.77	12.36	16.02	24.00	15.70	11.06
8) Scheldt	7.28	2.74	4.31	3.64	3.59	3.74	4.63	4.57	3.63
9) Weser	11.43	18.97	11.80	10.52	10.37	9.72	16.21	12.59	9.58
10) Firth of Forth	2.72	3.76	2.06	3.01	3.00	2.84	2.85	3.59	3.66
11) Tyne	1.81	2.25	1.18	2.04	1.92	1.78	2.09	2.70	2.05
12) Tees	1.33	1.78	0.94	1.59	1.27	1.45	1.49	1.99	1.55
13) Humber	10.76	12.10	7.16	10.51	7.68	11.11	12.03	13.87	9.60
14) Wash	5.46	4.39	3.08	3.91	1.96	2.72	5.24	4.77	3.21
15) Thames	4.47	3.23	2.41	2.13	0.96	1.57	3.52	3.20	2.38
16) Eider	0.67	0.97	0.47	0.70	0.68	0.67	0.63	0.58	0.57
Sum	178.2	207.4	128.1	133.7	131.6	142.9	172.9	160.7	134.4

1340

1341

1342

1343

1344

1345

1346

1347

1348

1349 **Table A2: River numbers in Fig. 1, their positions and source of data**

Number in Fig. 1	Name	River mouth position	Data source
1	Elbe	53°53'20"N 08°55'00"E	Pätsch & Lenhart (2008); TA-, DIC- and nitrate- concentrations by Amann (2015)
2	Ems	53°29'20"N 06°55'00"E	Pätsch & Lenhart (2008)
3	Noordzeekanaal	52°17'20"N 04°15'00"E	Pätsch & Lenhart (2008); TA-, DIC- and nitrate-

			concentrations from waterbase.nl
4	Ijsselmeer (east)	53°17'20"N 05°15'00"E	As above
5	Ijsselmeer (west)	53°05'20"N 04°55'00"E	As above
6	Nieuwe Waterweg	52°05'20"N 03°55'00"E	As above
7	Haringvliet	51°53'20"N 03°55'00"E	As above
8	Scheldt	51°29'20"N 03°15'00"E	As above
9	Weser	53°53'20"N 08°15'00"E	Pätsch & Lenhart (2008)
10	Firth of Forth	56°05'20"N 02°45'00"W	HASEC (2012)
11	Tyne	55°05'20"N 01°25'00"W	HASEC (2012)
12	Tees	54°41'20"N 01°05'00"W	HASEC (2012)
13	Humber	53°41'20"N 00°25'00"W	HASEC (2012)
14	Wash	52°53'20"N 00°15'00"E	HASEC (2012): sum of 4 rivers: Nene, Ouse, Welland and Witham
15	Thames	51°29'20"N 00°55'00"E	HASEC (2012)
16	Eider	54°05'20"N 08°55'00"E	Johannsen et al, 2008

1350

1351 **Table A3: Monthly values of TA, DIC and NO₃ concentrations [$\mu\text{mol kg}^{-1}$] of rivers, the annual**
1352 **mean and the standard deviation**

River parameter	Jan	Feb	Mar	Apr	May	Jun	Jul	Aug	Sep	Oct	Nov	Dec	Mean	SD
Elbe TA	2380	2272	2293	2083	2017	1967	1916	1768	1988	2156	2342	2488	2139	218
Noordzeekanaal TA	3762	3550	3524	3441	4748	3278	3419	3183	3027	3299	3210	3413	3488	441
Nieuwe Waterweg TA	2778	2708	2765	3006	2883	2658	2876	2695	2834	2761	2834	2927	2810	102
Haringvliet TA	2588	2635	2532	3666	2826	2829	2659	2660	2496	2816	2758	2585	2754	309
Scheldt TA	3781	3863	3708	3725	3758	3626	3722	3514	3367	3666	3825	3801	3696	140
Ijsselmeer TA	2829	3005	2472	2259	2611	1864	1672	1419	1445	2172	2286	2551	2215	521
Elbe DIC	2415	2319	2362	2179	2093	2025	1956	1853	2018	2200	2428	2512	2197	211
Noordzeekanaal DIC	3748	3579	3470	3334	3901	3252	3331	3136	2977	3214	3183	3405	3378	264
Nieuwe Waterweg DIC	2861	2794	2823	2991	2879	2657	2886	2706	2828	2773	2907	3036	2845	108
Haringvliet DIC	2673	2735	2600	3661	2850	2846	2687	2681	2512	2859	2803	2670	2798	292
Scheldt DIC	3798	3909	3829	3737	3704	3592	3705	3490	3316	3648	3733	3868	3694	167
Ijsselmeer DIC	2824	3008	2458	2234	2576	1826	1636	1369	1399	2134	2285	2565	2193	538
Elbe NO ₃	247	330	277	225	193	161	129	103	112	157	267	164	197	72
Noordzeekanaal NO ₃	150	168	190	118	79	71	64	73	78	92	107	137	111	42
Nieuwe Waterweg NO ₃	232	243	231	195	150	140	132	135	113	145	201	220	178	47
Haringvliet NO ₃	233	252	218	200	143	144	133	117	128	127	143	228	172	50
Scheldt NO ₃	320	341	347	345	243	221	219	215	189	202	190	274	259	63
Ijsselmeer NO ₃	136	159	190	192	135	46	20	14	7	18	20	79	85	73

1353

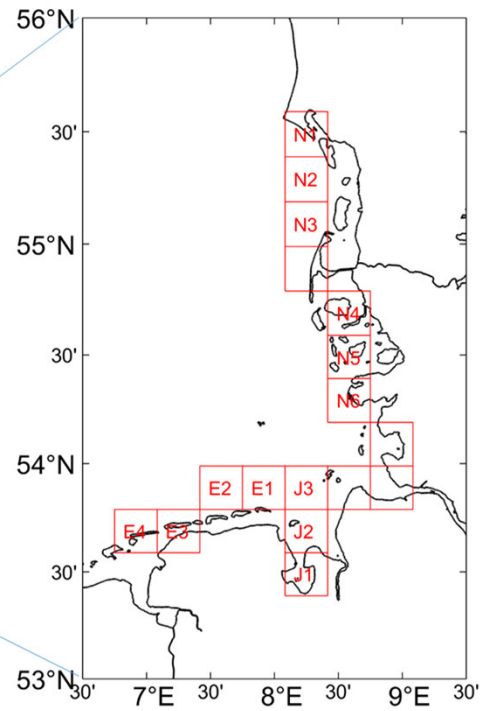
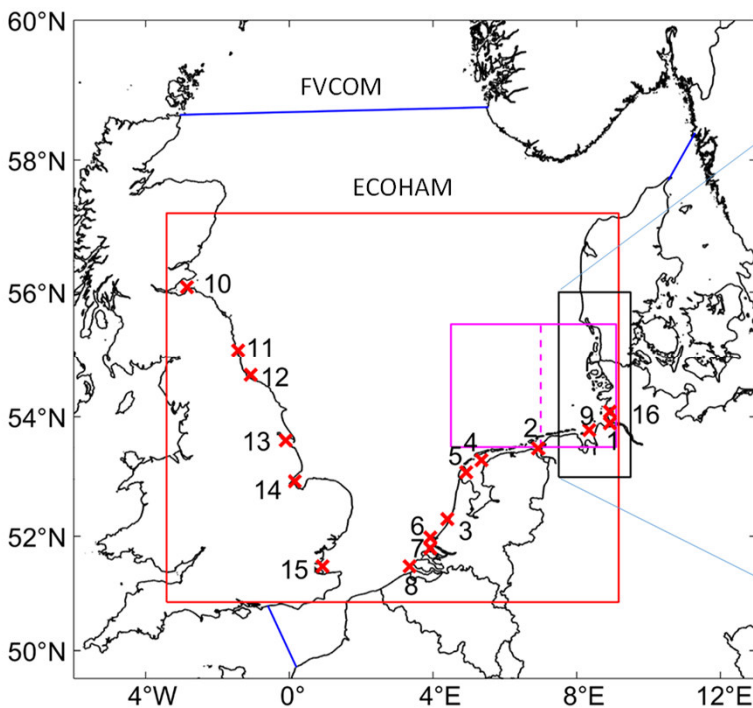
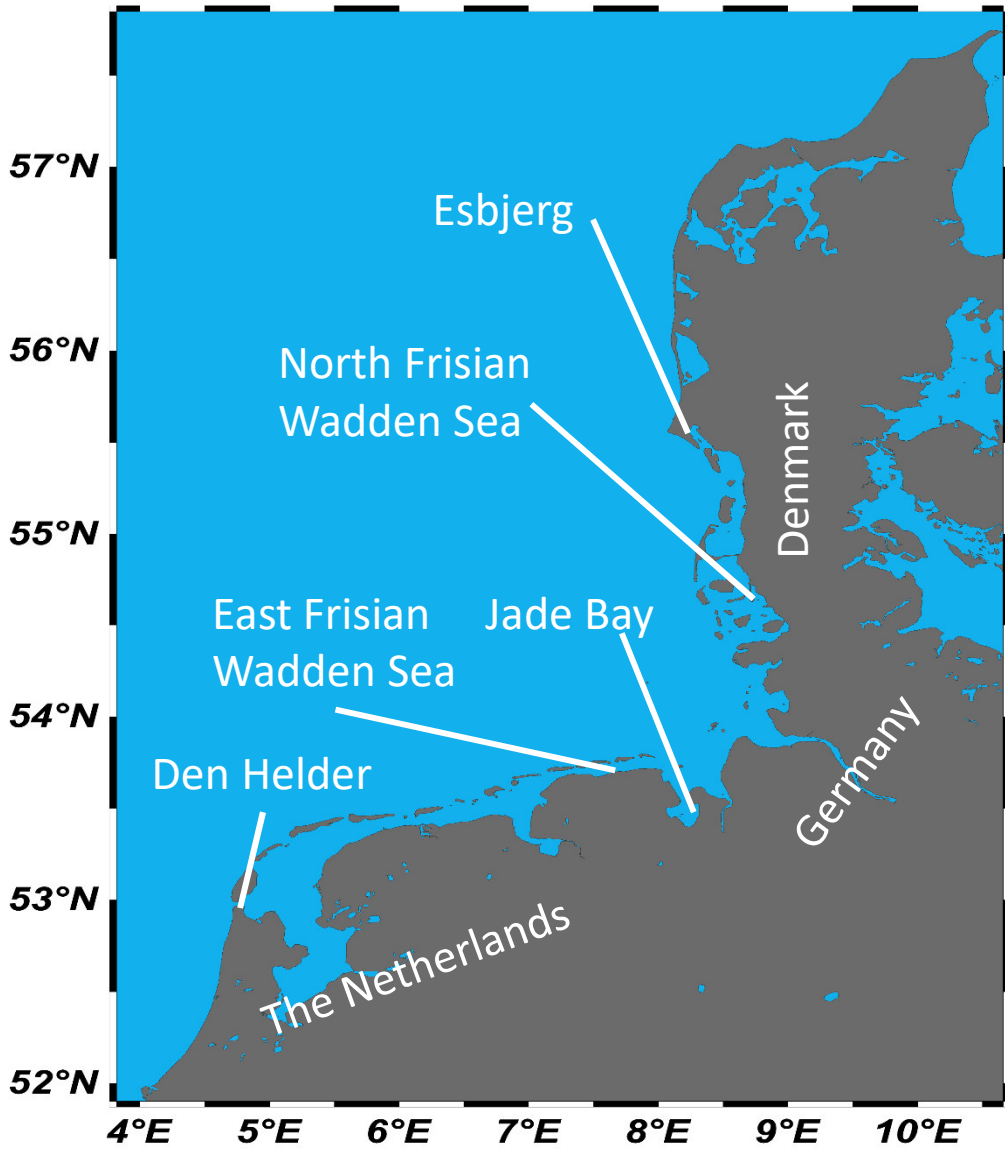


Fig. 1

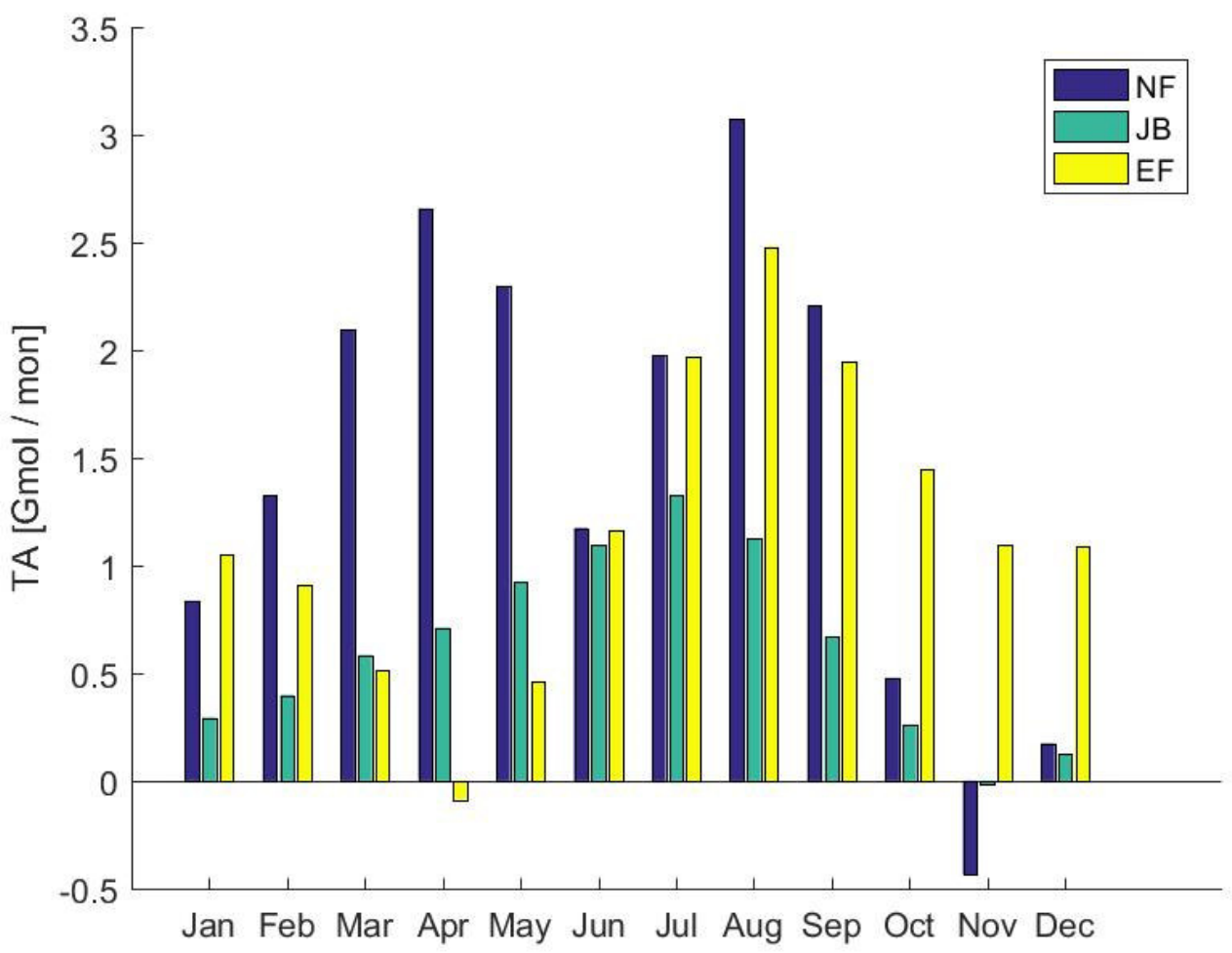
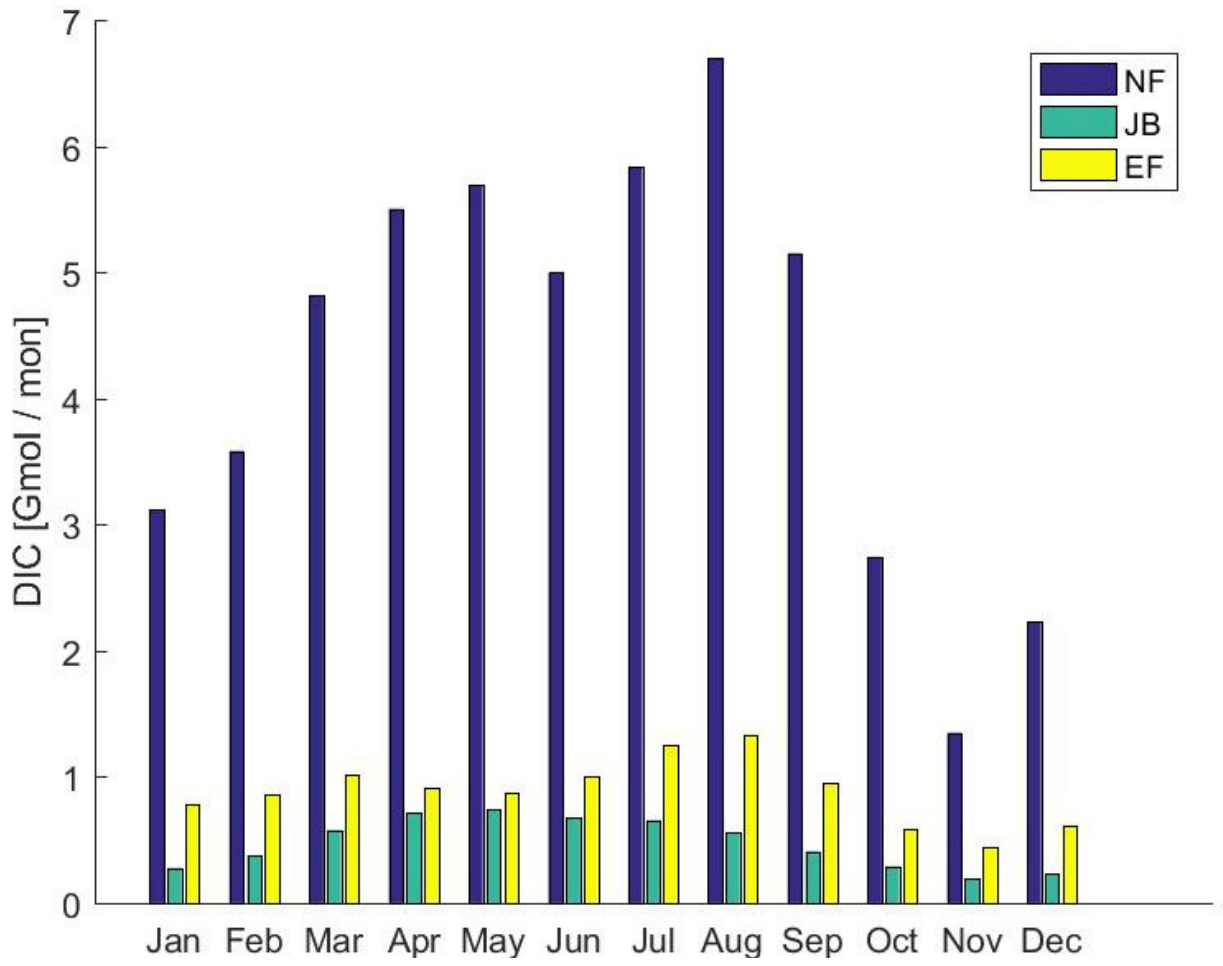


Fig. 2

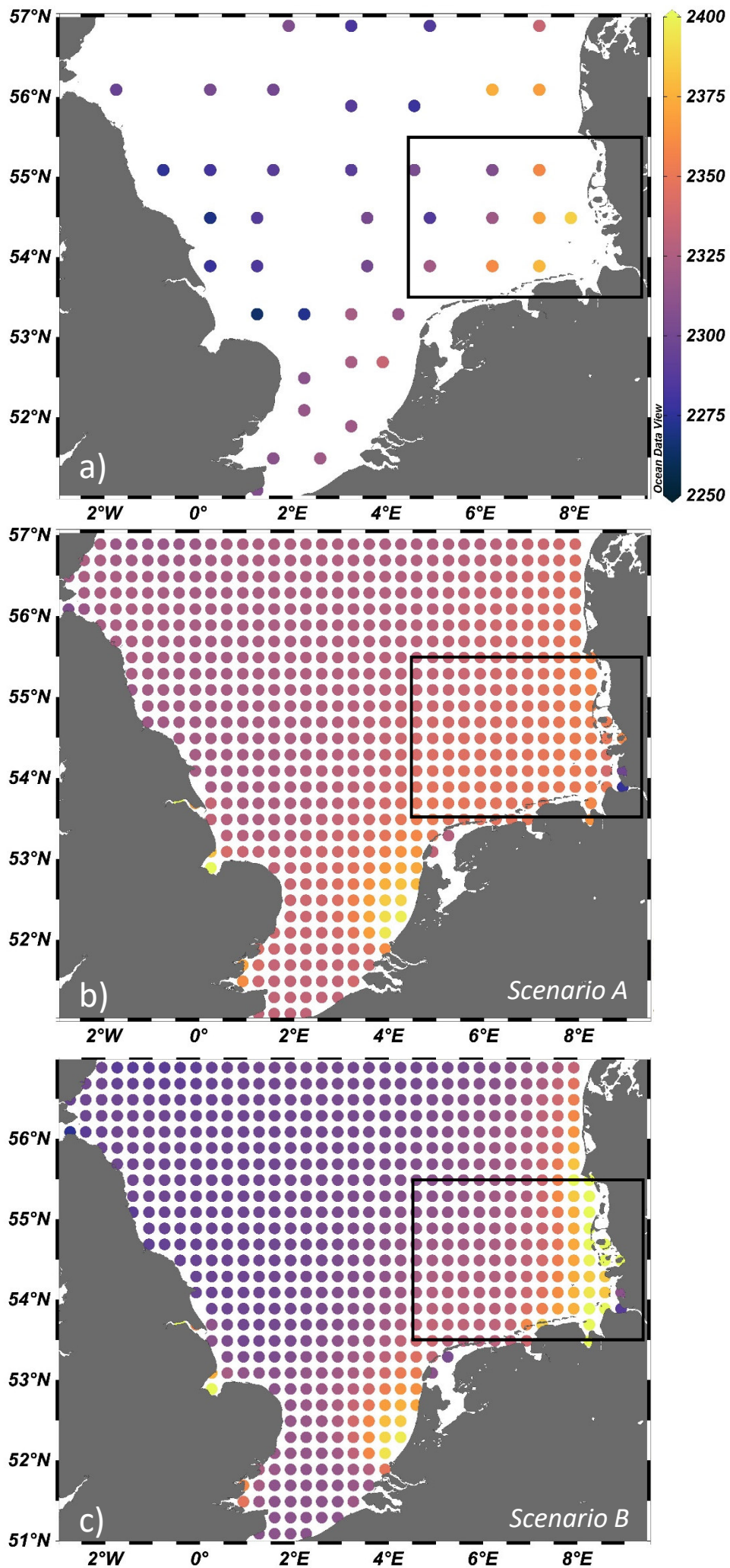


Fig. 3

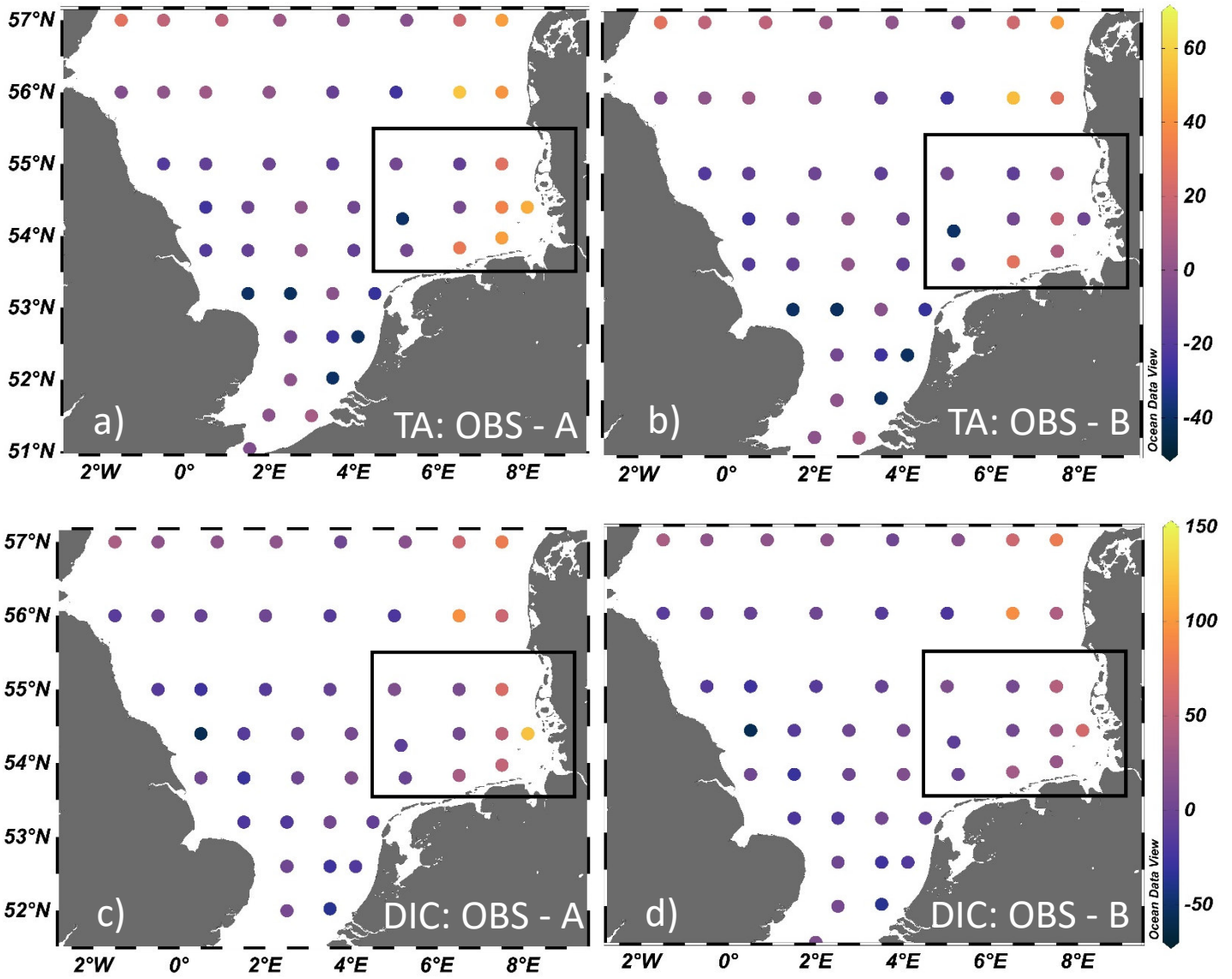


Fig. 4

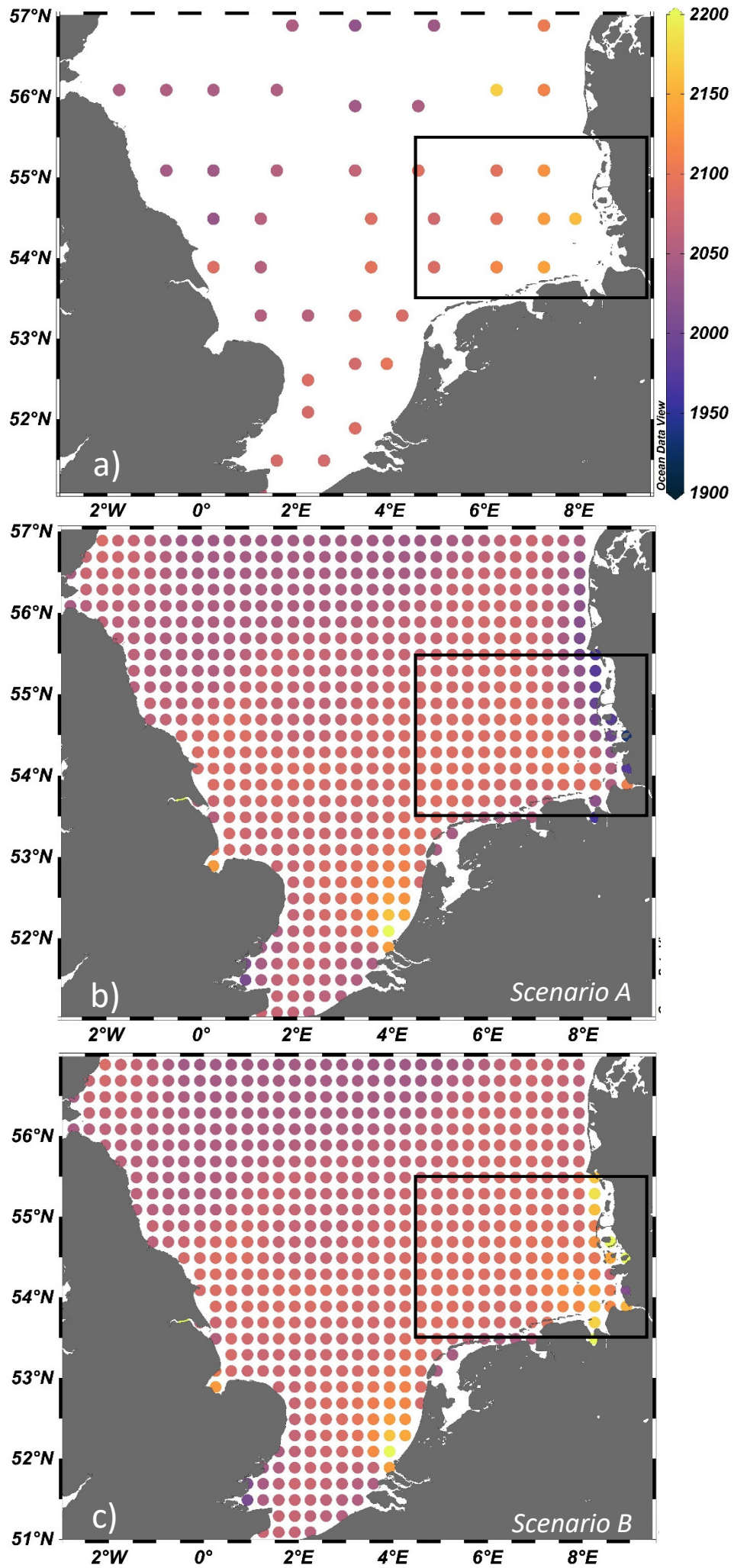


Fig. 5

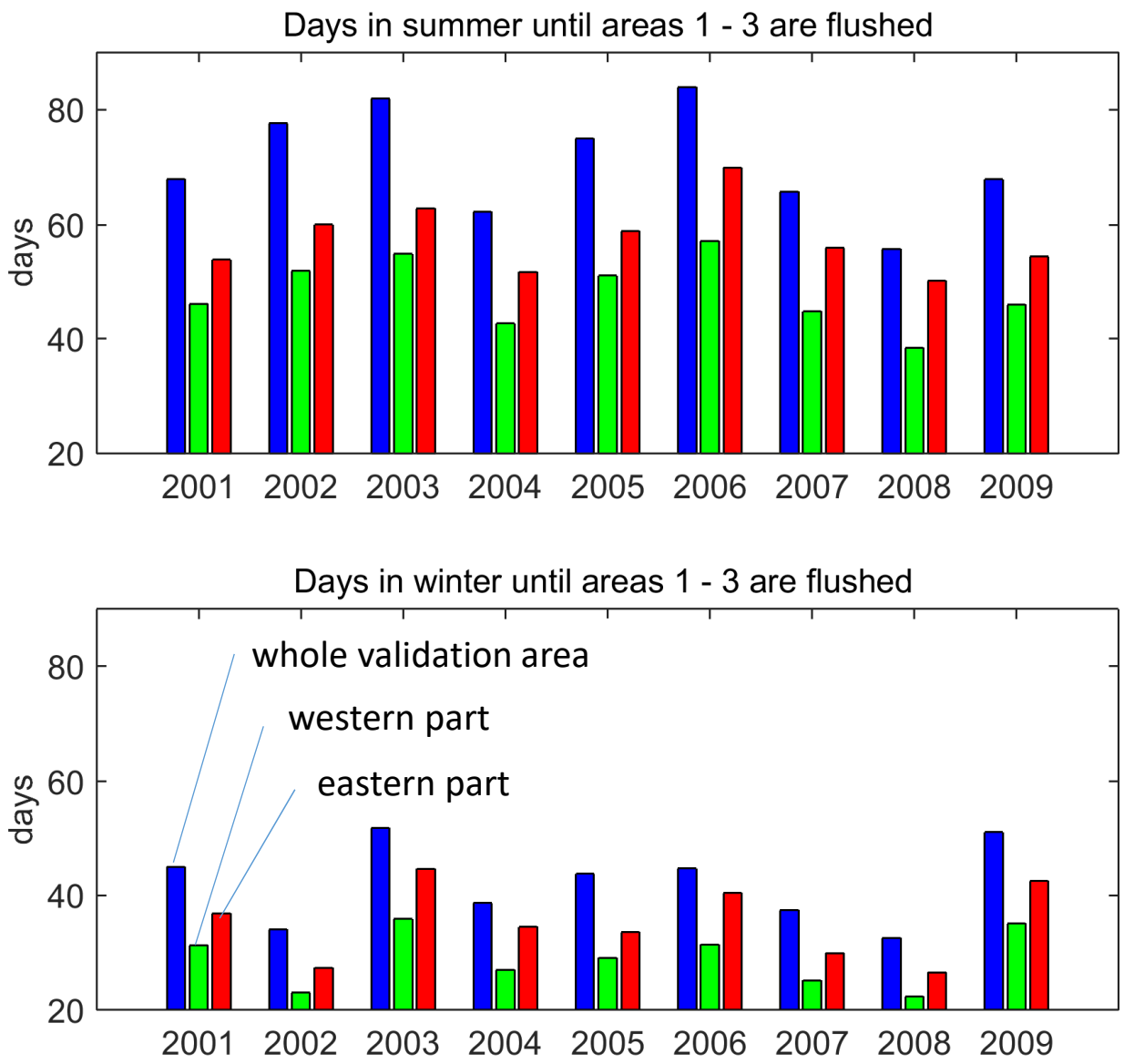


Fig. 6

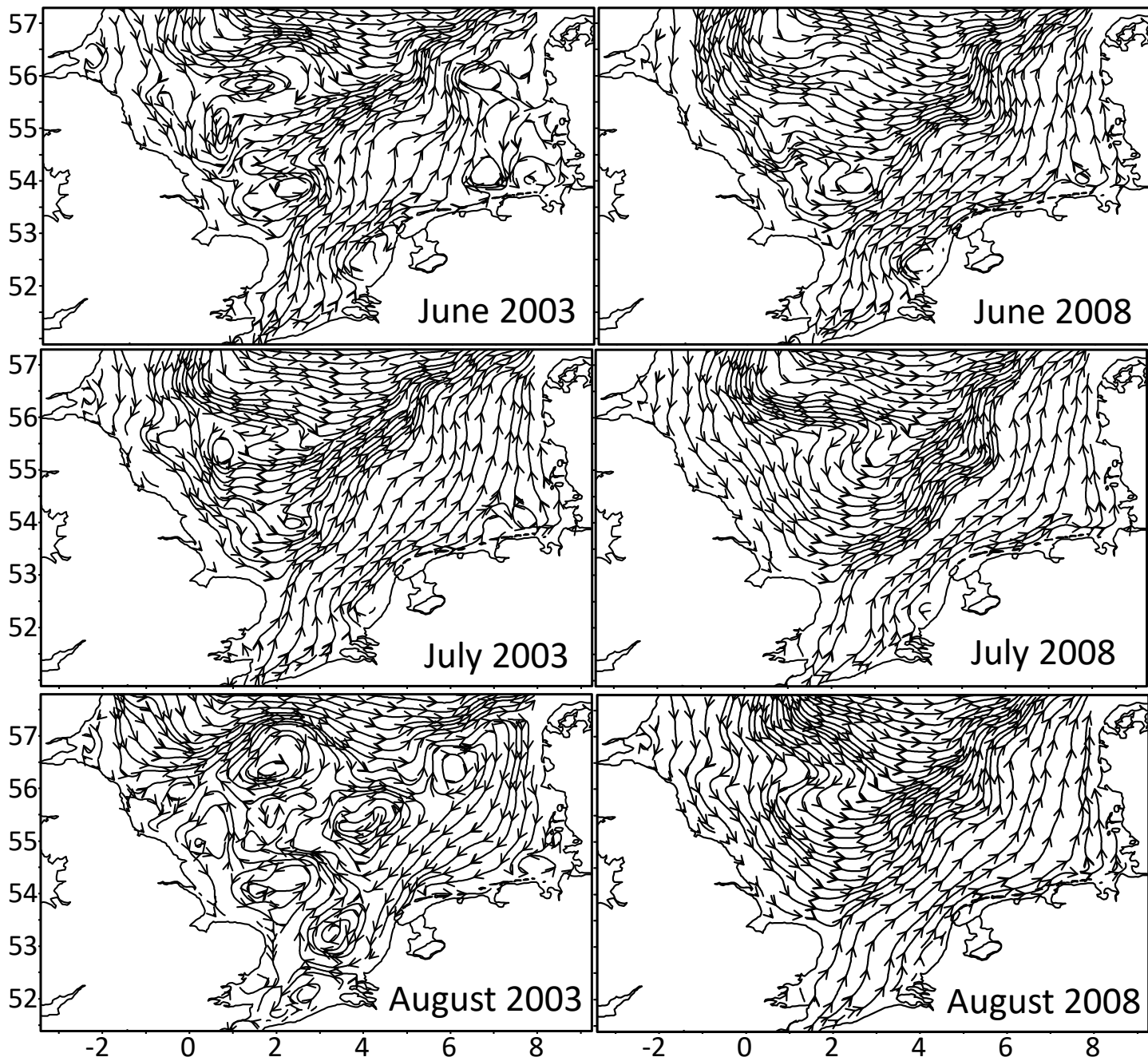


Fig. 7

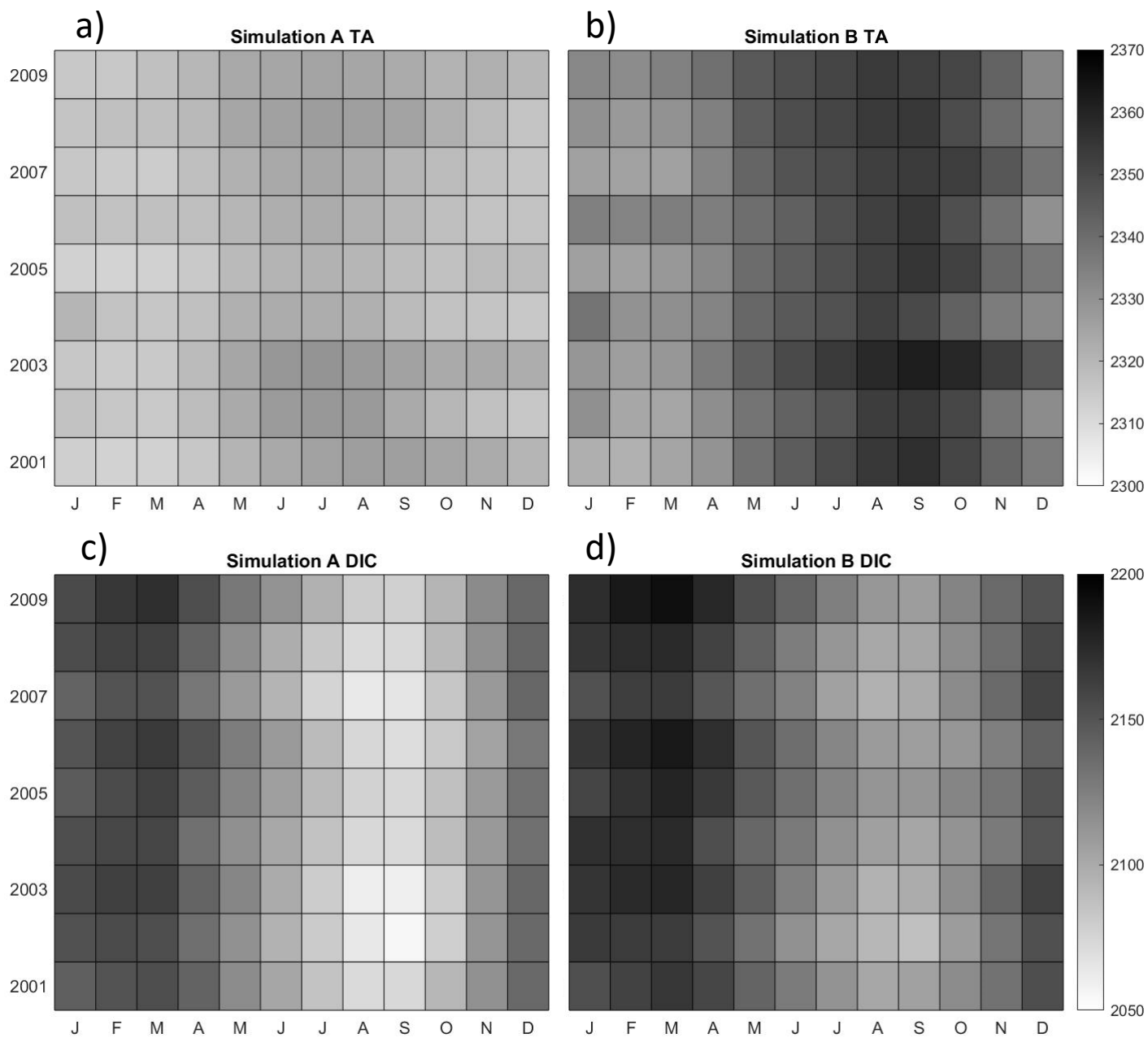


Fig. 8

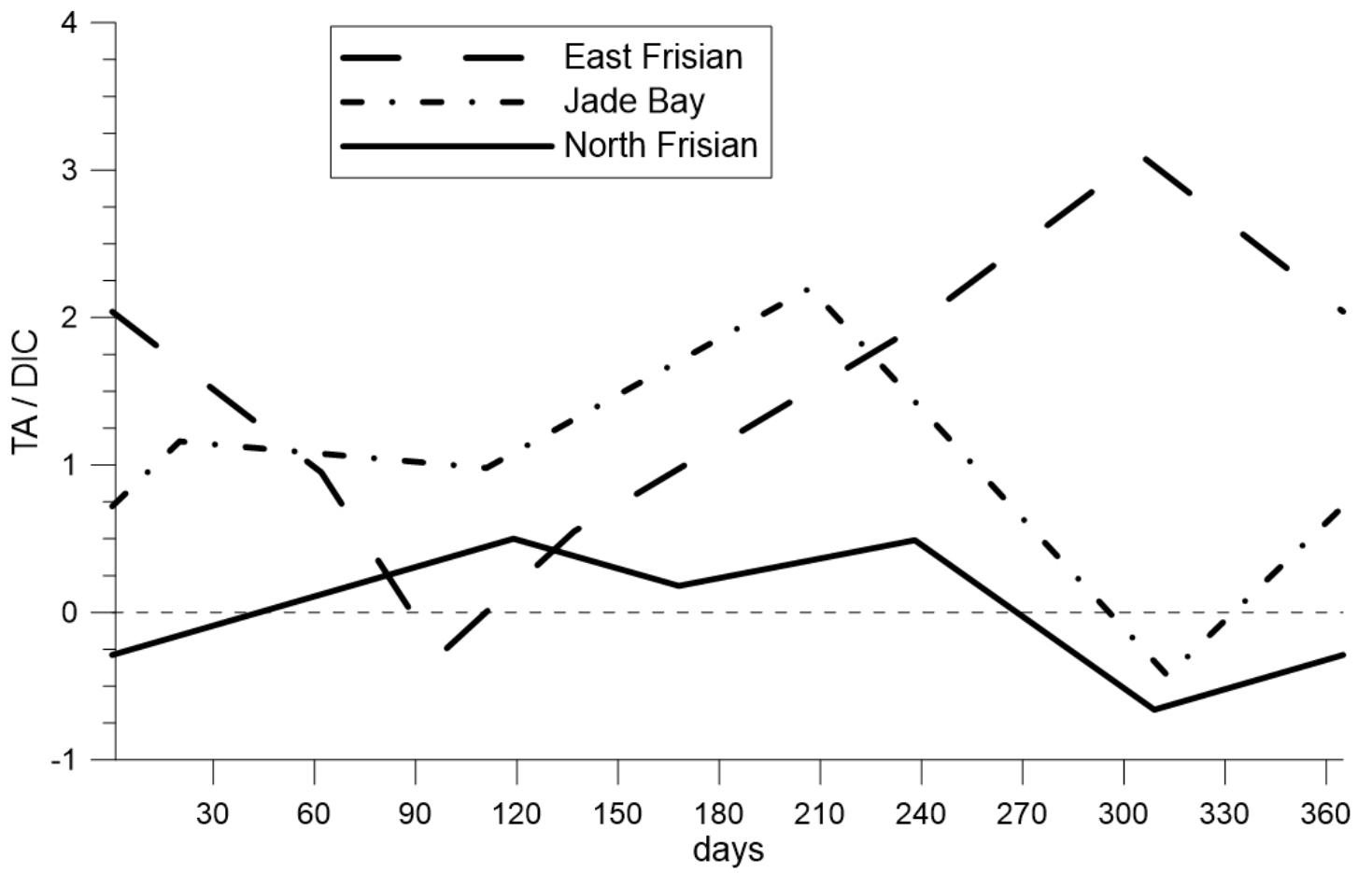


Fig. 9

The impact of intertidal areas on the carbonate system of the southern North Sea

Fabian Schwichtenberg^{1,6}, Johannes Pätsch^{1,5}, Michael Ernst Böttcher^{2,3,4}, Helmuth Thomas⁵, Vera Winde², Kay-Christian Emeis⁵

¹ Theoretical Oceanography, Universität Hamburg, Bundesstr. 53, D-20146 Hamburg, ~~Bundesstr. 53~~, Germany

² Geochemistry & Isotope Biogeochemistry Group, Department of Marine Geology, Leibniz Institute of Baltic Sea Research (IOW), Seestr. 15, D-18119 Warnemünde, Germany

³ Marine Geochemistry, University of Greifswald, Friedrich-Ludwig-Jahn Str. 17a, D-17489 Greifswald, Germany

⁴ Department of Maritime Systems, Interdisciplinary Faculty, University of Rostock, Albert-Einstein-~~Straße~~Str. 21, D-~~18059~~ Rostock, Germany

⁵ Institute of Coastal Research, Helmholtz Zentrum Geesthacht (HZG), Max-Planck-~~Str.~~ 1, D-21502 Geesthacht, Germany

⁶ Present Address: German Federal Maritime and Hydrographic Agency, Bernhard-Nocht-Str. 78, D-20359 Hamburg, Germany

Correspondence to Johannes Pätsch (~~johannes.paetsch@uni-hamburg.de~~johannes.paetsch@uni-hamburg.de)

Abstract

The coastal ocean is strongly affected by ocean acidification because ~~it is of its~~ shallow, ~~has a~~ water depths, low volume, and ~~is in close contact with~~ the closeness to terrestrial dynamics. Earlier observations of dissolved inorganic carbon (DIC) and total alkalinity (TA) in the southern part of the North Sea ~~and the German Bight~~, a Northwest-European shelf sea, ~~have~~ revealed lower acidification effects than expected. It has been assumed that anaerobic degradation and subsequent TA release in the adjacent back-barrier tidal areas ('Wadden Sea') in summer time is responsible for this phenomenon. ~~In~~ this study the exchange rates of TA and DIC between the Wadden Sea tidal basins and the North Sea and the consequences for the carbonate system in the German Bight are estimated using a 3-D ecosystem model. ~~Aim~~ The aim of this

29 ~~workstudy~~ is to ~~reproduce the~~ differentiate the various sources contributing to observed high
30 summer TA concentrations in the southern North Sea ~~and to differentiate the various sources~~
31 ~~contributing to these elevated values.~~ Observed. Measured TA and DIC concentrations in the
32 Wadden Sea are considered as model boundary conditions. This procedure acknowledges the
33 dynamic behaviour of the Wadden Sea as an area of effective production and decomposition
34 of organic material. ~~In addition, modelled tidal water mass exchange is used to transport~~
35 ~~material between the open North Sea and the Wadden Sea. In the model~~ According to the
36 modelling results, 39 Gmol TA yr⁻¹ were exported from the Wadden Sea into the North Sea,
37 which is lowerless than a previous estimate, but within a comparable range. ~~Furthermore,~~
38 ~~the~~ The interannual variabilities of TA and DIC concentrations, ~~which were~~ mainly driven by
39 hydrodynamic conditions, were examined for the years 2001 – 2009. VariabilityDynamics in
40 the carbonate system ~~of the German Bight is~~ found to be related to specific weather ~~in that~~
41 ~~the occurrence of weak meteorological “blocking situations” leads to enhanced accumulation~~
42 ~~of TA there.~~ conditions. The results suggest that the Wadden Sea is an important driver ~~of~~
43 the carbonate system ~~variability~~ in the southern North Sea. ~~According to the model results,~~
44 ~~on~~ On average 41-% of ~~all~~ TA massinventory changes in the German Bight ~~are~~ were caused by
45 ~~river~~ riverine input, 37-% by net transport from adjacent North Sea sectors, 16-% by Wadden
46 Sea export, and 6-% are caused by ~~the~~ internal net production of TA. ~~The effect~~ The dominant
47 role of river input for the TA inventory disappears when focussing on TA concentration ~~change~~
48 ~~are very low for river input, as these~~ changes due to the corresponding freshwater fluxes ~~on~~
49 ~~average slightly diluted~~ diluting the marine TA ~~concentration.~~ concentrations. The ratio of
50 exported TA ~~and~~ versus DIC reflects the dominant underlying biogeochemical processes in the
51 ~~different~~ Wadden Sea ~~areas.~~ Aerobic. Whereas, aerobic degradation of organic matter plays a
52 key role in the North Frisian Wadden Sea during all seasons of the year. ~~In the East Frisian~~
53 ~~Wadden Sea,~~ anaerobic degradation of organic matter dominated, ~~including denitrification,~~
54 ~~sulphate, and iron reduction~~ in the East Frisian Wadden Sea. Despite of the scarcity of high-
55 resolution field data it is shown that anaerobic degradation in the Wadden Sea is one of the
56 main contributors of elevated summer TA values in the southern North Sea.

57

58 1. Introduction

59 Shelf seas are highly productive areas constituting the interface between the inhabited coastal
60 areas and the global ocean. Although they represent only 7.6% of the world ocean's area,
61 current estimates assume that they contribute approximately 21% to total global ocean CO₂
62 sequestration (Borges, 2011). At the global scale the uncertainties of these estimates are
63 significant due to the lack of spatially and temporally resolved field data. Some studies
64 investigated regional carbon cycles in detail (e.g., Kempe & Pegler, 1991; Brasse et al., 1999;
65 Reimer et al., 1999; Thomas et al., 2004; 2009; Artioli et al., 2012; Lorkowski et al., 2012; Burt
66 et al., 2016; Shadwick et al., 2011; Laruelle et al., 2014; Carvalho et al., 2017) and pointed out
67 sources of uncertainties specifically for coastal settings.

68 However, natural pH variations dynamics in coastal- and shelf- regions, for example, can have
69 been shown to be up to an order of magnitude higher than in the open ocean (Provoost et al,
70 2010).

71 Also, the nearshore effects of CO₂ uptake and acidification are difficult to determine, because
72 of the shallow water depth and a possible superposition by benthic-pelagic coupling, and
73 strong variations in fluxes of TA are associated with inflow of nutrients from rivers, pelagic
74 nutrient driven production and respiration (Provoost et al., 2010), submarine groundwater
75 discharge (SGD; Winde et al., 2014), and from benthic-pelagic pore water exchange (e.g.,
76 Billerbeck et al., 2006; Riedel et al., 2010; Moore et al., 2011; Winde et al., 2014; Santos et al.,
77 2012; 2015; Brenner et al., 2016; Burt et al., 2014; 2016; Seibert et al., 2019). Finally, shifts
78 within the carbonate system are driven by impacts from watershed processes and
79 amplified/modulated by changes in ecosystem structure and metabolism (Duarte et al., 2013).

80 Berner et al. (1970) and Ben-Yakoov (1973) were among the first who investigated elevated
81 TA and pH variations caused by microbial dissimilatory sulphate reduction in the anoxic pore
82 water of sediments. At the Californian coast, the observed enhanced TA export from
83 sediments was related to the burial of reduced sulphur compounds (pyrite) (Dollar et al., 1991;
84 Smith & Hollibaugh, 1993; Chambers et al., 1994). Other studies conducted in the Satilla and
85 Altamaha estuaries and the adjacent continental shelf found non-conservative mixing lines of
86 TA versus salinity, which was attributed to anaerobic TA production in nearshore sediments
87 (Wang & Cai, 2004; Cai et al., 2010). Iron dynamics and pyrite formation in the Baltic Sea were

88 found to impact benthic TA generation from the sediments (Gustafsson et al., 2019; Łukawska-
89 Matuszewska and Graca, 2017).

90 The focus of the present study is the southern part of the North Sea, located on the Northwest
91 European Shelf. This shallow part of the North Sea is connected with the tidal basins of the
92 Wadden Sea via ~~deep~~ channels between barrier islands enabling an exchange of water, and
93 dissolved and suspended material (Rullkötter, 2009; Lettmann et al., 2009; Kohlmeier and
94 Ebenhöf, 2009). The Wadden Sea extends from Den Helder (The Netherlands) in the west to
95 Esbjerg (Denmark) in the north and covers an area of about 9500 km² (Ehlers, 1994). The
96 entire system is characterised by semidiurnal tides with a tidal range between 1.5 m in the
97 westernmost part and 4 m in the estuaries of the rivers Weser and Elbe (Streif, 1990). During
98 low tide about 50% of the area are falling dry (van Beusekom et al., 2019). Large rivers
99 discharge nutrients into the Wadden Sea, which in turn shows a high degree of eutrophication,
100 aggravated by mineralisation of organic material imported into the Wadden Sea from the
101 open North Sea (van Beusekom et al., 2012).

102 In comparison to the central and northern part of the North Sea, TA concentrations in the
103 southern part are significantly elevated during summer (Salt et al., 2013; Thomas et al., 2009;
104 Brenner et al., 2016; Burt et al., 2016). The observed high TA concentrations have been
105 attributed to an impact from the adjacent tidal areas (Hoppema, 1990; Kempe & Pegler, 1991;
106 Brasse et al., 1999; Reimer et al., 1999; Thomas et al., 2009; Winde et al., 2014), but this impact
107 has not been rigorously quantified. Using several assumptions, Thomas et al. (2009) calculated
108 an annual TA export from the Wadden Sea / Southern Bight of 73 Gmol TA yr⁻¹ to close the
109 TA budget for the ~~entire~~southern North Sea.

110 The aim of this study is to reproduce the elevated summer concentrations of TA in the
111 southern North Sea with a 3D biogeochemical model that has TA as prognostic variable. With
112 this tool ~~in~~at hand, we balance the budget TA in the relevant area on an annual basis.
113 Quantifying the different budget terms, like river input, Wadden Sea export, internal pelagic
114 and benthic production, degradation and respiration allows us to determine the most
115 important contributors to TA variations. In this way we refine the budget terms by Thomas et
116 al. (2009) and replace the original closing term by data. The new results are discussed on the
117 background of the budget approach proposed by Thomas et al. (2009).

118 2. Methods

119 2.1. Model specifications

120 2.1.1. Model domain and validation area

121 The ECOHAM model domain for this study (Fig.-1) was first applied by Pätsch et al. (2010). For
122 model validations (magenta: validation area, Fig.-1), an area was chosen that includes the
123 German Bight as well as parts ~~of~~ along the Danish and the Dutch coast. The western boundary
124 of the validation area is situated at 4.5°-E. The southern and northern boundaries are at 53.5°
125 and 55.5°-N, respectively. The validation area is divided by the magenta dashed line at 7°-E
126 into the western and eastern part. For the calculation of box averages of DIC and TA a bias
127 towards the deeper areas with more volume and more data should be avoided. Therefore,
128 each water column covered with data within the validation area delivered one mean value,
129 which is calculated by vertical averaging. These mean water column averages were
130 horizontally interpolated onto the model grid. After this procedure average box values were
131 calculated. In case of box-averaging model output, the same procedure was applied, but
132 without horizontal interpolation.

133 2.1.2. The hydrodynamic module

134 The physical parameters temperature, salinity, horizontal and vertical advection as well as
135 turbulent mixing were calculated by the submodule HAMSOM (Backhaus, 1985), which was
136 integrated in the ECOHAM model. It is a baroclinic primitive equation model using the
137 hydrostatic and Boussinesq approximation. It is applied to several regional sea areas
138 worldwide- ([Mayer et al., 2018](#); [Su & Pohlmann, 2009](#)). Details are described by Backhaus &
139 Hainbucher (1987) and Pohlmann (1996). The hydrodynamic model ran prior to the
140 biogeochemical part. Daily result fields were stored for driving the biogeochemical model in
141 offline mode. Surface elevation, temperature and salinity resulting from the Northwest-
142 European Shelf model application (Lorkowski et al., 2012) were used as boundary conditions
143 at the southern and northern boundaries. The temperature of the shelf run by Lorkowski et
144 al. (2012) showed a constant offset compared with observations (their Fig.-3), because
145 incoming solar radiation was calculated too high. For the present simulations the shelf run has
146 been repeated with adequate solar radiation forcing.

147 River-induced horizontal transport due to the hydraulic gradient is incorporated (Große et al.,
148 2017; Kerimoglu et al., 2018). This component of the hydrodynamic horizontal transport
149 corresponds to the amount of freshwater discharge.

150 Within this study we use the term flushing time. It is the average time when a basin is filled
151 with ~~lateral~~laterally advected water. The flushing time ~~is depending~~depends on the specific
152 basin. ~~Large~~large basins have usually higher flushing times than smaller basins. High flushing
153 times correspond with low water renewal times.

154 ***2.1.3. The biogeochemical module***

155 The relevant biogeochemical processes and their parameterisations have been detailed in
156 Lorkowski et al. (2012). In former model setups TA was restored to prescribed values derived
157 from observations (Thomas et al., 2009) with a relaxation time of two weeks (Kühn et al., 2010;
158 Lorkowski et al., 2012). The changes in TA treatment for the study at hand is described below.
159 Results from the Northwest-~~European Shelf~~ model application (Lorkowski et al., 2012) were
160 used as boundary conditions for the recent biogeochemical simulations at the southern and
161 northern boundaries (Fig.-1).

162 The main model extension was the introduction of a prognostic treatment of TA in order to
163 study the impact of biogeochemical and physical driven changes of TA onto the carbonate
164 system and especially on acidification (Pätsch et al., 2018). The physical part contains
165 advective and mixing processes as well as dilution by riverine freshwater input. The pelagic
166 biogeochemical part is driven by planktonic production and respiration, formation and
167 dissolution of calcite, pelagic and benthic degradation and remineralisation, and also by
168 atmospheric deposition of reduced and oxidised nitrogen. All these processes impact TA.
169 ~~Benthic~~In this model version benthic denitrification ~~and other anaerobic processes have~~has
170 no impact on pelagic TA concentrations ~~in this model version.~~ Other benthic anaerobic
171 processes are not considered. Only the carbonate ions from benthic calcite dilution ~~and~~
172 ~~the~~increase pelagic TA concentrations. Aerobic remineralisation ~~products~~releases ammonium
173 and phosphate, which enter the pelagic system across the benthic-pelagic interface and alter
174 the pelagic TA concentration. The theoretical background to this has been outlined by Wolf-
175 Gladrow et al. (2007).

176 The years 2001 to 2009 were simulated with 3 spin up years in 2000. Two different scenarios
177 (A and B) were conducted. Scenario-A is the reference scenario without implementation of
178 any Wadden Sea processes. For scenario-B we used the same model configuration as for
179 scenario-A and additionally implemented Wadden Sea export rates of TA and DIC as described
180 ~~above~~in section 2.3.1. The respective Wadden Sea export rates (Fig.-2) are calculated by the
181 temporal integration of the product of wad_sta and wad_exc over one month (see section
182 2.3.1, equation 2).

183 **2.2. External sources and boundary conditions**

184 **2.2.1. Freshwater discharge**

185 Daily data of freshwater fluxes from 16 rivers were used (Fig.-1). For the German Bight and
186 the other continental rivers daily observations of runoff provided by Pätsch & Lenhart (2008)
187 were incorporated. The discharges of the rivers Elbe, Weser and Ems were increased by 21%,
188 19% and 30% in order to take additional drainage into account that originated from the area
189 downstream of the respective points of observation (Radach and Pätsch, 2007). The respective
190 tracer loads were increased accordingly. The data of Neal (2002) were implemented for the
191 British rivers for all years with daily values for freshwater. The annual amounts of freshwater
192 of the different rivers are shown in the appendix (Table-A1). Riverine freshwater discharge
193 was also considered for the calculation of the concentrations of all biogeochemical tracers in
194 the model.

195 **2.2.2. River input**

196 **Data sources**

197 River load data for the main continental rivers were taken from the report by Pätsch & Lenhart
198 (2008) that was kept up to date continuously so that data for the years 2007 – 2009 were also
199 available (https://wiki.cen.uni-hamburg.de/ifm/ECOHAM/DATA_RIVER). They calculated
200 daily loads of nutrients and organic matter based on data provided by the different river
201 authorities. Additionally, loads of the River Eider were calculated according to Johannsen et
202 al. (2008).

203 Up to now, all ECOHAM applications used constant riverine DIC concentrations. TA was not
204 used. For the study at hand we introduced time varying riverine TA and DIC concentrations.

205 New data of freshwater discharge were introduced, as well as TA and DIC loads for the British
 206 rivers (Neal, 2002). Monthly mean concentrations of nitrate, TA and DIC were added for the
 207 Dutch rivers (www.waterbase.nl) and for the German river Elbe (Amann et al., 2015). The
 208 Dutch river data were observed in the years 2007 – 2009. The river Elbe data were taken in
 209 the years 2009 – 2011. These concentration data were prescribed for all simulation years as
 210 mean annual cycle.

211 The data sources and positions of the river mouths of all 16 rivers are shown in Table A2 and
 212 in Fig. 1. The respective riverine concentrations of TA and DIC are given in Table A3. ~~The Dutch
 213 data were observed in the years 2007 – 2009. The river Elbe data stem from the years 2009 –
 214 2011.~~ A3. Schwichtenberg (2013) describes the river data in detail.

215 A few small flood gates (“Siel”) and rivers transport fresh water from the recharge areas into
 216 the intertidal areas (Streif, 1990). The recharge areas for these inlets differ considerably from
 217 each other, leading to different relative contributions for the fresh water input. Whereas the
 218 catchments of Schweiburger Siel (22.2 km²) and the Hooksiel Binnentief are only of minor
 219 importance, the Vareler Siel, the Eckenwarder Siel, and the Maade Siel are of medium
 220 importance, and the highest contribution may originate from the Wangersiel, the Dangaster
 221 Siel, and the Jade-Wapeler Siel (Lipinski, 1999).

222

223 **Effective river input**

224 In order to analyse the net effect ~~of~~ on concentrations in the sea due to river input, the
 225 effective river input (Riv_{eff} [Gmol_{-yr}⁻¹]) is introduced:

226

$$Riv_{eff} = \frac{\Delta C|_{riv}}{\rho \cdot yr} \cdot V \cdot C Riv_{eff} = \frac{\Delta C|_{riv}}{\rho \cdot yr} \cdot V \cdot C \quad (1)$$

227

228 with $\Delta C|_{riv}$ [μmol_{-kg}⁻¹]: the concentration change in the river mouth cell due to river load
 229 riv and the freshwater flux from the river. V [l] is the volume of the river mouth cell, ρ [kg_{-l}⁻¹]
 230 density of water, yr is one year, C [10^{-15} l⁻¹] is a constant.

231 Bulk alkalinity discharged by rivers is quite large but most of the rivers entering the North Sea
232 (here the German Bight) have lower TA concentrations than the sea water. In case of identical
233 concentrations, the effective river load Riv_{eff} is zero. The TA related molecules enter the sea,
234 and in most cases, they are leaving it via transport. In case of tracing or budgeting both the
235 real TA river discharge and the transport must be recognized. In order to understand TA
236 concentration changes in the sea Riv_{eff} is appropriate.

237

238 **2.2.3. Meteorological forcing**

239 The meteorological forcing was provided by NCEP Reanalysis (Kalnay et al., 1996) and
240 interpolated on the model grid field. It consisted of six-hourly fields of air temperature,
241 relative humidity, cloud coverage, wind speed, atmospheric pressure, and wind stress for
242 every year. 2-hourly and daily mean short wave radiation were calculated from astronomic
243 insolation and cloudiness with an improved formula (Lorkowski et al., 2012).

244 **2.3. The Wadden Sea**

245 **2.3.1. Implementation of Wadden Sea dynamics**

246 For the present study the exchange of TA and DIC between North Sea and Wadden Sea was
247 implemented into the model by defining sinks and sources of TA and DIC for some of the
248 south-eastern cells of the North Sea grid (Fig.-1). The cells with adjacent Wadden Sea were
249 separated into three exchange areas: The East Frisian, the North Frisian Wadden Sea and the
250 Jade Bay, marked by "E", "N" and "J" (Fig.-1, right side).

251 Two parameters were determined in order to quantify the TA and DIC exchange between the
252 Wadden Sea and the North Sea.

- 253 1. Concentration changes of pelagic TA and DIC in the Wadden Sea during one tide, and
- 254 2. Water mass exchange between the back-barrier islands and the open sea during one
255 tide

256 Measured concentrations of TA and DIC (Winde, 2013; Winde et al., 2014) as well as modelled
257 water mass exchange rates of the export areas by Grashorn (2015) served as bases for the

258 calculated exchange. Details on flux calculations and measurements are described below. The
259 daily Wadden Sea exchange of TA and DIC was calculated as:

$$wad_flu = \frac{wad_sta * wad_exc}{vol} \quad (2) \quad (2)$$

$$wad_flu = \frac{wad_sta * wad_exc}{vol}$$

261
262 Differences in measured concentrations in the Wadden Sea during rising and falling water
263 levels, as described in section 2.3.2, were temporally interpolated and summarized as *wad_sta*
264 [mmol·m⁻³]. Modelled daily Wadden Sea exchange rates of water masses (tidal prisms during
265 falling water level) were defined as *wad_exc* [m³·d⁻¹], and the volume of the corresponding
266 North Sea grid cell was *vol* [m³]. *wad_flu* [mmol·m⁻³·d⁻¹] were the daily concentration changes
267 of TA and DIC in the respective North Sea grid cells.

268 In fact, some amounts of the tidal prisms return without mixing with North Sea water, and
269 calculations of Wadden Sea – North Sea exchange should therefore consider flushing times in
270 the respective back-barrier areas. Since differences in measured concentrations between
271 rising and falling water levels were used, this effect is already assumed to be represented in
272 the data. This approach enabled the use of tidal prisms without consideration of any flushing
273 times.

274 **2.3.2. Wadden Sea - measurements**

275 The flux calculations for the Wadden Sea – North Sea exchange were carried out in tidal basins
276 of the East and North Frisian Wadden Sea (Spiekeroog Island, Sylt-Rømø) as well as in the Jade
277 Bay. For the present study seawater samples representing tidal cycles during different seasons
278 (Winde, 2013). The mean concentrations of TA and DIC during rising and falling water levels
279 and the respective differences (Δ TA and Δ DIC) are given in Table_1. Measurements in August
280 2002 were taken from Moore et al. (2011). The Δ -values were used as *wad_sta* and were
281 linearly interpolated between the times of observations for the simulations. In this procedure,
282 the linear progress of the Δ -values does not represent the natural behaviour perfectly,

283 especially if only few data are available. As a consequence, possible short events of high TA
284 and DIC export rates that occurred in periods outside the observation periods may have been
285 missed.

286 Due to the low number of concentration measurements a statistical analysis of uncertainties
287 of Δ TA and Δ DIC was not possible. They were measured with a lag of 2 hours after low tide
288 and high tide. This was done in order to obtain representative concentrations of rising and
289 falling water levels. As a consequence, only 2 - 3 measurements for each location and season
290 were considered for calculations of Δ TA and Δ DIC.

291 **2.3.3. Wadden Sea – modelling the exchange rates**

292 Grashorn (2015) performed the hydrodynamic computations of exchanged water masses
293 (*wad_exc*) with the model FVCOM (Chen et al., 2003) by adding up the cumulative seaward
294 transport during falling water level (tidal prisms) between the back-barrier islands that were
295 located near the respective ECOHAM cells with adjacent Wadden Sea area. These values are
296 given in Table-2 for each ECOHAM cell in the respective export areas. The definition of the
297 first cell N1 and the last cell E4 is in accordance to the clockwise order in Fig.-1 (right side).
298 The mean daily runoff of all N-, J- and E-positions was $8.1\text{-km}^3\text{-d}^{-1}$, $0.8\text{-km}^3\text{-d}^{-1}$ and $2.3\text{-km}^3\text{-d}^{-1}$
299 respectively.

300 **2.3.4. Additional Sampling of DIC and TA**

301 DIC and TA concentrations for selected freshwater inlets sampled in October 2010 and May
302 2011 are presented in Table-3. Sampling and analyses took place as described by Winde et al.
303 (2014) and are here reported for completeness and input for discussion only. The autumn data
304 are deposited under doi:10.1594/PANGEA.841976. The samples for TA measurements were
305 filled without headspace into pre-cleaned 12-ccm Exetainer[®], filled with ~~0.1 ml~~ 1 ml saturated
306 HgCl₂ solution. The samples for DIC analysis were completely filled into 250-ccm ground-glass-
307 stoppered bottles, and then poisoned with 100-µl of a saturated HgCl₂ solution. The DIC
308 concentrations were determined at IOW by coulometric titration according to Johnson et al.
309 (1993), using reference material provided by A. Dickson (University of California, San Diego;
310 Dickson et al., 2003) for the calibration (batch 102). TA was measured by potentiometric
311 titration using HCl using a Schott titri plus equipped with an IOline electrode A157. Standard

312 deviations for DIC and TA measurements were better than ± 2 and $\pm 10 \mu\text{mol kg}^{-1}$,
313 respectively.

315 **2.4. Statistical analysis**

316 A statistical overview of the simulation results in comparison to the observations (Salt et al.,
317 2013) is given in Table 4 and 5. In the validation area (magenta box in Fig. 1) observations of
318 10 different stations were available, each with four to six measurements at different depths
319 (51 measured points). Measured TA and DIC concentrations of each point were compared with
320 modelled TA and DIC concentrations in the respective grid cells, respectively. The standard
321 deviations (Stdv), the root ~~mean~~ mean square errors (RMSE), and correlation coefficients (r)
322 were calculated for each simulation. In addition to the year 2008, which we focus on in this
323 study, observations were performed at the same positions in summer 2005 and 2001. These
324 data are also statistically compared with the model results.

325 **3. Results**

326 **3.1. Model validation - TA concentrations in summer 2008**

327 The results of scenarios A and B were compared with observations of TA in August 2008 (Salt
328 et al., 2013) for surface water. The observations revealed high TA concentrations in the
329 German Bight (east of 7°E and south of 55°N) and around the Danish coast (around 56°N) as
330 shown in Fig. 3a. The observed concentrations in these areas ranged between 2350 and
331 $2387 \mu\text{mol TA kg}^{-1}$. These findings were in accordance with observed TA concentrations in
332 August / September 2001 (Thomas et al., 2009). TA concentrations in other parts of the
333 observation domain ranged between $2270 \mu\text{mol TA kg}^{-1}$ near the British coast ($53^\circ \text{N} - 56^\circ \text{N}$)
334 and $2330 \mu\text{mol TA kg}^{-1}$ near the Dutch coast and the Channel. In the validation box the overall
335 average and the standard deviation of all observed TA concentrations (Stdv) was 2334 and
336 $33 \mu\text{mol TA kg}^{-1}$, respectively.

337 In scenario A the simulated surface TA concentrations showed a more homogeneous pattern
338 than observations with maximum values of $2396 \mu\text{mol TA kg}^{-1}$ at the western part of the
339 Dutch coast and even higher ($2450 \mu\text{mol TA kg}^{-1}$) in the river mouth of the Wash estuary at
340 the British coast. Minimum values of 2235 and $2274 \mu\text{mol TA kg}^{-1}$ were simulated at the
341 mouths of the rivers Elbe and Firth of Forth. The modelled TA concentration ranged from 2332

342 to 2351 $\mu\text{mol TA kg}^{-1}$ in the German Bight and in the Jade Bay. Strongest underestimations
343 in relation to observations are located in a band close to the coast stretching from the East
344 Frisian Islands to 57° N at the Danish coast (Fig. 4a). The deviation of simulation results of
345 scenario A from observations in the validation box was represented by a RMSE of
346 28 $\mu\text{mol TA kg}^{-1}$. The standard deviation was 7 $\mu\text{mol TA kg}^{-1}$ and the correlation amounted
347 to $r = 0.77$ (Table 4). In the years 2005 and 2001 similar statistical values are found, but the
348 correlation coefficient was smaller.

349 The scenario B was based on a Wadden Sea export of TA and DIC as described above. The
350 major difference in TA concentrations of this scenario compared to A occurred east of 6.5° E.
351 Surface TA concentrations there peaked in the Jade Bay (2769 $\mu\text{mol TA kg}^{-1}$) and were
352 elevated off the North Frisian and Danish coasts from 54.2° to 56° N ($> 2400 \mu\text{mol TA kg}^{-1}$).
353 Strongest underestimations in relation to observations are noted off the Danish coast
354 between 56° and 57° N (Fig. 4b). In the German Bight the model overestimated the
355 observations slightly, while at the East Frisian Islands the model underestimates TA. When
356 approaching the Dutch Frisian Islands the simulation overestimates TA compared to
357 observations and strongest overestimations can be seen near the river mouth of River Rhine.
358 Compared to scenario A the simulation of scenario B was closer to the observations in terms
359 of RMSE (18 $\mu\text{mol TA kg}^{-1}$) and the standard deviation (Stdv = 22 $\mu\text{mol TA kg}^{-1}$). Also, the
360 correlation ($r = 0.86$) improved (Table 4). In the years 2001 and 2005 the observed mean
361 values are slightly overestimated by the model. The statistical values for 2001 are better than
362 for 2005, where scenario A better compares with the observations.

364 **3.2. Model validation - DIC concentrations in summer 2008**

365 Analogously to TA the simulation results were compared with surface observations of DIC
366 concentrations in summer 2008 (Salt et al., 2013). They also revealed high values in the
367 German Bight (east of 7° E and south of 55° N) and around the Danish coast (near 56° N)
368 which is shown in Fig. 5. The observed DIC concentrations in these areas ranged between
369 2110 and 2173 $\mu\text{mol DIC kg}^{-1}$. Observed DIC concentrations in other parts of the model
370 domain ranged between 2030 and 2070 $\mu\text{mol DIC kg}^{-1}$ in the north western part and 2080 -
371 2117 $\mu\text{mol DIC kg}^{-1}$ at the Dutch coast. In the validation box the overall average and the

372 standard deviation of all observed DIC concentrations were 2108 and 25.09- $\mu\text{mol-DIC-kg}^{-1}$,
373 respectively.

374 The DIC concentrations in scenario-A ranged between 1935 and 1977- $\mu\text{mol-DIC-kg}^{-1}$ at the
375 North Frisian and -Danish coast (54.5° N - 55.5° N) and 1965- $\mu\text{mol-DIC-kg}^{-1}$ in the Jade Bay.
376 Maxima of up to 2164- $\mu\text{mol-DIC-kg}^{-1}$ were modelled at the western part of the Dutch coast
377 north of the mouth of River Rhine (Fig.-5). The DIC concentrations in the German Bight showed
378 a heterogeneous pattern in the model, and sometimes values decreased from west to east,
379 which contrasts the observations (Fig.-5a). This may be the reason for the negative correlation
380 coefficient $r = -0.64$ between model and observations (Table-5). The significant deviation
381 from observation of results from scenario-A is also indicated by the RMSE of 43- $\mu\text{mol-DIC-kg}^{-1}$
382 ¹, and a standard deviation of 14- $\mu\text{mol-DIC-kg}^{-1}$. In 2001 and 2005 the simulation results of
383 this scenario-A are better, which is expressed in positive correlation coefficients and small
384 RMSE values.

385 In scenario-B the surface DIC concentrations at the Wadden Sea coasts increased: The North
386 Frisian coast shows concentrations of up to 2200- $\mu\text{mol-DIC-kg}^{-1}$ while the German Bight has
387 values of 2100 – 2160- $\mu\text{mol-DIC-kg}^{-1}$, and Jade Bay concentrations were higher than
388 2250- $\mu\text{mol-DIC-kg}^{-1}$. The other areas are comparable to scenario-A. In scenario-B the RMSE
389 in the validation box decreased to 26- $\mu\text{mol-DIC-kg}^{-1}$ in comparison to scenario-A. The
390 standard deviation decreased to 9.1- $\mu\text{mol-DIC-kg}^{-1}$, and the correlation improved to $r = 0.55$
391 (Table-5). The average values are close to the observed ones for all years, even though in 2005
392 a large RMSE was found.

393 The comparison between observations and simulation results of scenario-A (Fig.-4c) clearly
394 show model underestimations in the south-eastern area and are strongest in the inner
395 German Bight towards the North Frisian coast ($> 120\text{-}\mu\text{mol-DIC-kg}^{-1}$). Scenario-B also models
396 values lower than observations in the south-eastern area (Fig.-4d), but the agreement
397 between observation and model results is reasonable. Only off the Danish coast near 6.5° E,
398 56° N the model underestimates DIC by 93- $\mu\text{mol-DIC-kg}^{-1}$.

3.3. Hydrodynamic conditions and flushing times

The calculations of Wadden Sea TA export in Thomas et al. (2009) were based on several assumptions concerning riverine input of bulk TA and nitrate, atmospheric deposition of NO_x, water column inventories of nitrate and the exchange between the Southern Bight and the adjacent North Sea (Lenhart et al., 1995). The latter was computed by considering that the water in the Southern Bight is flushed with water of the adjacent open North Sea at time scales of six weeks. For the study at hand, flushing times in the validation area in summer and winter are presented for the years 2001 to 2009 in Fig. 6. Additionally, monthly mean flow patterns of the model area are presented for June, July and August for the years 2003 and 2008, respectively (Fig. 7). They were chosen to highlight the pattern in summer 2003 with one of the highest flushing times (lowest water renewal times), and that in 2008 corresponding to one of the lowest flushing times (highest water renewal times).

The flushing times were determined for the three areas 1 – validation area, 2 – western part of the validation area, 3 – eastern part of the validation area. They were calculated by dividing the total volume of the respective areas 1 – 3 by the total inflow into the areas $m^3 \cdot (m^3 \cdot s^{-1})^{-1}$. Flushing times (rounded to integer values) were consistently higher in summer than in winter, meaning that highest inflow occurred in winter. Summer flushing times in the whole validation area ranged from 54 days in 2008 to 81 days in 2003 and 2006, whereas the winter values in the same area ranged from 32 days in 2008 to 51 days in 2003 and 2009. The flushing times in the western and eastern part of the validation area were smaller due to the smaller box sizes. Due to the position, flushing times in the western part were consistently shorter than in the eastern part. These differences ranged from 5 days in winter 2002 to 14 days in summer 2006 and 2008. The interannual variabilities of all areas were higher in summer than in winter.

The North Sea is mainly characterised by an anti-clockwise circulation pattern (Otto et al., 1990; Pätsch et al., 2017). This can be observed for the summer months in 2008 (Fig. 7). More disturbed circulation patterns in the south-eastern part of the model domain occurred in June 2003: In the German Bight and in the adjacent western area two gyres with reversed rotating direction are dominant. In August 2003 the complete eastern part shows a clockwise rotation which is due to the effect of easterly winds as opposed to prevalent westerlies. In this context such a situation is called meteorological blocking situation.

3.4. Seasonal and interannual variability of TA and DIC concentrations

The period from 2001 to 2009 was simulated for the scenarios A and B. For both scenarios monthly mean surface concentrations of TA were calculated in the validation area and are shown in Fig. 8a and 8b. The highest TA concentration in scenario A was $2329 \mu\text{mol TA kg}^{-1}$ and occurred in July 2003. The lowest TA concentrations in each year were about 2313 to $2318 \mu\text{mol TA kg}^{-1}$ and occurred in February and March. Scenario B showed generally higher values: Summer concentrations were in the range of 2348 to $2362 \mu\text{mol TA kg}^{-1}$ and the values peaked in 2003. The lowest values occurred in the years 2004 – 2008. Also winter values were higher in scenario B than in scenario A: They range from 2322 to $2335 \mu\text{mol TA kg}^{-1}$.

Corresponding to TA, monthly mean surface DIC concentrations in the validation area are shown in Fig. 8c and 8d. In scenario A the concentrations increased from October to February and decreased from March to August (Fig. 8c). In scenario B the time interval with increasing concentrations was extended into March. Maximum values of 2152 to $2172 \mu\text{mol DIC kg}^{-1}$ in scenario A occur in February and March of each model year, and minimum values of 2060 to $2080 \mu\text{mol DIC kg}^{-1}$ in August. Scenario B shows generally higher values: Highest values in February and March are 2161 to $2191 \mu\text{mol DIC kg}^{-1}$. Lowest values in August range from 2095 to $2112 \mu\text{mol DIC kg}^{-1}$. The amplitude of the annual cycle is smaller in scenario B, because the Wadden Sea export shows highest values in summer (Fig. 2).

The pattern of the monthly TA and DIC concentrations of the reference scenario A differ drastically in that TA does not show a strong seasonal variability, whereas DIC does vary significantly. In case of DIC this is due to the biological drawdown during summer. On the other hand, the additional input (scenario B) from the Wadden Sea in summer creates a strong seasonality for TA and instead flattens the variations in DIC.

4. Discussion

Thomas et al. (2009) estimated the contribution of shallow intertidal and subtidal areas to the alkalinity budget of the SE North Sea. That estimate (by closure of mass fluxes) was about

458 $73 \text{ Gmol TA yr}^{-1}$ originating from the Wadden Sea fringing the southern and eastern coast.
459 These calculations were based on observations from the CANOBA dataset in 2001 and 2002.
460 The observed high TA concentrations in the south-eastern North Sea were also encountered
461 in August 2008 (Salt et al., 2013) and these measurements were used for the main model
462 validation in this study. Our simulations result in $39 \text{ Gmol TA yr}^{-1}$ as export from the Wadden
463 Sea into the North Sea. Former modelling studies of the carbonate system of the North Sea
464 (Artioli et al., 2012; Lorkowski et al., 2012) did not consider the Wadden Sea as a source of TA
465 and DIC, and good to reasonable agreement to observations from the CANOBA dataset was
466 only achieved in the open North Sea in 2001 / 2002 (Thomas et al., 2009). Subsequent
467 simulations that included TA export from aerobic and anaerobic processes in the sediment
468 improved the agreement between data and models (Pätsch et al., 2018). When focusing on
469 the German Bight, however, the observed high TA concentrations in summer measurements
470 east of 7° E could not be simulated satisfactorily.

471 The present study confirms the Wadden Sea as an important TA source for the German Bight
472 and quantifies the annual Wadden Sea TA export rate to $39 \text{ Gmol TA yr}^{-1}$. Additionally, the
473 contributions by most important rivers have been more precisely quantified and narrow down
474 uncertainties in the budgets of TA and DIC in the German Bight. All steps that were required
475 to calculate the budget including uncertainties are discussed in the following.

476

477 ***4.1. Uncertainties of Wadden Sea – German Bight exchange rates of TA and DIC***

478 The Wadden Sea is an area of effective benthic decomposition of organic material (Böttcher
479 et al., 2004; Billerbeck et al., 2006; Al-Rai et al., 2009; van Beusekom et al., 2012) originating
480 both from land and from the North Sea (Thomas et al., 2009). In general, anaerobic
481 decomposition of the organic matter generates TA and increases the CO_2 buffer capacity of
482 seawater. On longer time scales TA can only be generated by processes that involve
483 permanent loss of anaerobic remineralisation products (Hu and Cai, 2011). A second
484 precondition is the nutrient availability to produce organic matter, which in turn serves as
485 necessary component of anaerobic decomposition (Gustafsson et al., 2019). The Wadden Sea
486 export rates of TA and DIC modelled in the present study are based on concentration
487 measurements during tidal cycles in the years 2002 and 2009 to 2011 (Table 1), and on

488 calculated tidal prisms of two day-periods that are considered to be representative of annual
489 mean values. This approach introduces uncertainties with respect to the true amplitudes of
490 concentrations differences in the tidal cycle and in seasonality due to the fact that differences
491 in concentrations during falling and rising water levels were linearly interpolated. These
492 interpolated values are based on four to five measurements in the three export areas and
493 were conducted in different years. Consequently, the approach does not reproduce the exact
494 TA and DIC concentrations in the years 2001 to 2009, because only meteorological forcing,
495 river loads and nitrogen deposition were specified for these particular years. The simulation
496 of scenario-B thus only approximates Wadden Sea export rates. More measurements
497 distributed with higher resolution over the annual cycle would clearly improve our estimates.
498 Nevertheless, the implementation of Wadden Sea export rates here results in improved
499 reproduction of observed high TA concentrations in the German Bight in summer in
500 comparison to the reference run A (Fig.-3).

501 We calculated the sensitivity of our modelled annual TA export rates on uncertainties of the
502 Δ -values of Table-1. As the different areas North- and East Frisian Wadden Sea and Jade Bay
503 has different exchange rates of water, for each region the uncertainty of $1\text{-}\mu\text{mol-kg}^{-1}$ in ΔTA
504 at all times has been calculated. The East Frisian Wadden Sea export would differ by
505 $0.84\text{-Gmol-TA-yr}^{-1}$, the Jade Bay export by $0.09\text{-Gmol-TA-yr}^{-1}$ and the North Frisian export by
506 3-Gmol-TA-yr^{-1} .

507 Primary processes that contribute to the TA generation in the Wadden Sea are denitrification,
508 sulphate reduction, or processes that are coupled to sulphate reduction and other processes
509 (Thomas et al., 2009). In our model, the implemented benthic denitrification does not
510 generate TA (Seitzinger & Giblin, 1996), because modelled benthic denitrification does not
511 consume nitrate (Pätsch & Kühn, 2008). Benthic denitrification is coupled to nitrification in the
512 upper layer of the sediment (Raaphorst et al., 1990), giving reason for neglecting TA
513 generation by this process in the model. The modelled production of N_2 by benthic
514 denitrification falls in the range of $20\text{--}25\text{-Gmol-N-yr}^{-1}$ in the validation area, which would
515 result in a TA production of about $19\text{--}23\text{-Gmol-TA-yr}^{-1}$ (Brenner et al., 2016). In the model
516 nitrate uptake by phytoplankton produces about $40\text{-Gmol-TA-yr}^{-1}$, which partly compensates
517 the missing TA generation by benthic denitrification. This amount of nitrate would not fully be
518 available for primary production if parts of it would be consumed by denitrification. Different

519 from this, the TA budget of Thomas et al. (2009) included estimates for the entire benthic
520 denitrification as a TA generating process.

521 Sulphate reduction (not modelled here) also contributes to alkalinity generation. On longer
522 time scales the net effect is vanishing as the major part of the reduced components are
523 immediately re-oxidized~~oxidised~~ in contact with oxygen. Iron- and sulphate- reduction
524 generates TA but only their reaction product iron sulphide (essentially pyrite) conserves the
525 reduced components from re-oxidation. As the formation of pyrite consumes TA, the TA
526 contribution of iron reduction in the North Sea is assumed to be small and to balance that of
527 pyrite formation (Brenner et al., 2016).

528 Atmospheric nitrogen deposition is taken into account in the simulations. Oxidised N-species
529 (NO_x) dominate reduced species (NH_y) slightly in the validation area during 6 out of 9
530 simulation years. This implies that the deposition of dissolved inorganic nitrogen decreases TA
531 in 6 of 9 years. The average decrease within 6 years is about $0.4 \text{ Gmol TA yr}^{-1}$, whereas the
532 average increase within 3 years is only $0.1 \text{ Gmol TA yr}^{-1}$. Thomas et al. (2009) also assumed
533 a dominance of oxidised species and consequently defined a negative contribution to the TA
534 budget.

535 Dissolution of biogenic carbonates may be an efficient additional enhancement of the CO_2
536 buffer capacity (that is: source of TA), since most of the tidal flat surface sediments contain
537 carbonate shell debris (Hild, 1997). On the other hand, shallow oxidation of biogenic methane
538 formed in deep and shallow tidal flat sediments (not modelled) (Höpner & Michaelis, 1994;
539 Neira & Rackemann, 1996; Böttcher et al., 2007) has the potential to lower the buffer capacity,
540 thus counteracting or balancing the respective effect of carbonate dissolution. The impact of
541 methane oxidation on the developing TA / DIC ratio in surface sediments, however, is
542 complex and controlled by a number of superimposing biogeochemical processes (e.g., Akam
543 et al., 2020).

544 The net effect of evaporation and precipitation in the Wadden Sea also has to be considered
545 in budgeting TA. Although these processes are balanced in the North Sea (Schott, 1966),
546 enhanced evaporation can occur in the Wadden Sea due to increased heating during low tide
547 around noon. Onken & Riethmüller (2010) estimated an annual negative freshwater budget
548 in the Hörnum Basin based on long-term hydrographic time series from observations in a tidal

549 channel. From this data a mean salinity difference between flood and ebb currents of
550 approximately -0.02 is calculated. This would result in an increased TA concentration of
551 $1\text{-}\mu\text{mol-TA-kg}^{-1}$, which is within the range of the ~~inaccuracy~~uncertainty of measurements.
552 Furthermore, the enhanced evaporation estimated from subtle salinity changes interferes
553 with potential input of submarine groundwater into the tidal basins, that been identified by
554 Moore et al. (2011), Winde et al. (2014), and Santos et al. (2015). The magnitude of this input
555 is difficult to estimate at present, for example from salinity differences between flood and ebb
556 tides, because the composition of SGD passing the sediment-water interfacial mixing zone has
557 to be known. Although first characteristics have been reported (Moore et al., 2011; Winde et
558 al., 2014; Santos et al., 2015), the quantitative effect of additional DIC, TA, and nutrient input
559 via both fresh and recirculated SGD into the Wadden Sea remains unclear.

560 An input of potential significance are small inlets that provide fresh water as well as DIC and
561 TA (Table-3). The current data base for seasonal dynamics of this source, however, is limited
562 and, therefore, this source cannot yet be considered quantitatively in budgeting approaches.

563

564 **4.2 TA / DIC ratios over the course of the year**

565

566

567 Ratios of TA and DIC generated in the tidal basins (Table-1) give some indication of the
568 dominant biogeochemical mineralisation and re-oxidation processes occurring in the
569 sediments of individual Wadden Sea sectors, although these processes have not been
570 explicitly modelled here (Chen & Wang, 1999; Zeebe & Wolf-Gladrow, 2001; Thomas et al.
571 2009; Sippo et al., 2016; Wurgaft et al., 2019; Akam et al., 2020). Candidate processes are
572 numerous and the export ratios certainly express various combinations, but the most
573 quantitatively relevant likely are aerobic degradation of organic material (resulting in a
574 reduction of TA due to nitrification of ammonia to nitrate with a TA / DIC ratio of -0.16),
575 denitrification (TA / DIC ratio of 0.8, see Rassmann et al., 2020), and anaerobic processes
576 related to sulphate reduction of organoclastic material (TA / DIC ratio of 1, see Sippo et al.,
577 2016). Other processes are aerobic (adding only DIC) and anaerobic (TA / DIC ratio of 2)
578 oxidation of upward diffusing methane, oxidation of sedimentary sulphides upon
579 resuspension into an aerated water column (no effect on TA / DIC) followed by oxidation of

580 iron (~~adding~~consuming TA), and nitrification of ammonium (consuming TA, TA/DIC ratio is -
581 2, see Pätsch et al., 2018 and Zhai et al. 2017).

582 The TA/DIC export ratios of DIC and TA for the individual tidal basins in three Wadden Sea
583 sectors (East Frisian, Jade Bay and North Frisian) as calculated from observed Δ TA and Δ DIC
584 over tidal cycles in different seasons are depicted in Fig. 9. They may give an indication of
585 regionally and seasonally varying processes occurring in the sediments of the three study
586 regions. The ratios vary between 0.2 and 0.5 in the North Frisian Wadden Sea with slightly
587 more TA than DIC generated in spring, summer and autumn, and winter having a negative
588 ratio of -0.5. The winter ratio coincides with very small measured differences of DIC in
589 imported and exported waters (Δ DIC = -2 μ mol kg^{-1}) and the negative TA/DIC ratio may
590 thus be spurious. The range of ratios in the other seasons is consistent with sulphate reduction
591 and denitrification as the dominant processes in the North Frisian tidal basins.

592 The TA / DIC ratios in the Jade Bay samples were consistently higher than those in the North
593 Frisian tidal basin and vary between 1 and 2 in spring and summer, suggesting a significant
594 contribution by organoclastic sulphate reduction and anaerobic oxidation of methane
595 (Al-Raei et al., 2009). The negative ratio of -0.4 in autumn is difficult to explain with
596 remineralisation or re-oxidation processes, but as with the fall ratio in Frisian tidal basin, it
597 coincides with a small change in Δ DIC (-3 μ mol kg^{-1}) at positive Δ TA (8 μ mol kg^{-1}). Taken at
598 face value, the resulting negative ratio of -0.4 implicates a re-oxidation of pyrite, normally ~~on~~at
599 timescales of early diagenesis thermodynamically stable (Hu and Cai, 2011), possibly
600 promoted by increasing wind forces and associated aeration and sulphide oxidation of anoxic
601 sediment layers (Kowalski et al., 2013). The DIC export rate from Jade Bay had its minimum in
602 autumn, consistent with a limited supply and mineralisation of organic matter, possibly
603 modified by seasonally changing impacts from small tidal inlets (Table 3).

604 The TA / DIC ratio of the East Frisian Wadden Sea is in the approximate range of those in Jade
605 Bay, but has one unusually high ratio in November caused by a significant increase in TA of
606 14 μ mol kg^{-1} at a low increase of 5 μ mol kg^{-1} in DIC. Barring an analytical artefact, the
607 maximum ratio of 3 may reflect a short-term effect of iron reduction.

608 Based on these results, processes in the North Frisian Wadden Sea export area differ from the
609 East Frisian Wadden Sea and the Jade Bay areas. The DIC export rates suggest that significant

610 amounts of organic matter were degraded in North Frisian tidal basins, possibly controlled by
611 higher daily exchanged water masses in the North Frisian ($8.1 \text{ km}^3 \text{ d}^{-1}$) than in the East Frisian
612 Wadden Sea ($2.3 \text{ km}^3 \text{ d}^{-1}$) and in the Jade Bay ($0.8 \text{ km}^3 \text{ d}^{-1}$) (compare Table 2). On the other
613 hand, TA export rates of the North Frisian and the East Frisian Wadden Sea were in the same
614 range.

615 Regional differences in organic matter mineralisation in the Wadden Sea have been discussed
616 by van Beusekom et al. (2012) and Kowalski et al. (2013) in the context of connectivity with
617 the open North Sea and influences of eutrophication and sedimentology. They suggested that
618 the organic matter turnover in the entire Wadden Sea is governed by organic matter import
619 from the North Sea, but that regionally different eutrophication effects as well as sediment
620 compositions modulate this general pattern. The reason for regional differences may be
621 related to the shape and size of the individual tidal basins. van Beusekom et al. (2012) found
622 that wider tidal basins with a large distance between barrier islands and mainland, as is the
623 case in the North Frisian Wadden Sea, generally have a lower eutrophication status than
624 narrower basins predominating in the East Frisian Wadden Sea. Together with the high water
625 exchange rate the accumulation of organic matter is reduced in the North Frisian Wadden Sea
626 and the oxygen demand per volume is lower than in the more narrow eutrophicated basins.
627 Therefore, aerobic degradation of organic matter dominated in the North Frisian Wadden Sea,
628 where the distance between barrier islands and mainland is large. This leads to less TA
629 production (in relation to DIC production) than in the East Frisian Wadden Sea, where
630 anaerobic degradation of organic matter dominated in more restricted tidal basins.

631

632 **4.3. TA budgets and variability of TA mass inventory in the German Bight**

633 Modelled TA and DIC concentrations in the German Bight have a high interannual and seasonal
634 variability (Fig. 8). The interannual variability of the model results are mainly driven by the
635 physical prescribed environment. Overall, the TA variability is more sensitive to Wadden Sea
636 export rates than DIC variability, because the latter is dominated by biological processes.
637 However, the inclusion of Wadden Sea DIC export rates improved correspondence with
638 observed DIC concentrations in the near-coastal North Sea.

639 It is a logical step to attribute the TA variability to variabilities of the different sources. In order
640 to calculate a realistic budget, scenario_B was considered. Annual and seasonal budgets of TA
641 sources and sinks in this scenario are shown in Table_6. Note that Riv_{eff} is not taken into
642 account for the budget calculations. This is explained in the Method Section [2.2.2](#) “River
643 Input”.

644 Comparing the absolute values of all sources and sinks of the mean year results in a relative
645 ranking of the processes. 41% of all TA massinventory changes in the validation area were
646 due to river loads, 37% were due to net transport, 16% were due to Wadden Sea export
647 rates, 6% were due to internal processes. River input ranged from 78 to 152 $Gmol_TA_yr^{-1}$
648 and had the highest absolute variability of all TA sources in the validation area. This is mostly
649 due to the high variability of annual freshwater discharge, which is indicated by low (negative)
650 values of Riv_{eff} . The latter values show that the riverine TA loads together with the freshwater
651 flux induce a small dilution of TA in the validation area for each year. Certainly, this ranking
652 depends mainly on the characteristics of the Elbe estuary. Due to the high concentration of
653 TA in rivers Rhine and Meuse (Netherlands) they had an effective river input of
654 +24 $Gmol_TA_yr^{-1}$ in 2008, which constitutes a much greater impact on TA concentration
655 changes than the Elbe river. In a sensitivity test, we switched off the TA loads of rivers Rhine
656 and Meuse for the year 2008 and found that the net flow of $-71 Gmol_TA_yr^{-1}$ decreased to
657 $-80 Gmol_TA_yr^{-1}$, which indicates that water entering the validation box from the western
658 boundary is less TA-rich in the test case than in the reference run.

659 At seasonal time scales (Table_6 lower part) the net transport dominated the variations from
660 October to March, while internal processes play a more important role from April to June
661 (28%). The impact of effective river input was less than 5% in every quarter. The Wadden
662 Sea TA export rates had an impact of 36% on TA mass changes in the validation area from
663 July to September. Note that these percentages are related to the sum of the absolute values
664 of the budgeting terms.

665 Summing up the sources and sinks, Wadden Sea exchange rates, internal processes and
666 effective river loads resulted in highest sums in 2002 and 2003 (51 and 52 $Gmol_TA_yr^{-1}$) and
667 lowest in 2009 (44 $Gmol_TA_yr^{-1}$). For the consideration of TA variation we excluded net
668 transport and actual river loads, because these fluxes are diluted and do not necessarily

669 change the TA concentrations. In agreement with this, the highest TA concentrations were
670 simulated in summer 2003 (Fig.-8). The high interannual variability of summer concentrations
671 was driven essentially by hydrodynamic differences between the years. Flushing times and
672 their interannual variability were higher in summer than in winter (Fig.-6) of every year. High
673 flushing times or less strong circulation do have an accumulating effect on exported TA in the
674 validation area. To understand the reasons of the different flushing times monthly stream
675 patterns were analysed (Fig.-7). Distinct anticlockwise stream patterns defined the
676 hydrodynamic conditions in every winter. Summer stream patterns were in most years
677 weaker, especially in the German Bight (compare Fig.-7, June-2003). In August-2003 the
678 eastern part of the German Bight shows a clockwise rotation, which transports TA-enriched
679 water from July back to the Wadden-Sea area for further enrichment. This could explain the
680 highest concentrations in summer 2003.

681 Thomas et al. (2009) estimated that $73 \text{ Gmol TA yr}^{-1}$ were produced in the Wadden Sea. Their
682 calculations were based on measurements in 2001 and 2002. The presented model was
683 validated with data measured in August 2008 (Salt et al., 2013) at the same positions. High TA
684 concentrations in the German Bight were observed in summer 2001 and in summer 2008. Due
685 to the scarcity of data, the West Frisian Wadden Sea was not considered in the simulations,
686 but, as the western area is much larger than the eastern area, the amount of exported TA from
687 that area can be assumed to be in the same range as from the East Frisian Wadden Sea (10 to
688 $14 \text{ Gmol TA yr}^{-1}$). With additional export from the West Frisian Wadden Sea, the maximum
689 overall Wadden Sea export may be as high as $53 \text{ Gmol TA yr}^{-1}$. Thus, the TA export from the
690 Wadden Sea calculated in this study is 20 to $34 \text{ Gmol TA yr}^{-1}$ lower than that assumed in
691 the study of Thomas et al. (2009). This is mainly due to the flushing time that was assumed by
692 Thomas et al. (2009). They considered the water masses to be flushed within six weeks
693 (Lenhart et al., 1995). Flushing times calculated in the present study were significantly longer
694 and more variable in summer. Since the Wadden Sea export calculated by Thomas et al. (2009)
695 was defined as a closing term for the TA budget, underestimated summerly flushing times led
696 to an overestimation of the exchange with the adjacent North Sea.

697 Table-4 shows that our scenario-B underestimates the observed TA concentration by about
698 $5.1 \text{ } \mu\text{mol kg}^{-1}$ in 2008. Scenario-A has lower TA concentration than scenario-B in the
699 validation area. The difference is about $11 \text{ } \mu\text{mol kg}^{-1}$. This means that the Wadden Sea export

700 of 39 Gmol TA yr⁻¹ results in a concentration difference of 11 μmol kg⁻¹. Assuming linearity,
701 the deviation between scenario B and the observations (5.1 μmol kg⁻¹) would be
702 compensated by an additional Wadden Sea export of about 18 Gmol TA yr⁻¹. If we assume
703 that the deviation between observation and scenario B is entirely due to uncertainties or
704 errors in the Wadden Sea export estimate, then the uncertainty of this export is
705 18 Gmol TA yr⁻¹.

706 Another problematic aspect in the TA export estimate by Thomas et al. (2009) is the fact that
707 their TA budget merges the sources of anaerobic TA generation from sediment and from the
708 Wadden Sea into a single source “anaerobic processes in the Wadden Sea”. Burt et al. (2014)
709 found a sediment TA generation of 12 mmol TA m⁻² d⁻¹ at one station in the German Bight
710 based on Ra-measurements. This fits into the range of microbial gross sulphate reduction rates
711 reported by Al-Raei et al. (2009) in the ~~backbarrier~~back-barrier tidal areas of Spiekeroog island,
712 and by Brenner et al. (2016) at the Dutch coast. Within the latter paper, the different sources
713 of TA from the sediment were quantified. The largest term was benthic calcite dissolution,
714 which would be cancelled out in terms of TA generation assuming a steady-state
715 compensation by biogenic calcite production. Extrapolating the southern North Sea TA
716 generation (without calcite dissolution) from the data for one station of Brenner et al. (2016)
717 results in an annual TA production of 12.2 Gmol in the German Bight (Area = 28.415 km²).
718 This is likely an upper limit of sediment TA generation, as the measurements were done in
719 summer when seasonal fluxes are maximal. This calculation reduces the annual Wadden Sea
720 TA generation estimated by Thomas et al. (2009) from 73 to 61 Gmol, which is still higher than
721 our present estimate. In spite of the unidentified additional TA-fluxes, both the estimate by
722 Thomas et al. (2009) and our present model-based quantification confirm the importance of
723 the Wadden-Sea export fluxes of TA on the North Sea carbonate system at present and in the
724 future.

725 **4.4. 4.4 The impact of exported TA and DIC on the North Sea and influences on** 726 **export magnitude**

727 Observed high TA and DIC concentrations in the SE North Sea are mainly caused by TA and DIC
728 export from the Wadden Sea (Fig. 3-5). TA concentrations could be better reproduced than
729 DIC concentrations in the model experiments, which was mainly due to the higher sensitivity

730 of DIC to modelled biology. Nevertheless, from a present point of view the Wadden Sea is the
731 main driver of TA concentrations in the German Bight. Future forecast studies of the evolution
732 of the carbonate system in the German Bight will have to specifically focus on the Wadden
733 Sea and on processes occurring there. In this context the Wadden Sea evolution during future
734 sea level rise is the most important factor. The balance between sediment supply from the
735 North Sea and sea level rise is a general precondition for the persistence of the Wadden Sea
736 (Flemming and Davis, 1994; van Koningsveld et al., 2008). An accelerating sea level rise could
737 lead to a deficient sediment supply from the North Sea and shift the balance at first in the
738 largest tidal basins and at last in the smallest basins. (CPSL, 2001; van Goor et al., 2003). The
739 share of intertidal flats as potential sedimentation areas is larger in smaller tidal basins (van
740 Beusekom et al., 2012), whereas larger basins have a larger share of subtidal areas. Thus,
741 assuming an accelerating sea level rise, large tidal basins will turn into lagoons, while tidal flats
742 may still exist in smaller tidal basins. This effect could decrease the overall Wadden Sea export
743 rates of TA, because sediments would no longer be exposed to the atmosphere and the
744 products of sulphate reduction would ~~reoxidise~~re-oxidise in the water column. Moreover,
745 benthic-pelagic exchange in the former intertidal flats would be more diffusive and less
746 advective than today due to a lowering of the hydraulic gradients during ebb tides, when parts
747 of the sediment become unsaturated with water. This would decrease TA export into the
748 North Sea. Caused by changes in hydrography and sea level the sedimentological composition
749 may also change. If sediments become more sandy, aerobic degradation of organic matter is
750 likely to become more important (de Beer et al., 2005). In fine grained silt diffusive transport
751 plays a key role, while in the upper layer of coarse (sandy) sediments advection is the
752 dominant process. Regionally, the North Frisian Wadden Sea will be more affected by rising
753 sea level because there the tidal basins are larger than the tidal basins in the East Frisian
754 Wadden Sea and even larger than the inner Jade Bay.

755 The Wadden Sea export of TA and DIC is driven by the turnover of organic material. Decreasing
756 anthropogenic eutrophication can lead to decreasing phytoplankton biomass and production
757 (Cadée & Hegeman, 2002; van Beusekom et al., 2009). Thus, the natural variability of the
758 North Sea primary production becomes more important in determining the organic matter
759 turnover in the Wadden Sea (McQuatters-Gollop et al., 2007; McQuatters-Gollop & Vermaat,
760 2011). pH values in Dutch coastal waters decreased from 1990 to 2006 drastically. Changes in

761 nutrient variability were identified as possible drivers (Provoost et al., 2010), which is
762 consistent with model simulations by Borges and Gypens (2010). Moreover, despite the
763 assumption of decreasing overall TA export rates from the Wadden Sea the impact of the
764 North Frisian Wadden Sea on the carbonate system of the German Bight could potentially
765 adjust to a change of tidal prisms and thus a modulation in imported organic matter. If less
766 organic matter is remineralised in the North Frisian Wadden Sea, less TA and DIC will be
767 exported into the North Sea.

768 In the context of climate change, processes that have impact on the freshwater budget of tidal
769 mud flats will gain in importance. Future climate change will have an impact in coastal
770 hydrology due to changes in ground water formation rates (Faneca Sánchez et al., 2012;
771 Sulzbacher et al., 2012), that may change both surface and subterranean run-off into the
772 North Sea. An increasing discharge of small rivers and groundwater into the Wadden Sea is
773 likely to increase DIC, TA, and possibly nutrient loads and may enhance the production of
774 organic matter. Evaporation could also increase due to increased warming and become a more
775 important process than today (Onken & Riethmüller, 2010), as will methane cycling change
776 due to nutrient changes, sea level and temperature rise (e.g., Höpner and Michaelis, 1994;
777 Akam et al., 2020).

778 Concluding, in the course of climate change the North Frisian Wadden Sea will be affected first
779 by sea level rise, which will result in decreased TA and DIC export rates due to less turnover of
780 organic matter there. This could lead to a decreased buffering capacity in the German Bight
781 for atmospheric CO₂. Overall, less organic matter will be remineralised in the Wadden Sea.

782

783

784 **5 Conclusion and Outlook**

785

786 We present a budget calculation of TA sources in the German Bight and relate 16% of the
787 annual TA ~~mass inventory~~ changes to TA exports from the Wadden Sea. The impact of riverine
788 bulk TA ~~is seems to be~~ less important ~~in the German Bight than the contribution from the~~
789 ~~Wadden Sea~~ due to the comparatively low TA concentrations in the Elbe estuary, a finding
790 that has to be proven by future research.

791 The evolution of the carbonate system in the German Bight under future ~~anthropogenic or~~
792 ~~climate change~~changes depends on the ~~evolution~~development of the Wadden Sea. The
793 amount of TA and DIC that is exported from the Wadden Sea depends on the amount of
794 organic matter and / or nutrient that ~~is~~are imported from the North Sea and finally
795 remineralised in the Wadden Sea. Decreasing riverine nutrient loads ~~have~~ led to decreasing
796 phytoplankton biomass and production (Cadée & Hegeman, 2002; van Beusekom et al., 2009),
797 a trend that is expected to continue in the future (European Water Framework Directive).
798 However, altered natural dynamics of nutrient cycling and productivity can override the
799 decreasing riverine nutrient loads (van Beusekom et al., 2012), but these will not generate TA
800 in the magnitude of denitrification of ~~riverborne~~river-borne nitrate.

801 ~~In the context of sea~~Sea level rise, in the North Frisian Wadden Sea will potentially be more
802 affected by a loss of intertidal areas than the East Frisian Wadden Sea (van Beusekom et al.,
803 2012). This effect ~~is~~will likely ~~to~~ reduce the turnover of organic material in this ~~sector~~region of
804 the Wadden Sea, which ~~will~~may decrease TA production and ~~decrease the overall input~~transfer
805 into the southern North Sea.

806 Thomas et al. (2009) estimated that the Wadden Sea facilitates approximately 7 – 10% of the
807 annual CO₂ uptake of the North Sea. This is motivation for model studies on the future role of
808 the Wadden Sea in the CO₂ balance of the North Sea under regional climate change.

809 Future research will also have to address the composition and amount of submarine ground
810 water discharge, as well as the magnitude and seasonal dynamics in discharge and
811 composition of small water inlets at the coast, which are ~~currently~~in this study only implicitly
812 included and in other studies mostly ignored due to a lacking data base.

813

814 **Data availability**

815 The river data are available at [https://wiki.cen.uni-](https://wiki.cen.uni-hamburg.de/ifm/ECOHAM/DATA_RIVER)
816 [hamburg.de/ifm/ECOHAM/DATA_RIVER](https://wiki.cen.uni-hamburg.de/ifm/ECOHAM/DATA_RIVER) and www.waterbase.nl. Meteorological data are
817 stored at <https://psl.noaa.gov/>. The North Sea TA and DIC data are
818 stored at <https://doi.org/10.1594/PANGAEA.4>
819 stored at <https://doi.org/10.1594/PANGAEA.438791>

820 (2001), <https://doi.org/10.1594/PANGAEA.441686>
821 ~~(2005)~~.<https://doi.org/10.1594/PANGAEA.441686> (2005). The data of the North Sea cruise
822 2008 have not been published, yet, but can be requested via the CODIS data portal
823 (<http://www.nioz.nl/portals-en>; registration required). Additional Wadden Sea TA and DIC
824 data are deposited under doi:10.1594/PANGAEA.841976.

825

826 **Author contributions**

827 The scientific concept for this study was originally developed by JP and MEB. FS wrote the
828 basic manuscript ~~with~~as part of his PhD thesis. VW provided field analytical data, as part of
829 her PhD thesis. JP developed the original text further with ~~input~~contributions from all co-
830 authors.

831 **Competing interests**

832 The authors declare that they have no conflict of interest.

833

834 **Acknowledgements**

835 ~~na~~The authors appreciate the two constructive reviews, which greatly helped to improve the
836 manuscript, and the editorial handling by Jack Middelburg. I. Lorkowski, Wilfried W. Kühn, and
837 Fabian F. Große are acknowledged for stimulating discussions, S. Grashorn for providing tidal
838 prisms and P. Escher for laboratory support. This work was financially supported by BMBF
839 during the Joint Research Project BIOACID (TP_5.1, ~~support code~~ 03F0608L and TP_3.4.1,
840 ~~support code~~ 03F0608F), with further support from Leibniz Institute for Baltic Sea Research.
841 We also acknowledge the support by the Cluster of Excellence 'CliSAP' (EXC177), University of
842 Hamburg, funded by the German Science Foundation (DFG) and the support by the German
843 Academic Exchange service (DAAD, MOPGA-GRI, #57429828) with funds of the German
844 Federal Ministry of Education and Research (BMBF). We used NCEP Reanalysis data provided
845 by the NOAA/OAR/ESRL PSL, Boulder, Colorado, USA, from their Web site at
846 <https://psl.noaa.gov/>L.

847

848

849 **Tables**

850 **Table-1: Mean TA and DIC concentrations [$\mu\text{mol}\cdot\text{l}^{-1}$] during rising and falling water levels**
 851 **and the respective differences (Δ -values) that were used as wad_sta in (1). Areas are the**
 852 **North Frisian (N), the East Frisian (E) Wadden Sea and the Jade Bay (J).**

Area	Date	TA (rising)	TA (falling)	Δ TA	DIC (rising)	DIC (falling)	Δ DIC
N	29.04.2009	2343	2355	12	2082*	2106	24
	17.06.2009	2328	2332	4	2170	2190	20
	26.08.2009	2238	2252	14	2077	2105	28
	05.11.2009	2335	2333	-2	2205	2209	4
J	20.01.2010	2429	2443	14	2380	2392	12
	21.04.2010	2415	2448	33	2099	2132	33
	26.07.2010	2424	2485	61	2159	2187	28
	09.11.2010	2402	2399	-3	2302	2310	8
E	03.03.2010	2379	2393	14	2313	2328	15
	07.04.2010	2346	2342	-4	2068	2082	14
	17./18.05.2011	2445	2451	6	2209	2221	12
	20.08.2002	2377	2414	37	2010	2030	20
	01.11.2010	2423	2439	16	2293	2298	5

853 *: This value was estimated.

854

855 **Table-2: Daily Wadden Sea runoff to the North Sea at different export areas.**

Position	wad_exc [$10^6 \text{ m}^3 \text{ d}^{-1}$]
N1	273
N2	1225
N3	1416
N4	1128
N5	4038
N6	18
J1 - J3	251
E1	380
E2	634
E3	437
E4	857

856

857

858

859 **Table_3: Examples for the carbonate system composition of small fresh water inlets**
 860 **draining into the Jade Bay and the backbarrier tidal area of Spiekeroog Island, given in**
 861 **($\mu\text{mol}\cdot\text{kg}^{-1}$). Autumn results (A) (October 31st, 2010) are taken from Winde et al. (2014);**
 862 **spring sampling (S) took place on May 20th, 2011.**

Site	Position	DIC(A)	-TA(A)	DIC(S)	TA(S)
Neuharlingersiel	53°41.944 N 7°42.170 E	2319	1773	1915	1878
Harlesiel	53°42.376 N 7°48.538 E	3651	3183	1939	1983
Wanger- Horumersiel	53°41.015 N 8°1.170 E	5405	4880	6270	6602
Hooksiel	53°38.421 N 8°4.805 E	2875	3105	3035	3302
Maade	53°33.534 N 8°7.082 E	5047	4448	5960	6228
Mariensiel	53°30.895 N 8°2.873 E	6455	5904	3665	3536
Dangaster Siel	53°26.737N 8°6.577 E	1868	1246	1647	1498
Wappelersiel	53°23.414 N 8°12.437 E	1373	630	1358	1152
Schweiburger Siel	53°24.725 N 8°16.968 E	4397	3579	4656	4493
Eckenwarder Siel	53°31.249 N 8°16.527 E	6542	6050	2119	4005

863
 864
 865
 866

867
868
869
870

871
872
873

874
875
876
877
878
879
880
881
882

Table 4: Averages ($\mu\text{mol}\cdot\text{kg}^{-1}$), standard deviations ($\mu\text{mol}\cdot\text{kg}^{-1}$), RMSE ($\mu\text{mol}\cdot\text{kg}^{-1}$), and correlation coefficients r for the observed TA concentrations and the corresponding scenarios A and B within the validation area.

TA	Average	Stdv	RMSE	r
Obs 2008	2333.52	32.51		
Obs 2005	2332.09	21.69		
Obs 2001	2333.83	33.19		
Sim A 2008	2327.64	6.84	27.97	0.77
Sim A 2005	2322.16	5.21	22.05	0.45
Sim A 2001	2329.79	5.32	31.89	0.24
Sim B 2008	2338.60	22.09	-18.34	-0.86
Sim B 2005	2339.48	26.81	31.81	0.18
Sim B 2001	2342.96	17.28	30.07	0.47

883
884
885
886
887
888
889
890
891
892
893
894
895
896

Table_5: Averages ($\mu\text{mol}\cdot\text{kg}^{-1}$), standard deviations ($\mu\text{mol}\cdot\text{kg}^{-1}$), RMSE ($\mu\text{mol}\cdot\text{kg}^{-1}$), and correlation coefficients r for the observed DIC concentrations and the corresponding scenarios A and B within the validation area.

DIC	Average	Stdv	RMSE	r
Obs 2008	2107.05	24.23		
Obs 2005	2098.20	33.42		
Obs 2001	2105.49	25.21		
Sim A 2008	2080.93	14.24	-43.48	-0.64
Sim A 2005	2083.53	21.94	26.97	0.73
Sim A 2001	2077.53	17.61	38.89	0.22
Sim B 2008	2091.15	9.25	-25.87	-0.55
Sim B 2005	2101.26	10.97	33.96	0.10
Sim B 2001	2092.69	11.71	25.33	0.48

897

898 **Table 6: Annual TA budgets in the validation area of the years 2001 to 2009, annual**
 899 **averages and seasonal budgets of ~~from~~ January to March, April to June, July to September**
 900 **and October to December [Gmol]. Net Flow is the annual net TA transport across the**
 901 **boundaries of the validation area. Negative values indicate a net export from the**
 902 **validation area to the adjacent North Sea. Δ content indicates the difference of the TA**
 903 **contents between the last and the first time steps of the simulated year or quarter.**

	Wadden Sea export Gmol/yr	internal processes Gmol/yr	river loads Gmol/yr	Riv _{eff} Gmol/yr	net flow Gmol/yr	Δ content Gmol
2001	39	13	87	-5	38	177
2002	39	19	152	-7	-223	-13
2003	39	16	91	-3	-98	48
2004	39	13	78	-5	-8	122
2005	39	12	89	-5	-98	42
2006	39	12	88	-4	-56	83
2007	39	12	110	-5	-132	29
2008	39	14	93	-5	-71	75
2009	39	10	83	-5	-151	-19
Average	Gmol/yr 39	Gmol/yr 14	Gmol/yr 101	Gmol/yr -5	Gmol/yr -89	Gmol 65
t = 3 mon	Gmol/t	Gmol/t	Gmol/t	Gmol/t	Gmol/t	Gmol
Jan - Mar	-7	-1	38	-1	-49	-5
Apr - Jun	10	15	23	-2	6	54

Jul -						
Sep	17	-2	15	-2	13	43
Oct -						
Dec	4	1	25	0	-56	-26

6. Figure Captions

Figure-1: Upper panel: Map of the ~~southeastern~~south-eastern North Sea and the bordering land. Lower panel: Model domains of ECOHAM (red) and FVCOM (blue), positions of rivers 1 – 16 (left, see Table-2) and the Wadden Sea export areas grid cells (right). The magenta edges identify the validation area, western and eastern part separated by the magenta dashed line.

Figure-2: Monthly Wadden Sea export of DIC and TA [$\text{Gmol}_{\text{mon}}^{-1}$] at the North Frisian coast-(N), East Frisian coast-(E) and the Jade Bay in scenario-B. The export rates were calculated for DIC and TA based on measured concentrations and simulated water fluxes.

Figure-3: Surface TA concentrations [$\mu\text{mol}_{\text{TA}}\text{kg}^{-1}$] in August-2008 observed-(a) and simulated with scenario-A-(b) and B-(c). The black lines indicate the validation box.

Figure-4: Differences between TA surface summer observations and results from scenario-A-(a) and B-(b) and the differences between DIC surface observations and results from scenario-A-(c) and B-(d), all in $\mu\text{mol}_{\text{kg}}^{-1}$. The black lines indicate the validation box.

Figure-5: Surface DIC concentrations [$\mu\text{mol}_{\text{DIC}}\text{kg}^{-1}$] in August-2008 observed-(a) and simulated with scenario-A-(b) and B-(c). The black lines indicate the validation box.

Figure-6: Flushing times in the validation area in summer (June to August) and winter (January to March). The whole validation area is represented in blue, green is the western part of the validation area (4.5°E to 7°E) and red is the eastern part (east of 7°E).

Figure-7: Monthly mean simulated streamlines for summer months 2003 and 2008.

925 Figure_8: Simulated monthly mean concentrations of TA (scenario_A_(a), scenario_B_(b))
926 [$\mu\text{mol_TA_kg}^{-1}$] and DIC (scenario_A_(c), scenario_B_(d)) [$\mu\text{mol_DIC_kg}^{-1}$] in the validation area
927 for the years 2001-2009.

928 ~~Fig. Figure~~ 9: Temporally interpolated TA/DIC ratio of the export rates in the North Frisian,
929 East Frisian, and Jade Bay. These ratios are calculated using the Δ -values of Table_1.

930

931 **7. References**

932
933 Akam, S.A., Coffin, R.B., Abdulla, H.A.N., and Lyons T.W.: ~~Dissovlved~~Dissolved inorganic
934 carbon pump in methane-charged shallow marine sediments: State of the art and new
935 model perspectives. *Frontiers in Marine Sciences* 7, 206, DOI: 10.3389/FMARS.2020.00206,
936 2020.

937 Al-~~Rai~~Raei, A.M., Bosselmann, K., Böttcher, M.E., Hespeneide, B., and Tauber, F.: Seasonal
938 dynamics of microbial sulfate reduction in temperate intertidal surface sediments: Controls
939 by temperature and organic matter. *Ocean Dynamics* 59, 351-370, 2009.

940 Amann, T., Weiss, A., and Hartmann, J.: Inorganic Carbon Fluxes in the Inner Elbe Estuary,
941 Germany, *Estuaries and Coasts* 38(1), 192-210, doi:10.1007/s12237-014-9785-6, 2015.

942
943 Artioli, Y., Blackford, J. C., Butenschön, M., Holt, J. T., Wakelin, S. L., Thomas, H., Borges, A.
944 V., and Allen, J. I.: The carbonate system in the North Sea: Sensitivity and model validation,
945 *Journal of Marine Systems*, 102-104, 1-13, doi:10.1016/j.jmarsys.2012.04.006, 2012.

946
947 Backhaus, J.O.: A three-dimensional model for the simulation of shelf sea dynamics, *Ocean*
948 *Dynamics*, 38(4), 165–187, doi:10.1016/0278-4343(84)90044-X, 1985.

949
950 Backhaus, J.O., and Hainbucher, D.: A finite difference general circulation model for shelf
951 seas and its application to low frequency variability on the North European Shelf, *Elsevier*
952 *Oceanography Series*, 45, 221–244, doi:~~10.1016/S0422-9894(08)70450-1~~10.1016/S0422-
953 9894(08)70450-1, 1987.

954
955 Ben-Yaakov, S.: pH BUFFERING OF PORE WATER OF RECENT ANOXIC MARINE SEDIMENTS,
956 *Limnology and Oceanography*, 18, doi: 10.4319/lo.1973.18.1.0086, 1973.

957
958 Berner, R. A., Scott, M. R., and Thomlinson, C.: Carbonate alkalinity in the pore waters of
959 anoxic marine sediments. *Limnology & Oceanography*, 15, 544–549,
960 doi:10.4319/lo.1970.15.4.0544, 1970.

961
962 Billerbeck, M., Werner, U., Polerecky, L., Walpersdorf, E., de Beer, D., [and](#) Hüttel, M.:
963 Surficial and deep pore water circulation governs spatial and temporal scales of nutrient
964 recycling in intertidal sand flat sediment. *Mar Ecol Prog Ser* 326, 61-76, 2006.
965
966 Böttcher, M.E., Al-Raei, A.M., Hilker, Y., Heuer, V., Hinrichs, K.-U., [and](#) Segl, M.: Methane and
967 organic matter as sources for excess carbon dioxide in intertidal surface sands:
968 Biogeochemical and stable isotope evidence. *Geochimica et Cosmochim Acta* 71, A111,
969 2007.
970
971 Böttcher, M.E., Hespeneide, B., Brumsack, H.-J., [and](#) Bosselmann, K.: Stable isotope
972 biogeochemistry of the sulfur cycle in modern marine sediments: I. Seasonal dynamics in a
973 temperate intertidal sandy surface sediment. *Isotopes Environ. Health Stud.* 40, 267-283,
974 2004.
975
976 Borges, A. V.: Present day carbon dioxide fluxes in the coastal ocean and possible feedbacks
977 under global change, In *Oceans and the atmospheric carbon content* (P.M. da Silva Duarte &
978 J.M. Santana Casiano Eds), Chapter 3, 47-77, doi:10.1007/978-90-481-9821-4, 2011.
979
980 Borges, A. V. and Gypens, N.: Carbonate chemistry in the coastal zone responds more
981 strongly to eutrophication than to ocean acidification. *Limn. Oceanogr.* 55(1): 346-353, 2010.
982
983 Brasse, J., Reimer, A., Seifert, R., and Michaelis, W.: The influence of intertidal mudflats on
984 the dissolved inorganic carbon and total alkalinity distribution in the German Bight,
985 southeastern North Sea, *J. Sea Res.* 42, 93-103, doi: 10.1016/S1385-1101(99)00020-9, 1999.
986
987 Brenner, H., Braeckman, U., Le Guitton, M., [and](#) Meysman, F. J. R.: The impact of
988 sedimentary alkalinity release on the water column CO₂ system in the North Sea,
989 *Biogeosciences*, 13(3), 841-863, doi:10.5194/bg-13-841-2016, 2016.

990

991 Burt, W. J., Thomas, H., Pätsch, J., Omar, A. M., Schrum, C., Daewel, U., Brenner, H., and de
992 Baar, H. J. W.: -Radium isotopes as a tracer of sediment-water column exchange in the North
993 Sea, *Global Biogeochemical Cycles* 28, pp 19,
994 [doi:10.1002/2014GB004825](https://doi.org/10.1002/2014GB004825)~~doi:10.1002/2014GB004825~~, 2014.

995

996 Burt, W. J., Thomas, H., Hagens, M., Pätsch, J., Clargo, N. M., Salt, L. A., Winde, V., and
997 Böttcher, M. E.: Carbon sources in the North Sea evaluated by means of radium and stable
998 carbon isotope tracers, *Limnology and Oceanography*, 61(2), 666-683,
999 [doi:10.1002/lno.10243](https://doi.org/10.1002/lno.10243)~~doi:10.1002/lno.10243~~, 2016.

1000

1001 Cadée, G. C., and Hegeman, J.: Phytoplankton in the Marsdiep at the end of the 20th century;
1002 30 years monitoring biomass, primary production, and Phaeocystis blooms, *J. Sea Res.* ~~48,~~
1003 ~~97-110~~, [doi:10.1016/S1385-1101\(02\)00161-2](https://doi.org/10.1016/S1385-1101(02)00161-2)~~48, 97-110, doi:10.1016/S1385-1101(02)00161-~~
1004 ~~2~~, 2002.

1005

1006 Cai, W.-J., Hu, X., Huang, W.-J., Jiang, L.-Q., Wang, Y., Peng, T.-H., and Zhang, X.: Surface
1007 ocean alkalinity distribution in the western North Atlantic Ocean margins, *Journal of*
1008 *Geophysical Research*, 115, C08014, [doi:10.1029/2009JC005482](https://doi.org/10.1029/2009JC005482), 2010.

1009

1010 Carvalho, A. C. O., Marins, R. V., Dias, F. J. S., Rezende, C. E., Lefèvre, N., Cavalcante, M. S.,
1011 and Eschrique, S. A.: Air-sea CO₂ fluxes for the Brazilian northeast continental shelf in a
1012 climatic transition region, *Journal of Marine Systems*, 173, 70-80,
1013 [doi:10.1016/j.jmarsys.2017.04.009](https://doi.org/10.1016/j.jmarsys.2017.04.009)~~doi:10.1016/j.jmarsys.2017.04.009~~, 2017.

1014

1015 Chambers, R. M., Hollibaugh, J. T., and Vink, S. M.: Sulfate reduction and sediment
1016 metabolism in Tomales Bay, California, *Biogeochemistry*, 25, 1–18, [doi:10.1007/BF00000509](https://doi.org/10.1007/BF00000509),
1017 1994.

1018

1019 Chen, C.-T. A., [and](#) Wang, S.-L.: Carbon, alkalinity and nutrient budgets on the East China Sea
1020 continental shelf. *Journal of Geophysical Research*, 104, 20,675–20,686,
1021 [doi:10.1029/1999JC900055](https://doi.org/10.1029/1999JC900055), 1999.

1022
1023 Chen, C., Liu, H., and Beardsley, R. C.: An Unstructured Grid, Finite-Volume, Three-
1024 Dimensional, Primitive Equations Ocean Model: Application to Coastal Ocean and Estuaries, J
1025 Atmos Oceanic Technol, 20 (1), 159-186,
1026 ~~doi:10.1175/1520-0426(2003)020<0159:AUGFVT>2.0.CO;2, 2003.~~
1027
1028 ~~doi:10.1175/1520-0426(2003)020<0159:AUGFVT>2.0.CO;2, 2003.~~
1029
1030 CPSL, ~~2001~~. Final Report of the Trilateral Working Group on Coastal Protection and Sea Level
1031 Rise. Wadden Sea Ecosystem No. 13. Common Wadden Sea Secretariat, Wilhelmshaven,
1032 Germany. ~~2001~~.
1033
1034 de Beer, D., ~~Wenzhöfer~~Wenzhöfer, F., ~~Ferdelman~~Ferdelman, T.G., Boehme, S., Huettel, M.,
1035 van Beusekom, J., Böttcher, M.E., Musat, N., ~~Dubilier~~Dubilier, N.: ~~Transport~~Transport and
1036 ~~mineralization~~mineralization rates in North Sea sandy ~~intertidal sediments~~intertidal
1037 ~~sediments~~ (Sylt-Rømø Basin, ~~Waddensea~~). ~~Limnol. Oceanogr~~Waddensea). ~~Limnol. Oceanogr.~~
1038 50, 113-127, 2005.

1039
1040 Dickson, A.G., Afghan, J.D., Anderson, G.C.: Reference materials for oceanic CO₂ analysis: a
1041 method for the certification of total alkalinity. Marine Chemistry 80, 185-197, 2003.
1042
1043 Dollar, S. J., Smith, S. V., Vink, S. M., Obrebski, S., and Hollibaugh, J.T.: Annual cycle of
1044 benthic nutrient fluxes in Tomales Bay, California, and contribution of the benthos to total
1045 ecosystem metabolism, Marine Ecology Progress Series, 79, 115–125,
1046 doi:10.3354/meps079115, 1991.
1047
1048 Duarte, C. M., Hendriks, I. E., Moore, T. S., Olsen, Y. S., Steckbauer, A., Ramajo, L.,
1049 Carstensen, J., Trotter, J. A., ~~and~~ McCulloch, M. Is Ocean Acidification an Open-Ocean
1050 Syndrome? Understanding Anthropogenic Impacts on Seawater pH. Estuaries and Coasts
1051 36(2): 221-236. 2013.

1052
1053 Ehlers, J.: Geomorphologie und Hydrologie des Wattenmeeres. In: Lozan, J.L., Rachor, E., Von

1054 Westernhagen, H., Lenz, W. (Eds.), Warnsignale aus dem Wattenmeer. Blackwell
1055 Wissenschaftsverlag, Berlin, pp. 1–11. 1994.
1056
1057 Faneca Sàncchez, M., Gunnink, J. L., van Baaren, E. S., Oude Essink, G. H. P., Siemon, B.,
1058 Auken, E., Elderhorst, W., de Louw, P. G. B.: Modelling climate change effects on a Dutch
1059 coastal groundwater system using airborne electromagnetic measurements. *Hydrol. Earth
1060 Syst. Sci.* 16(12), 4499-4516, 2012.

1061
1062 Flemming, B. W., and Davis, R. A. J.: Holocene evolution, morphodynamics and
1063 sedimentology of the Spiekeroog barrier island system (southern North Sea). *Senckenb.
1064 Marit.* 25, 117-155, 1994.
1065
1066 Große, F., Kreuz, M., Lenhart, H.-J., Pätsch, J., and Pohlmann, T.: A Novel Modeling Approach
1067 to Quantify the Influence of Nitrogen Inputs on the Oxygen Dynamics of the North Sea,
1068 *Frontiers in Marine Science* 4(383), pp 21, doi:10.3389/fmars.2017.00383, 2017.
1069
1070 Grashorn, S., Lettmann, K. A., Wolff, J.-O., Badewien, T. H., and Stanev, E. V.: East Frisian
1071 Wadden Sea hydrodynamics and wave effects in an unstructured-grid model, *Ocean
1072 Dynamics* 65(3), 419-434, doi:10.1007/s10236-014-0807-5, 2015.
1073
1074 Gustafsson, E., Hagens, M., Sun, X., Reed, D. C., Humborg, C., Slomp, C. P., Gustafsson, B. G.:
1075 Sedimentary alkalinity generation and long-term alkalinity development in the Baltic Sea.
1076 *Biogeosciences* 16(2): 437-456, 2019.

1077 HASEC: OSPAR Convention for the Protection of the Marine Environment of the North-East
1078 Atlantic. Meeting of the Hazardous Substances and Eutrophication Committee (HASEC), Oslo
1079 27 February – 2 March 2012.
1080
1081 Hild, A.: Geochemie der Sedimente und Schwebstoffe im Rückseitenwatt von Spiekeroog
1082 und ihre Beeinflussung durch biologische Aktivität. *Forschungszentrum Terramare Berichte*
1083 5, 71 pp., 1997.

1084 Höpner, T., and Michaelis, H.: Sogenannte ‚Schwarze Flecken‘ – ein Eutrophierungssymptom
1085 des Wattenmeeres. In: L. Lozán, E. Rachor, K. Reise, H. von Westernhagen und W. Lenz.
1086 Warnsignale aus dem Wattenmeer. Berlin: Blackwell, 153-159, 1997.
1087
1088 Hoppema, J. M. J.; The distribution and seasonal variation of alkalinity in the southern bight
1089 of the North Sea and in the western Wadden Sea, Netherlands Journal of Sea Research, 26
1090 (1), 11-23, doi: 10.1016/0077-7579(90)90053-J, 1990.
1091
1092 Hu, X. and Cai, W.-J.: An assessment of ocean margin anaerobic processes on oceanic
1093 alkalinity budget. Global Biogeochemical Cycles 25: 1-11, 2011.
1094
1095 Johannsen, A., Dähnke, K., and Emeis, K.-C.: Isotopic composition of nitrate in five German
1096 rivers discharging into the North Sea, Organic Geochemistry, 39, 1678-1689
1097 doi:10.1016/j.orggeochem.2008.03.004, 2008.
1098
1099 Johnson, K.M., Wills, K.D., Buttler, D.B., Johnson, W.K., and Wong, C.S.: Coulometric total
1100 carbon dioxide analysis for marine studies: maximizing the performance of an automated
1101 gas extraction system and coulometric detector. Marine Chemistry 44, 167-187, 1993.
1102
1103 Kalnay, E., Kanamitsu, M., Kistler, R., Collins, W., Deaven, D., Gandin, L., Iredell, M., Saha S.,
1104 White, G., Woollen, J., Zhu, Y., Chelliah, M., Ebisuzaki, W., Higgins, W., Janowiak, J., Mo, K.C.,
1105 Ropelewski, C., Wang, J., Leetmaa, A., Reynolds, R., Jenne, R., and Joseph, D.: The
1106 NCEP/NCAR 40-year reanalysis project, Bulletin of The American Meteorological Society,
1107 77(3), 437–471, doi: ~~10.1175/1520-0477(1996)077<0437:TNYRP>2.0.CO;2~~10.1175/1520-
1108 0477(1996)077<0437:TNYRP>2.0.CO;2, 1996.
1109
1110 Kempe, S. and Pegler, K.: Sinks and sources of CO₂ in coastal seas: the North Sea, Tellus 43 B,
1111 224-235, doi: ~~10.3402/tellusb.v43i2.15268~~10.3402/tellusb.v43i2.15268, 1991.
1112
1113 Kerimoglu, O., Große, F., Kreuz, M., Lenhart, H.-J., and van Beusekom, J. E. E.: A model-based
1114 projection of historical state of a coastal ecosystem: Relevance of phytoplankton

1115 stoichiometry, *Science of The Total Environment* 639, 1311-1323,
1116 doi:10.1016/j.scitotenv.2018.05.215, 2018.

1117

1118 Kohlmeier, C., and Ebenhöf, W.: Modelling the biogeochemistry of a tidal flat ecosystem
1119 with EcoTiM, *Ocean Dynamics*, 59(2), 393-415, doi: 10.1007/s10236-009-0188-3, 2009.

1120

1121 Kowalski, N., Dellwig, O., Beck, M., Gräwe, U., Pierau, N., Nägler, T., Badewien, T., Brumsack,
1122 H.-J., van Beusekom, J.E., and Böttcher, M. E. Pelagic molybdenum concentration anomalies
1123 and the impact of sediment resuspension on the molybdenum budget in two tidal systems of
1124 the North Sea. *Geochimica et Cosmochimica Acta* 119, 198-211, 2013.

1125

1126 Kühn, W., Pätsch, J., Thomas, H., Borges, A. V., Schiettecatte, L.-S., Bozec, Y., and Prowe, A. E.
1127 F.: Nitrogen and carbon cycling in the North Sea and exchange with the North Atlantic-A
1128 model study, Part II: Carbon budget and fluxes, *Continental Shelf Research*, 30, 1701-1716,
1129 doi:10.1016/j.csr.2010.07.001, 2010.

1130

1131 Laruelle, G. G., Lauerwald, R., Pfeil, B., and Regnier, P.: Regionalized global budget of the CO₂
1132 exchange at the air-water interface in continental shelf seas, *Global Biogeochemical Cycles*,
1133 28 (11), 1199-1214, doi: 10.1002/2014gb004832, 2014.

1134

1135 Lenhart, H.-J., Radach, G., Backhaus, J. O., and Pohlmann, T.: Simulations of the North Sea
1136 circulation, its variability, and its implementation as hydrodynamical forcing in ERSEM, *Neth.*
1137 *J. Sea Res.*, 33, 271–299, doi:10.1016/0077-7579(95)90050-0, 1995.

1138

1139 Lettmann, K. A., Wolff, J.-O., and Badewien, T.H.: Modeling the impact of wind and waves on
1140 suspended particulate matter fluxes in the East Frisian Wadden Sea (southern North Sea),
1141 *Ocean Dynamics*, 59(2), 239-262, doi: 10.1007/s10236-009-0194-5, 2009.

1142

1143 Lipinski, M.: Nährstoffelemente und Spurenmetalle in Wasserproben der Hunte und Jade.
1144 Diploma thesis, C.v.O. University of Oldenburg, 82 pp., 1999.

1145

1146 Lorkowski, I., Pätsch, J., Moll, A., and Kühn, W.: Interannual variability of carbon fluxes in the
1147 North Sea from 1970 to 2006 – Competing effects of abiotic and biotic drivers on the gas-
1148 exchange of CO₂, Estuarine, Coastal and Shelf Science, 100, 38-57,
1149 doi:10.1016/j.ecss.2011.11.037, 2012.

1150

1151 Łukawska-Matuszewska, K. and Graca, B.: Pore water alkalinity below the permanent
1152 halocline in the Gdańsk Deep (Baltic Sea) - Concentration variability and benthic fluxes.
1153 Marine Chemistry 204: 49-61, 2017.

1154

1155 Mayer, B., Rixen, T., and Pohlmann, T.: The Spatial and Temporal Variability of Air-Sea CO₂
1156 Fluxes and the Effect of Net Coral Reef Calcification in the Indonesian Seas: A Numerical
1157 Sensitivity Study. Frontiers in Marine Science 5(116), 2018.

1158

1159 McQuatters-Gollop, A., Raitos, D. E., Edwards, M., Pradhan, Y., Mee, L. D., Lavender, S. J.,
1160 and Attrill, ~~and~~ M. J.: A long-term chlorophyll data set reveals regime shift in North Sea
1161 phytoplankton biomass unconnected to nutrient trends, Limnology & Oceanography, 52,
1162 635-648, doi:~~10.4319/lo.2007.52.2.0635~~10.4319/lo.2007.52.2.0635, 2007.

1163

1164 McQuatters-Gollop, A., and Vermaat, J. E.: Covariance among North Sea ecosystem state
1165 indicators during the past 50 years e contrasts between coastal and open waters, Journal of
1166 Sea Research, 65, 284-292, doi:~~10.1016/j.seares.2010.12.004~~10.1016/j.seares.2010.12.004,
1167 2011.

1168

1169 Moore, W.S., Beck, M., Riedel, T., Rutgers van der Loeff, M., Dellwig, O., Shaw, T.J.,
1170 Schnetger, B., and Brumsack, H.-J.: Radium-based pore water fluxes of silica, alkalinity,
1171 manganese, DOC, and uranium: A decade of studies in the German Wadden Sea, Geochimica
1172 et Cosmochimica Acta, 75, 6535 – 6555,
1173 doi:~~10.1016/j.gca.2011.08.037~~10.1016/j.gca.2011.08.037, 2011.

1174

1175 Neal, C.: Calcite saturation in eastern UK rivers, The Science of the Total Environment, -282-
1176 283, 311-326, doi:~~10.1016/S0048-9697(01)00921-4~~10.1016/S0048-9697(01)00921-4, 2002.

1177
1178 Neira, C., and Rackemann, M.: Black spots produced by buried macroalgae in intertidal sandy
1179 sediments of the Wadden Sea: Effects on the meiobenthos. *J. Sea Res.*, 36, 153 - 170, 1996.
1180
1181 Onken, R., and Riethmüller, R.: Determination of the freshwater budget of tidal flats from
1182 measurements near a tidal inlet, *Continental Shelf Research*, 30, 924-933,
1183 doi:10.1016/j.csr.2010.02.004, 2010.
1184
1185 Otto, L., Zimmerman, J.T.F., Furnes, G.K., Mork, M., Saetre, R., and Becker, G.: Review of the
1186 physical oceanography of the North Sea, *Netherlands Journal of Sea Research*, 26 (2-4), 161–
1187 238, doi:10.1016/0077-7579(90)90091-T, 1990.
1188
1189 Pätsch, J., and Kühn, W.: Nitrogen and carbon cycling in the North Sea and exchange with
1190 the North Atlantic – a model study Part I: Nitrogen budget and fluxes, *Continental Shelf*
1191 *Research*, 28, 767–787, doi: ~~10.1016/j.csr.2007.12.013~~10.1016/j.csr.2007.12.013, 2008.
1192
1193 Pätsch, J., and Lenhart, H.-J.: Daily Loads of Nutrients, Total Alkalinity, Dissolved Inorganic
1194 Carbon and Dissolved Organic Carbon of the European Continental Rivers for the Years
1195 1977–2006, *Berichte aus dem Zentrum für Meeres- und Klimaforschung*
1196 ~~(https://wiki.cen.uni-hamburg.de/ifm/ECOHAM/DATA_RIVER), 2008.~~
1197 ~~(https://wiki.cen.uni-hamburg.de/ifm/ECOHAM/DATA_RIVER), 2008.~~
1198
1199 Pätsch, J., Serna, A., Dähnke, K., Schlarbaum, T., Johannsen, A., and Emeis, K.-C.: Nitrogen
1200 cycling in the German Bight (SE North Sea) - Clues from modelling stable nitrogen isotopes.
1201 *Continental Shelf Research*, 30, 203-213,
1202 doi:~~10.1016/j.csr.2009.11.003~~10.1016/j.csr.2009.11.003, 2010.
1203
1204 Pätsch, J., Kühn, W., and Six, K. D.: Interannual sedimentary effluxes of alkalinity in the
1205 southern North Sea: model results compared with summer observations, *Biogeosciences*
1206 15(11), 3293-3309, doi: 10.5194/bg-15-3293-2018, 2018.
1207

1208 Pätsch, J., Burchard, H., Dieterich, C., Gräwe, U., Gröger, M., Mathis, M., Kapitza, H.,
1209 Bersch, M., Moll, A., Pohlmann, T., Su, J., Ho-Hagemann, H.T.M., Schulz, A., Elizalde, A., and
1210 Eden, C.: An evaluation of the North Sea circulation in global and regional models relevant
1211 for ecosystem simulations, *Ocean Modelling*, 116, 70-95,
1212 doi:10.1016/j.ocemod.2017.06.005, 2017.

1213

1214 Pohlmann, T.: Predicting the thermocline in a circulation model of the North Sea – Part I:
1215 model description, calibration and verification, *Continental Shelf Research*, 16(2), 131–146,
1216 doi:10.1016/0278-4343(95)90885-S, 1996.

1217

1218 Provoost, P., van Heuven, S., Soetaert, K., Laane, R. W. P. M., and Middelburg, J. J.: Seasonal
1219 and long-term changes in pH in the Dutch coastal zone, *Biogeoscience*, 7, 3869-3878,
1220 doi:10.5194/bg-7-3869-2010, 2010.

1221

1222 Raaphorst, W., Kloosterhuis H. T., Cramer, A., and Bakker, K. J. M.: Nutrient early diagenesis
1223 in the sandy sediments of the Dogger Bank area, North Sea: pore water results, *Neth. J. Sea.*
1224 *Res.*, 26(1), 25-52, doi: 10.1016/0077-7579(90)90054-K, 1990.

1225

1226 Radach, G. and Pätsch, J.: Variability of Continental Riverine Freshwater and Nutrient Inputs
1227 into the North Sea for the Years 1977-2000 and Its Consequences for the Assessment of
1228 Eutrophication, *Estuaries and Coasts* 30(1), 66-81, doi: 10.1007/BF02782968, 2007.

1229

1230 Rassmann, J., Eitel, E. M., Lansard, B., Cathalot, C., Brandily, C., Taillefert, M., and Rabouille,
1231 C.: Benthic alkalinity and dissolved inorganic carbon fluxes in the Rhône River prodelta
1232 generated by decoupled aerobic and anaerobic processes. *Biogeosciences*, 17, 13-33,
1233 doi:10.5194/bg-17-13-2020, 2020.

1234

1235 Reimer, S., Brasse, S., Doerffer, R., Dürselen, C. D., Kempe, S., Michaelis, W., and Seifert, R.:
1236 Carbon cycling in the German Bight: An estimate of transformation processes and transport,
1237 *Deutsche Hydr. Zeitschr.* 51, 313-329, doi: /10.1007/BF02764179, 1999.

1238

1239 Riedel, T., Lettmann, K., Beck, M., and Brumsack, H.-J.: Tidal variations in groundwater
1240 storage and associated discharge from an intertidal coastal aquifer. Journal of Geophysical
1241 Research 115, 1-10, 2010.

1242

1243 Rullkötter, J.: The back-barrier tidal flats in the southern North Sea—a multidisciplinary
1244 approach to reveal the main driving forces shaping the system, Ocean Dynamics, 59(2), 157-
1245 165, doi: 10.1007/s10236-009-0197-2, 2009.

1246

1247 Salt, L. -A., Thomas, H., Prowe, A. E. F., Borges, A. V., Bozec, Y., and de Baar, H. J. W.:
1248 Variability of North Sea pH and CO₂ in response to North Atlantic Oscillation forcing, Journal
1249 of Geophysical Research, Biogeosciences, 118, pp 9, doi:10.1002/2013JG002306, 2013.

1250

1251 Santos, I. R., Eyre, B. ~~D., and Huettel, M.: The driving forces of porewater and groundwater~~
1252 ~~flow in permeable coastal sediments: A review~~D., and Huettel, M.: The driving forces of
1253 porewater and groundwater flow in permeable coastal sediments: A review, Estuarine,
1254 Coastal and Shelf Science, 98, 1-15,
1255 doi:~~10.1016/j.ecss.2011.10.024~~10.1016/j.ecss.2011.10.024, 2012.

1256

1257 Santos, I. R., Beck, M., Brumsack, H.-J., Maher, D.T., Dittmar, T., Waska, H., and Schnetger,
1258 B.: Porewater exchange as a driver of carbon dynamics across a terrestrial-marine transect:
1259 Insights from coupled ²²²Rn and pCO₂ observations in the German Wadden Sea, Marine
1260 Chemistry, 171, 10-20,
1261 doi:~~10.1016/j.marchem.2015.02.005~~10.1016/j.marchem.2015.02.005, 2015.

1262

1263 Schott, F.: Der Oberflächensalzgehalt in der Nordsee, Deutsche Hydr. Zeitschr., Reihe A Nr. 9,
1264 SUPPL. A9, pp 1-29, 1966.

1265

1266 Schwichtenberg, F.: Drivers of the carbonate system variability in the southern North Sea:
1267 River input, anaerobic alkalinity generation in the Wadden Sea and internal processes,
1268 (Doktorarbeit/PhS), Universität Hamburg, Hamburg, Germany, 161 pp, 2013.

1270 Seibert, S.L., Greskowiak J., Prommer H., Böttcher M.E., Waska H., and Massmann G.:
1271 Modeling biogeochemical processes in a barrier island freshwater lens (Spiekeroog,
1272 Germany). *J. Hydrol.*, 575, 1133-1144, 2019.

1273

1274 Seitzinger, S., and Giblin, A.E.: Estimating denitrification in North Atlantic continental shelf
1275 sediments, *Biogeochemistry*, 35, 235–260, doi: 10.1007/BF02179829, 1996.

1276

1277 Shadwick, E. H., Thomas, H., Azetsu-Scott, K., Greenan, B. J. W., Head, E., and Horne, E.:
1278 Seasonal variability of dissolved inorganic carbon and surface water pCO₂ in the Scotian Shelf
1279 region of the Northwestern Atlantic, *Marine Chemistry*, 124 (1–4), 23-37,
1280 doi:10.1016/j.marchem.2010.11.004, 2011.

1281

1282 Sippo, J.Z., Maher, D.T., Tait, D.R., Holloway, C., Santos, I.R.: Are mangroves drivers or
1283 buffers of coastal acidification? Insights from alkalinity and dissolved inorganic carbon export
1284 estimates across a latitudinal transect. *Global Biogeochemical Cycles*, 30, 753-766, 2016.

1285

1286 Smith, S. V., and Hollibaugh, J. T.: Coastal metabolism and the oceanic organic carbon
1287 balance, *Reviews of Geophysics*, 31, 75–89, doi:10.1029/92RG02584, 1993.

1288

1289 Streif, H.: *Das ostfriesische Wattenmeer. Nordsee, Inseln, Watten und Marschen.* Gebrüder
1290 Borntraeger, Berlin, 1990.

1291

1292 [Su, J. and Pohlmann, T.: Wind and topography influence on an upwelling system at the](#)
1293 [eastern Hainan coast. *Journal of Geophysical Research: Oceans* 114\(C6\), 2009.](#)

1294

1295 Sulzbacher, H., Wiederhold, H., Siemon, B., Grinat, M., Igel, J., Burschil, T., Günther, T.,
1296 Hinsby, K.: Numerical modelling of climate change impacts on freshwater lenses on the
1297 North Sea Island of Borkum using hydrological and geophysical methods." *Hydrol. Earth Syst.*
1298 *Sci.* 16(10): 3621-3643, 2012.

1299

1300 Thomas, H., Bozec, Y., Elkalay, K., and de Baar, H. J. W.: Enhanced open ocean storage of CO₂

1301 from shelf sea pumping, *Science*, 304, 1005-1008, doi:10.1126/science.1095491, 2004.

1302

1303 Thomas, H., Schiettecatte, L.-S., Suykens, K., Kone, Y. J. M., Shadwick, E. H., Prowe, A. E. F.,
1304 Bozec, Y., De Baar, H. J. W., and Borges, A. V.: Enhanced ocean carbon storage from
1305 anaerobic alkalinity generation in coastal sediments, *Biogeosciences*, 6, 267-274,
1306 doi:10.5194/bg-6-267-2009, 2009.

1307

1308 van Beusekom, J. E. E., Carstensen, J., Dolch, T., Grage, A., Hofmeister, R., Lenhart, H.-J.,
1309 Kerimoglu, O., Kolbe, K., Pätsch, J., Rick, J., Rönn, L., and Ruiters, H.: Wadden Sea
1310 Eutrophication: Long-Term Trends and Regional Differences. *Frontiers in Marine Science*
1311 6(370), 2019

1312

1313 van Beusekom, J. E. E., Loebel, M., and Martens, P.: Distant riverine nutrient supply and local
1314 temperature drive the long-term phytoplankton development in a temperate coastal basin,
1315 *J. Sea Res.* ~~61, 26-33~~, doi:~~10.1016/j.seares.2008.06.00561, 26-33~~,
1316 doi:10.1016/j.seares.2008.06.005, 2009.

1317

1318 van Beusekom, J. E. E., Buschbaum, C., and Reise, K.: Wadden Sea tidal basins and the
1319 mediating role of the North Sea in ecological processes: scaling up of management? *Ocean &*
1320 *Coastal Management*, 68, 69-78,
1321 doi:~~10.1016/j.ocecoaman.2012.05.002~~10.1016/j.ocecoaman.2012.05.002, 2012.

1322

1323 van Goor, M. A., Zitman, T. J., Wang, Z. B., and Stive, M. J. F.: Impact of sea-level rise on the
1324 equilibrium state of tidal inlets, *Mar. Geol.* 202, 211-227, doi:~~10.1016/S0025-3227(03)00262-~~
1325 710.1016/S0025-3227(03)00262-7, 2003.

1326

1327 van Koningsveld, M., Mulder, J. P. M., Stive, M. J. F., Van der Valk, L., and Van der Weck,
1328 A.W.: Living with sea-level rise and climate change: a case study of the Netherlands, *J. Coast.*
1329 *Res.* 24, 367-379, doi:10.2112/07A-0010.1, 2008.

1330

1331 Wang, Z. A., and Cai, W.-J.: Carbon dioxide degassing and inorganic carbon export from a
1332 marsh-dominated estuary (the Duplin River): A marsh CO₂ pump, *Limnology &*

1333 Oceanography, 49, 341–354, doi:10.4319/lo.2004.49.2.0341, 2004.

1334

1335 Winde, V.: Zum Einfluss von benthischen und pelagischen Prozessen auf das Karbonatsystem
1336 des Wattenmeeres der Nordsee. Dr.rer.nat. thesis, EMA University of Greifswald, ~~2013~~2012.

1337

1338 Winde, V., Böttcher, M. E., Escher, P., Böning, P., Beck, M., Liebezeit, G., and Schneider, B.:
1339 Tidal and spatial variations of DI^{13}C and aquatic chemistry in a temperate tidal basin during
1340 winter time, Journal of Marine Systems, 129, 396-404,
1341 doi:~~10.1016/j.jmarsys.2013.08.005~~10.1016/j.jmarsys.2013.08.005, 2014.

1342

1343 Wolf-Gladrow, D. A., Zeebe, R. E., Klaas, C., Kortzinger, A., and Dickson, A. G.: Total alkalinity:
1344 The explicit conservative expression and its application to biogeochemical processes, Marine
1345 Chemistry, 106, 287–300, doi:10.1016/j.marchem.2007.01.006, 2007.

1346

1347 Wurgaft E., Findlay A.J., Vigderovich H., Herut B., ~~Sivan O.: Sulfate reduction rates in the~~
1348 ~~sediments of the Mediterranean continental shelf inferred from combined dissolved inorganic~~
1349 ~~carbon and total alkalinity profiles. Marine Chemistry, 211,64–74, 2019.~~and Sivan O.: Sulfate
1350 reduction rates in the sediments of the Mediterranean continental shelf inferred from
1351 combined dissolved inorganic carbon and total alkalinity profiles. Marine Chemistry, 211,64-
1352 74, 2019.

1353

1354 Zhai, W.-D., Yan, X.-L., and Qi, D.: Biogeochemical generation of dissolved inorganic carbon
1355 and nitrogen in the North Branch of inner Changjiang Estuary in a dry season. Estuarine,
1356 Coastal and Shelf Science 197: 136-149, 2017.

1357

1358 Zeebe, R.E., and Wolf-Gladrow, D. 2001. CO_2 in seawater: Equilibrium, Kinetics, Isotopes. 1st
1359 edn. ELSEVIERElsevier Science Ltd., 2001.

1360

1361

1362

1363

1364
1365
1366
1367
1368
1369
1370
1371
1372
1373
1374
1375
1376

8. Appendix

Table A1: Annual riverine freshwater discharge [km³-yr⁻¹]. The numbering refers to Fig. 1.

	2001	2002	2003	2004	2005	2006	2007	2008	2009
1) Elbe	23.05	43.38	23.95	19.56	25.56	26.98	26.61	24.62	24.28
2) Ems	3.47	4.48	3.15	3.52	2.99	2.54	4.32	3.32	2.58
3) Noordzeekanaal	3.21	2.98	2.49	3.05	3.03	2.96	1.55	3.05	2.46
4) IJsselmeer (east)	9.55	9.94	6.27	7.97	7.35	7.30	9.10	8.23	6.59
5) IJsselmeer (west)	9.55	9.94	6.27	7.97	7.35	7.30	9.10	8.23	6.59
6) Nieuwe Waterweg	50.37	51.33	34.72	42.91	41.61	44.21	49.59	49.76	44.69
7) Haringvliet	33.10	35.18	17.92	10.77	12.36	16.02	24.00	15.70	11.06
8) Scheldt	7.28	2.74	4.31	3.64	3.59	3.74	4.63	4.57	3.63
9) Weser	11.43	18.97	11.80	10.52	10.37	9.72	16.21	12.59	9.58
10) Firth of Forth	2.72	3.76	2.06	3.01	3.00	2.84	2.85	3.59	3.66
11) Tyne	1.81	2.25	1.18	2.04	1.92	1.78	2.09	2.70	2.05
12) Tees	1.33	1.78	0.94	1.59	1.27	1.45	1.49	1.99	1.55
13) Humber	10.76	12.10	7.16	10.51	7.68	11.11	12.03	13.87	9.60
14) Wash	5.46	4.39	3.08	3.91	1.96	2.72	5.24	4.77	3.21
15) Thames	4.47	3.23	2.41	2.13	0.96	1.57	3.52	3.20	2.38
16) Eider	0.67	0.97	0.47	0.70	0.68	0.67	0.63	0.58	0.57
Sum	178.2	207.4	128.1	133.7	131.6	142.9	172.9	160.7	134.4

1377
1378
1379
1380
1381
1382

1383 **Table A2: River numbers in Fig. 1, their positions and source of data**

Number in Fig. 1	Name	River mouth position	Data source
1	Elbe	53°53'20"N 08°55'00"E	Pätsch & Lenhart (2008); TA-, DIC- and nitrate- concentrations by Amann (2015)
2	Ems	53°29'20"N 06°55'00"E	Pätsch & Lenhart (2008)
3	Noordzeekanaal	52°17'20"N 04°15'00"E	Pätsch & Lenhart (2008); TA-, DIC- and nitrate- concentrations from waterbase.nl
4	IJsselmeer (east)	53°17'20"N 05°15'00"E	As above
5	IJsselmeer (west)	53°05'20"N 04°55'00"E	As above
6	Nieuwe Waterweg	52°05'20"N 03°55'00"E	As above
7	Haringvliet	51°53'20"N 03°55'00"E	As above
8	Scheldt	51°29'20"N 03°15'00"E	As above
9	Weser	53°53'20"N 08°15'00"E	Pätsch & Lenhart (2008)
10	Firth of Forth	56°05'20"N 02°45'00"W	HASEC (2012)
11	Tyne	55°05'20"N 01°25'00"W	HASEC (2012)
12	Tees	54°41'20"N 01°05'00"W	HASEC (2012)
13	Humber	53°41'20"N 00°25'00"W	HASEC (2012)
14	Wash	52°53'20"N 00°15'00"E	HASEC (2012): sum of 4 rivers: Nene, Ouse, Welland and Witham
15	Thames	51°29'20"N 00°55'00"E	HASEC (2012)
16	Eider	54°05'20"N 08°55'00"E	Johannsen et al, 2008

1384

1385

1386 **Table_A3: Monthly values of TA, DIC and NO₃ concentrations [$\mu\text{mol}\cdot\text{kg}^{-1}$] of rivers, the annual**

River parameter	Jan	Feb	Mar	Apr	May	Jun	Jul	Aug	Sep	Oct	Nov	Dec	Mean	SD
Elbe TA	2380	2272	2293	2083	2017	1967	1916	1768	1988	2156	2342	2488	2130	218
Noordzeekanaal TA	3762	3550	3524	3441	4748	3278	3410	3183	3027	3290	3210	3413	3488	441
Nieuwe Waterweg TA	2728	2768	2765	3095	2745	2858	2834	2888	2898	2791	2895	2892	Mean	SD
Elbe TA	2380	2272	2293	2083	2017	1967	1916	1768	1988	2156	2342	2488	2130	218
Noordzeekanaal TA	3762	3550	3524	3441	4748	3278	3410	3183	3027	3290	3210	3413	3488	441
Nieuwe Waterweg TA	2728	2768	2765	3095	2745	2858	2834	2888	2898	2791	2895	2892	Mean	SD
Haringvliet TA	2538	2635	2582	2686	2688	2628	2658	2669	2498	2806	2758	2582	2754	299
Noordzeekanaal-DIC	3788	3889	3708	3338	3968	3888	3732	3538	3967	3868	3885	3805	3898	280
Nieuwe Waterweg-DIC	2889	3008	2872	2999	2679	2867	2888	2708	2828	2772	2988	2858	2845	508
Haringvliet-DIC	2678	2738	2808	2689	2898	2826	2888	2883	2818	2889	2808	2678	2798	292
Noordzeekanaal-DIC	3798	3909	3828	3334	3804	3892	3805	3498	3978	3848	3788	3868	3898	264
Nieuwe Waterweg-DIC	2884	2988	2858	2884	2678	2888	2888	2788	2888	2774	2885	2888	2888	588
Elbe NO ₃	2873	2798	2888	3885	2888	2888	2889	2883	2512	2888	2888	2898	2788	282
Noordzeekanaal-NO ₃	3798	3889	3829	3739	3789	3582	3784	3488	3378	3648	3788	3888	3884	167
Nieuwe Waterweg-NO ₃	2824	3888	2488	2784	2578	1828	1836	1389	1389	2134	2285	2588	2188	538
Haringvliet-NO ₃	247	336	277	229	193	184	129	103	142	157	267	464	167	92
Noordzeekanaal-NO ₃	158	188	198	178	278	271	284	278	198	292	189	157	194	89
Nieuwe Waterweg-NO ₃	138	188	198	192	155	48	28	14	7	48	28	79	88	17
Haringvliet-NO ₃	232	243	231	195	150	140	132	135	113	145	201	220	178	
Scheldt-NO ₃	233	252	218	200	143	144	133	117	128	127	143	228	172	50
IJsselmeer-NO ₃	320	341	347	345	243	221	219	215	189	202	190	274	259	63
IJsselmeer-NO ₃	136	159	190	192	135	46	20	14	7	18	20	79	85	73

1387 mean and the standard deviation

1388

1389